

FINAL REPORT
for
Iowa Highway Research Board Project TR-760

**Reducing Uncertainties in Snow Fence Design:
Development of Methods for Estimation of Snow Drifting and the
Snow Relocation Coefficient**

Submitted by

Corey D. Markfort, Marian Muste, Hao Chen, and Mohsen Vahidzadeh

IIHR-Hydrosience & Engineering
and
Department of Civil and Environmental Engineering
The University of Iowa
Iowa City, IA

Sponsored by

The Iowa Highway Research Board

September 8, 2020

Disclaimer Notice

The contents of this report reflect the views of the authors, who are responsible for the facts and the accuracy of the information presented herein. The opinions, findings, and conclusions expressed in this publication are those of the authors and not necessarily of the sponsors. The sponsors assume no liability for the contents or use of the information contained in this document. This report does not constitute a standard, specification, or regulation.

The sponsors do not endorse products or manufacturers. Trademarks or manufacturer's names appear in this report only because they are considered essential to the objectives of the document.

Statement of Non-Discrimination

Federal and state laws prohibit employment and/or public accommodation discrimination on the basis of age, color, creed, disability, gender identity, national origin, pregnancy, race, religion sex, sexual orientation or veteran's status. If you believe you have been discriminated against, please contact the Iowa Civil Rights Commission at 800-457-4416 or Iowa Department of Transportation's affirmative action officer. If you need accommodations because of a disability to access the Iowa Department of Transportation's services, contact the agency's affirmative action officer at 800-262-0003.

The University of Iowa does not discriminate on the basis of race, color, age, religion, national origin, sexual orientation, gender identity, sex, marital status, disability, or status as a U.S. veteran. Inquiries can be directed to the Director of Equal Opportunity and Diversity at the University of Iowa, (319) 335-0705.

Acknowledgements

The study presented in this report was supported by the Iowa Highway Research Board (IHRB) Project: TRB-760. We would like to thank Ms. Tina Greenfield Huitt and all the members of the technical advisory committee for their support of the project. The preparation of the field test site and field measurements conducted as part of the present project were assisted by Bob Ellis with the Williams/Iowa Falls Maintenance Garages, Iowa DOT. Their support is greatly appreciated.

1. Report No. TR-760	2. Government Accession No. Optional	3. Recipient Catalog No. Optional	
4. Title and Subtitle Reducing Uncertainties in Snow Fence Design: Development of Methods for Estimation of Snow Drifting and the Snow Relocation Coefficient		5. Report Date September 10, 2020	
		6. Performing Organization Code: N/A	
7. Author(s): Markfort, C.D., Muste M., Chen H., Vahidzahdeh M.		8. Performing Organization Report No.	
9. Performing Organization Name and Address Dept. Civil and Environmental Engineering, The University of Iowa, Iowa City, IA, 52242		10. Work Unit No. (TR AIS) Not Required	
		11. Contract or Grant No. TR-760	
12. Sponsoring Organization Name and Address Iowa Department of Transportation 800 Lincoln Way Ames, Iowa 50010		13. Type of Report and Period Covered. Final Report for 08/15/2018 to 09/30/2020.	
		14. Sponsoring Agency Code TR-760	
15. Supplementary Notes None			
16. Abstract Blowing and drifting of snow is a major concern for transportation safety and road maintenance. Mitigation of snow drift on roadways is often achieved by installing temporary or permanent snow fences along the road segments affected by snow drift. Robust design of snow fences is critical for road safety and for maintaining clear and open roads during the winter season in the US Midwest, as well as for other states affected by large snow events. Reducing accumulation of snow on roadways also decreases the need for associated repairs due to damage caused to roads. The design of snow fences relies on empirical relations that do not necessarily apply to the U S Midwest. Majors changes are related to the accurate estimation of the snow relocation coefficient (SRC), a critical parameter for sizing snow fences and determining the required easement for snow storage. Currently, IDOT snow fence designers use a default value of SRC despite conditions vary widely across the state and from where SRC has been determined empirically. Estimation of SRC requires quantification of the snowfall and snowdrift fluxes at sites where snow fences are installed. The lack of available, reliable data to estimate the local value of SRC results in an inefficient and possibly inadequate design of the snow fence. The research described in this report addresses two critical questions related to snow fence design: 1) What is the seasonal snow relocation coefficient for Iowa? and, 2) What is the seasonal storage capacity of snow fences when accounting for successive storms and ablation between snow events? Estimation of the SRC in the field is a challenging problem as it requires accurate quantification of snowfall and snowdrift fluxes at the site where the snow fence is installed. Therefore, we first developed methods for accurate estimation of snowfall and snow drifting fluxes, building on prior research efforts. The methods include monitoring techniques designed to continuously acquire data without supervision as well as detailed field collection efforts, typically after major snowstorm events. A range of intrusive monitoring methods (i.e., direct snow depth measurements, topographic surveys of snow deposit profiles, and snow density measurements) and non-intrusive methods were used for quantification of meteorological conditions at snow fence installations and tracking changes in snow deposits during and between snowstorm events. The results of the study conducted at three snow fence sites suggest that the SRC estimates are significantly lower than the default value of 0.5, currently used for snow fence design. The study also found that additional storage capacity is available during the winter season due to ablation, comprised of compaction, sublimation or evaporation, and melting between storm events. The outcomes of the two-year project confirmed the reliability of the developed monitoring methods as well as the consistency of the results for the three experimental sites investigated during the study.			
17. Key Words Snow fence, Design uncertainty, Monitoring snow deposits, Field experiments, Snow transport		18. Distribution Statement No restrictions.	
19. Security Classification (of this report) Unclassified	20. Security Classification (of this page) Unclassified	21. No. of pages 77	22. Price N/A

This page left intentionally blank

Contents

Contents.....	i
Executive Summary	1
1. Introduction	3
1.1. Problem statement	3
1.2. Research needs	4
1.3. Research goal and objectives	5
2. Background	6
2.1. Snow relocation coefficient.....	6
2.1.1. Definition of snow relocation coefficient.....	6
2.1.2. Snow movement.....	6
2.1.3. Snow transport and evaporative losses	7
2.1.4. Estimation of SRC	9
2.2. Considerations on snow fences.....	10
2.2.1. Structural fences	11
2.2.2. Living fences	11
2.2.3. Design considerations	14
3. Experimental approach & implementation details	14
3.1. Experimental sites	14
3.1.1. Site selection criteria and experimental design	14
3.1.2. Description of experimental arrangements	19
3.2. Experimental instrumentation and data acquisition methods.....	23
3.2.1. Continuous monitoring	23
3.2.2. Synoptic monitoring.....	34
3.2.3. Uncertainty considerations	39
3.3. Complementary public data	41
3.3.1. Alternative sources for estimation of the local snowfall.....	41
3.3.2 Snow density	44
3.3.3 Wind speed	44
4. Data analysis	47
4.1. Snowstorm records	47
4.2. Snow deposit tracking	53

4.2.1. Snow deposit shape	53
4.2.2. Cross-sectional snow deposit profiles using webcam images.....	54
4.2.3. Snow volumes calculation	57
4.3. Data processing for estimation of SRC	58
4.3.1. Observational method (M1).....	58
4.3.2. Theoretical method (M2)	60
4.3.2. Uncertainty considerations for SRC calculation	64
5. Summary of results	65
5.1. SRC Estimates	65
5.2. Snow deposit volume change between events.....	66
6. Conclusion and future work	68
7. References.....	70

Executive Summary

Blowing and drifting of snow is a major concern for safety, transportation efficiency, and road maintenance in regions subject to intense snowfall and winds during the winter season. Snow blowing (or drifting) across and accumulating on the roadway leads to reduced driver visibility and induces ice formation on roads posing serious safety concerns and leading to an increased number of accidents. The impacts of snowfall and snowdrift on highway traffic are mitigated with a variety of methods and activities implemented before, during, and after snowstorms. The most commonly used mitigation measure is the deployment of snow fences. Snow fences can be temporarily or permanently installed along the roadway. They are deployed in areas prone to snowdrifting as either structural barrier (constructed using lightweight construction materials) or as living fences (composed of a combination of planted shrubs, trees and tall grasses) that act as a windbreak to effectively trap the snow before it blows onto the road.

The design of temporary and permanent snow fences relies on empirical relations developed for specific climatic regions. One essential design input is a snow relocation coefficient (SRC), which is the fraction of fallen snow relocated by wind from the upwind fetch area. The available SRC estimation methods are based on semi-empirical equations without provision for corrections to adapt these relationships for specific local site conditions. Currently, Iowa DOT snow fence designers use an estimated value of $SRC = 0.5$. Without being able to accurately estimate the Iowa local SRC values, the design of an efficient snow fence is often incomplete and prone to multiple sources of uncertainties. An additional source of uncertainty in the fence design is the effective seasonal capacity of a snow fence. Due to melting and sublimation, or ablation (occurring between snow events), the assumption of no snow losses currently used in the snow fence design may be unnecessarily conservative, and therefore the result of these relations at sites prone to snow drift in Iowa is uncertain.

Ensuing from the above considerations, the main research questions for the present research are: 1) What is the seasonal snow relocation coefficient for Iowa? and, 2) What is the seasonal storage capacity of the snow fences deployed in Iowa? Estimation of the SRC is however a complex undertaking as it requires accurate quantification of the snowfall and snowdrift fluxes at the site where the snow fence is installed. The current methods for measurement of snowfall are often subject to significant uncertainties because of unaccounted wind effects. Snowdrift fluxes are dependent on wind fetch length, wind speed, air and ground temperature, and ground cover characteristics. Consequently, the empirical relations for evaluation of the SRC are site-dependent and strongly correlated with the local meteorological conditions, topography, and the presence and type of ground cover. There are no established protocols for in-situ determination of the SRC in the presence or absence of snow fences. Therefore, prior to addressing the SRC-related question, this research first tackled improved methods for estimation of snowfall and snow drifting fluxes building on original concepts developed through prior research complemented by new innovations. Specifically, we improved and advanced methods to continuously acquire data in real time at the observation sites without need for human presence. In parallel, we developed a set of improved methods for acquiring data through site visits, typically made right after major snowstorm events occurred. The monitoring methods include intrusive measurements (i.e., direct snow depth

measurements, topographic surveys of the cross-sectional profiles of the snow deposits accumulated at the fences, and snow density measurements) and non-intrusive measurements for quantification of at-the-site meteorological conditions and of tracking of the changes in snow deposits during and between storms.

Seven different types of direct and close-range measurements were deployed at the experimental sites arranged in customized layouts to measure local meteorological variables and for tracking the snow deposits accumulated due to snow drifting. In addition to our own data, complementary data on meteorological conditions in the vicinity of the experimental sites were accessed from multiple public sources for validation and verification purposes. The selection of the experimental sites was made in consultation with Iowa DOT engineer representatives and the project Technical Advisory Committee to optimally analyze the snow drifting process. Specifically, sites located in open-field areas regularly exposed to high-severity snow drifting were selected. Preference was given to locations where the fence alignment was perpendicular to the dominant wind direction over most of the winter season. The fences at the three investigated sites (on US-20 and I-35 near Williams, and on a secondary road close to US-218 near Cedar Rapids) entailed permanent structural fences, living fences, and temporary lightweight fences. During the two-year project two of the sites were monitored for one winter season and one site (US-20) was monitored for two winters for validation of the result purposes.

The outcomes of the data analysis carried out through this study revealed that the SRC estimates are lower than the default value of 0.5 currently used for snow fence design by the Iowa DOT design office. This important result is confirmed by the implementation of two alternative methods for SRC estimation; one following the approach for defining SRC from Tabler's (2003), (method M1) and the other one being a hybrid of control-volume approach complemented by Tabler-inspired empirical relationships for snow transport based on wind speed and evaporation (method M2). The implications for an Iowa-specific value for SRC are supported by the results obtained at all three investigated sites. Furthermore, it was shown that the fences have considerable additional storage capacity when considering the whole winter season due to compaction, sublimation, and melting occurring between storm events. Both of these findings were anticipated by the Iowa DOT designers but not quantitatively confirmed through rigorous investigations. While not definitive and generalizable due to the fact that the two investigated winters are not equally representative (with the 2019-20 winter being milder than the 2018-19 one), the study results provide, for the first time, estimation of site-specific SRC values, documented by local measurements of all the relevant variables involved in the snow drift process.

The consistency of the results obtained for the three experimental sites investigated during the two-year study also confirmed the reliability of the developed monitoring methods. This is a secondary contribution of this project as the current protocols for quantifying snowdrift events is a challenging task with many of the methods still under development. Most conventional methods in this area (e.g., total station surveys, graduated stakes, and direct snow depth measurements) are outdated and require personnel to physically visit sites in the field during harsh winter conditions. During this, as well as through previous studies, we gradually developed our own set of protocols that are currently providing an adequate experimental package to confidently address the

estimation of the snow drifting process with high spatial and temporal resolution using non-intrusive, unassisted measurements communicated remotely in real time.

1. Introduction

1.1. Problem statement

Snowstorms accompanied by blowing and drifting are widespread in the Midwestern landscape, where winters experience strong winds and often times large amount of snowfall. There are several detrimental consequences caused by drifting snow. Most of the concerns are related to traffic safety as during the storms the drifting snow accumulates in addition to the snow that falls directly on the road leading to a dramatic reduction of vehicle maneuverability and drivers' visibility of the roads and traffic signs (Figure 1a). Drifting snow considerably increases the cost needed for snow and ice removal due to equipment expenses and snow removal crews (Tabler, 2003). Collectively, these cause an increase in the number of road accidents (Figure 1b). Drifting snow also is the main cause for ice formation on the roadway, which results in a reduction in effective road width (Figure 1c), making the safety barriers ineffective and impeding efficient snow removal. Under the worst conditions, snow drifting can cause roads to be impassible and require road closures. In the long term, the snow drifted on the road and its vicinity reduces the pavement life by blocking ditches, drains, and culverts.



Figure 1 Effects of snow blowing on Iowa's roads: a) reduced visibility; b) accidents, c) reduction of the effective road width (photos: Tsai, 2015, I-35 Hwy, Iowa).

The impacts of blowing and drifting snow are mitigated with a variety of methods and activities implemented before, during, and after snowstorms. The most common mitigation measure is the use of snow fences. Snow fence can be temporary or permanently installed along the road. They are deployed in areas prone to drifting snow as either structural barrier (constructed using lightweight construction materials) or by planting a combination of shrubs, trees and grasses that act as a windbreak (i.e., living fence) in the vicinity of the road.

Snow fences were initially used for protecting railroads and become widespread on roadways during the 1930s with the rapid increase of automobiles. The first studies on snow fence design started about the same time but the research slowed down soon because of increased availability and access to improved trucks and heavy snow-cleaning equipment. Current snow fence design guidelines are based on U.S Forest Service research conducted in the 1960s and 1970s (Martinelli et al., 1982). The research results implemented at I-80 in Wyoming led to between a third to half of the required snow-cleaning equipment, staffing, and maintenance costs. Snow fence was also

credited with preventing an average of 54 accidents and 35 injuries over the winter season (Tabler, 2003).

The effectiveness of snow fences in Wyoming provides strong evidence that snow fence can effectively reduce the impact of drifting snow. Similar to Wyoming, Iowa also experiences hazardous snow and blowing snow events. While snow fence is a good strategy to limit blowing snow from reaching the highway, their design relies on empirical relationships and assumptions for several key variables. An important factor used for determining the amount of snow that will blow onto the roadway and a fence must capture is the Snow Relocation Coefficient (SRC). It is the fraction of the fallen snow that is relocated by wind from the upwind source area or fetch. SRC depends on the amount and mobility of the snow in the fetch area as well as wind speeds sustained over the fetch area. Values of SRC typically vary from 0.15 for landscapes with dense and tall vegetation to 0.75 for open landscapes with short vegetation. In the open landscapes of Wyoming, as SRC of 0.75 is used, while the typical range of SRC used northeastern states is 0.15 to 0.3 (Tabler, 2003). Lacking sufficient local data for Iowa, and since Iowa is between Wyoming and the northeastern US, the Iowa Dept. of Transportation (IDOT) uses a value of 0.5, as recommended by Tabler (2003).

Currently, IDOT snow fence designers use an estimated value of SRC for snow fence design due to a lack of data and the empirical estimate is widely different from those previously measured. Without an accurately estimate for appropriate local values of SRC, the design of an efficient snow fence is, in most cases, incomplete.

1.2. Research needs

The performance of a snow fence depends on fence height, porosity, and the size of the bottom gap (Tabler and Jairell 1990; Tabler 1980, 1994). The correct determination of these design variables depends on estimation of snow relocation coefficient (SRC) for a specific site. The available SRC estimates are based on a set of empirical equations, without accounting for corrections to adapt these relationships for sites specific conditions, and therefore the result of these relations at sites prone to snow drift in Iowa is uncertain. Additional uncertainty comes from the effective seasonal capacity of a snow fence. Due to melting and sublimation, and ablation (all resulting in shrinking of the snow deposit between snowstorms), the current assumption of no snow losses in snow fence design may be unnecessarily conservative. These uncertainties in SRC and in the estimation of the capacity of the fences to retain snow result in improper snow fence design.

SRC estimation requires quantification of the snowfall and snow transported by wind at the site where the snow fence is installed. The current methods for measurement of snowfall are often subject to significant uncertainty due to wind effects. Estimation of snow transport is dependent on local meteorological conditions (e.g, wind speed, air and ground temperature), topography, fetch length, and ground cover characteristics. Consequently, the empirical relations for evaluation of the SRC are site-dependent and strongly correlated with the local meteorological conditions, topography, and the presence and type of ground cover. An additional uncertainty for monitoring snow transport is assumptions about snow water equivalent (SWE). The estimate is required for

converting snow volume to equivalent water volume, and is an input variable for snow fence design.

Currently, the Iowa DOT design guidelines for controlling snowdrifts and reducing the concentration of snow in air are based on the studies conducted by Tabler (1991, 1994, and 2003). These reports are considered “the best available information” in the field of mitigation of snow drift, and they represent the foundation for the Wyoming DOT Snow Drift Profiler (Tabler, 2006) that is the basis for the design tool used by IDOT. During previous discussions with the research team and IDOT engineers, including Brian Smith, Eric Weigel, Tina Greenfield Huitt with the IDOT Office of Design, two primary questions were identified for the design of snow fences:

- a) ***What is the seasonal snow relocation coefficient (SRC) for Iowa?*** How does the SRC vary with fetch length, ground cover, topographic features, and variation in snow characteristics for individual storms? Currently, a single SRC is used in the design (i.e., 0.5 as an interpolation from values estimated in Wyoming and Northeastern US region). However, values may vary depending on the local site and winter seasonal characteristics. For example, an average seasonal value of 0.25 may be a more appropriate estimate for Iowa.
- b) ***What is the seasonal storage capacity of the snow fences when accounting for successive storms and the ablation of accumulated snow deposits between snow events?*** How much volume is stored at the fences for each storm in succession during the winter season? How much does the drifted snow accumulated at snow fences subside between storms?

The proposed research addresses these specific questions by developing an in-situ field experimental program to measure specific values for SRC and quantify net accumulation of snow at snow fences continuously throughout the winter season. The monitoring approaches developed in this project can provide the necessary data to estimate SRC coefficients specifically for the climate and topographic conditions characteristic of Iowa.

1.3. Research goal and objectives

The current measurement protocols for snowfall and snowdrift quantification and evaluation of the design of snow fence efficiency are incomplete, costly, and are practically of unknown (presumably quite low) accuracy. Most of the pitfalls of measurement approaches are related to the fact that the measurements are acquired with intrusive sampling techniques, i.e., snow bags, snow traps, and snow boards. Data acquisition performed with these techniques require extended exposure to adverse, frigid, and windy conditions that pose a significant risk for personnel safety and health.

The research goal of this study is to develop, test, and deploy a set of new technologies to support the design and evaluation of snow fence performance using nonintrusive measurement technologies based on images of snow drift movement and of the accumulation of the snow at snow fences. Specifically, the objectives proposed for this study addresses three critical aspects of snow fence design that are needed by IDOT winter maintenance designers:

Objective 1. Estimation of local snowfall

Objective 2. Mapping of the accumulated snow at fences

2. Background

2.1. Snow relocation coefficient

2.1.1. Definition of snow relocation coefficient

The relocated snow (S_{rwe}), is the portion of the snowfall transferred by wind without consideration of the amount of snow retained by vegetation and topographic features, or snow that hardens or melts (Tabler, 2003). Therefore, the snow relocation coefficient (θ) is the proportion of winter snowfall water equivalent (S_{we}) relocated by wind (Tabler, 2003).

$$\theta = \frac{S_{rwe}}{S_{we}} \quad (1)$$

The area that contributes with transported snow in the downwind direction is labeled fetch. During its downwind movement, the snow evaporate specific amounts (Q_{evap}), pending on a combination of meteorological factors. Tabler (2003) suggests that 3 km is the maximum transport distance that the snow particle can travel before to completely evaporate. The amount of snow deposited at the fenced area is the actual snow transported by wind (Q_{dep}), as illustrated in Figure 2.

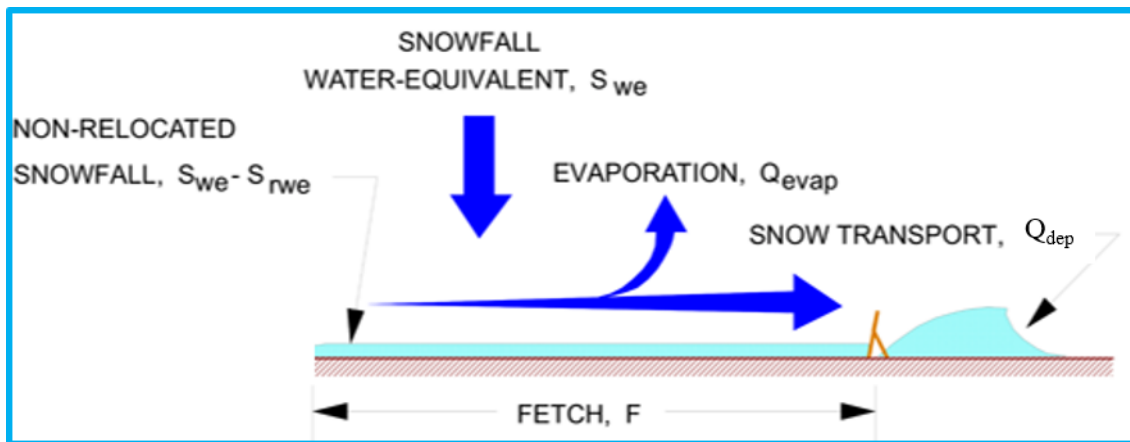


Figure 2. Diagram of the transport distance concept (adapted from Tabler 1975a)

2.1.2. Snow movement

Snow transport along the ground surface, also called snowdrift, occurs when snow particles in the layer of snow deposited on the ground are re-entrained by the wind. Surface snow particles previously deposited on the ground are entrained into the air when the wind speed is greater than about 12 mph which is equivalent to 5 m/s (Tabler et al., 1990; Kathleen 2009, and Mellor, 1965). There are three types of snow movement: creep, saltation, and turbulent diffusion. An illustration of the movements is schematically illustrated in Figure 3. The type of movement is determined by both particle size (typical ranges from infinitely small to 5 mm/0.2 inch).

The creep or rolling apply to the largest snow particles moving along the surface as snow sheets/dunes that migrate downwind. Approximately 25% of the total snow transported at low

wind speeds is transported by this mechanism (Tabler, 2003). Smaller particles move by the process of saltation where particles temporarily are entrained into the air and redeposited on the surface. Most of saltation particles are contained within 5cm (2 inches) from the surface. (Tabler 2003) The smallest snow particles are carried by the wind due to turbulent diffusion. A snow particle becomes suspended in the airstream because the gravitational force on the particle is less than lift force from the upward-moving air. In this mode of motion, the particles of snow are suspended in the air and do not typically make contact with the ground. As the suspended particles become smaller due to the evaporation, they tend to be carried higher above the surface. Pomeroy (1989, 1990) indicated that most snow carried by turbulent diffusion remains within about three feet of the ground, and most snow moves by turbulent diffusion.

Most of the snow transport along the ground surface occurs when snow particles in the layer of snow deposited on the ground are re-entrained by the wind. Surface snow particles previously deposited on the ground are entrained into the air when the wind speed is greater than about 5 m/s or 12 mph (Ohara, 2014). Although some snow particle can be found thousands of meters above the surface, most of the total suspended particle mass is within 1m above the surface (Pomeroy 1988, 1989). Therefore, Tabler suggests that snow transport above 5 meters (16 feet) can be ignored for drifting snow control (Tabler 2003). The goal of a snow capturing device is therefore to minimize the amount of drifted snow of all the above-described transport processes.

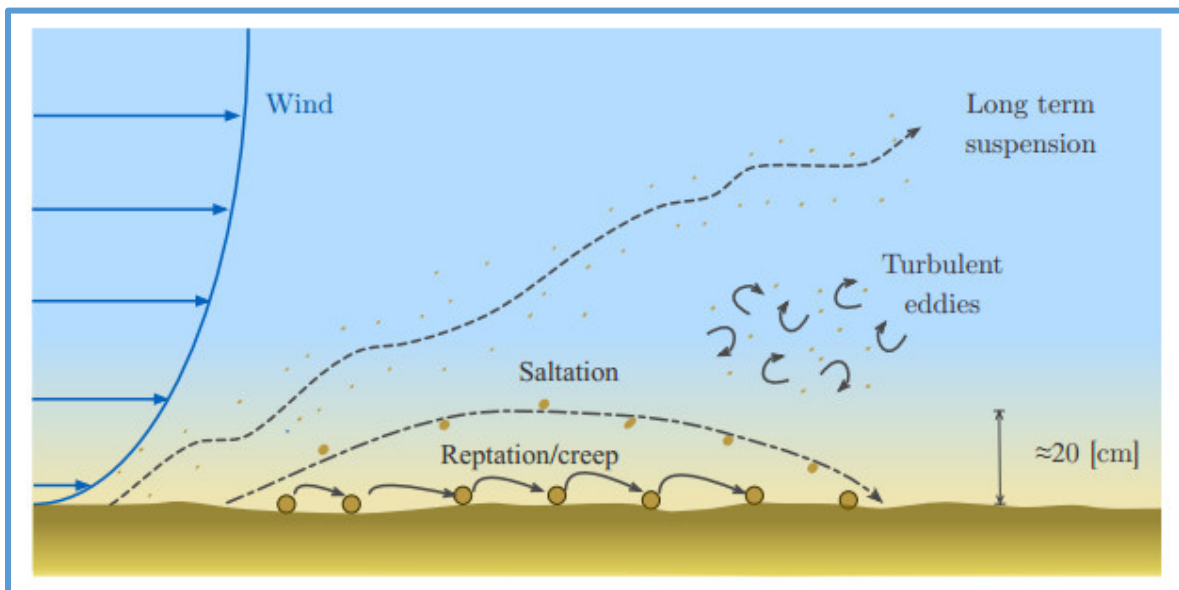


Figure 3 Diagram of snow movement (from Giudice 2019).

2.1.3. Snow transport and evaporative losses

In order to devise an effective mitigation strategy for snowdrifts, the amount of snow that is transported by wind needs to be quantified. Snow transport can be measured directly using instruments such as snow traps. However, such measurements are time consuming, might interfere with the transport process and are very difficult to obtain. With the advent of non-intrusive techniques, the quantification of snow transport has gained accuracy. An alternative approach for characterizing snow transport is using empirical models based on measurements of snow

accumulations around natural or man-made obstacles located in the wind fetch. Figure 4 shows a schematic for amount of snow that is transported due to wind and deposited behind a snow fence.

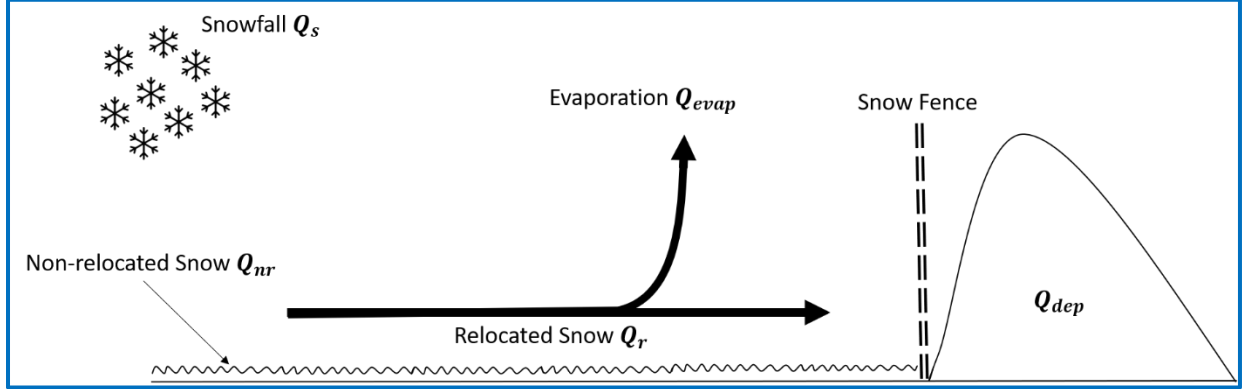


Figure 4 Schematic of snow transport in the presence of a snow fence.

In Figure 4, Q_s denotes the mass of snowfall, Q_r is the mass of relocated snow due to wind, and Q_{nr} is the mass of snow that remains on the ground after snow transport is completed by wind. The relation among these quantities is as follows:

$$Q_s = Q_r + Q_{nr} \quad (2)$$

Snow particles that are being transported by wind are subject to sublimation while airborne. Therefore, a fraction of relocated snow is lost to evaporation and sublimation before it reaches the snow fence. The mass of snow that is deposited at the snow fence is given by:

$$Q_{dep} = Q_r - Q_{evap} \quad (3)$$

Tabler (1991) argues that the wind speed at which snow particles are separated from the surface and start to move depend on condition of snow and air density. In general, it is assumed that the snow transport occurs when wind speed exceeds 5 m s^{-1} (11 mph). Furthermore, Tabler (1991) proposes that the majority of snow transport takes place within 5 m (16 feet) above ground, and the snow transport beyond this layer is negligible. The amount of snow transport that happens within 5 m (16 feet) above ground can be quantified as follows:

$$Q_{0-5} = \begin{cases} \frac{U_{10}^{3.8}}{233847} & U_{10} \geq 5 \\ 0 & U_{10} < 5 \end{cases} \quad (4)$$

where Q_{0-5} is the snow transport that happens up to 5 m (16 feet) above ground in kg s^{-1} per unit width across the wind, and U_{10} is wind speed in m s^{-1} at height of 10 m (33 feet). From this point forward, Q_{0-5} is replaced by Q for brevity. Wind speed is typically measured at 10 m (33 feet) above the ground. However, if wind speed records are from a height different than 10 m (33 feet), power law profile can be assumed for wind speed to find value of wind speed at this height:

$$\frac{U_z}{U_{10}} = \left(\frac{z}{10}\right)^{1/7} \quad (5)$$

where z is the height at which wind speed is measured.

Tabler (1993) argues that Equation (4), derived for sites with an infinitely long fetch area, needs to be modified for shorter fetch. The correction for shorter fetch length is given by:

$$Q_{cor} = Q (1 - 0.14^{F/L}) \quad (6)$$

where Q is the snow transport for a site with infinitely long fetch area given by Equation (4), Q_{cor} is the snow transport for a site with finite fetch, F is fetch length, and L is equal to 3 km (1.9 miles). Equation (6) represents the mass of snow that is blown away by wind and becomes airborne. However, some of it is lost due to sublimation before it can be deposited downstream the fence. Airborne particles of snow can only travel a finite distance before they disappear due to sublimation and the distance of travel depends on various factors including relative humidity, temperature, wind speed, solar radiation, etc. Tabler (2003) provides a relationship for estimation for mass of snow that is lost due to sublimation as a function of fetch length (see Figure 5).

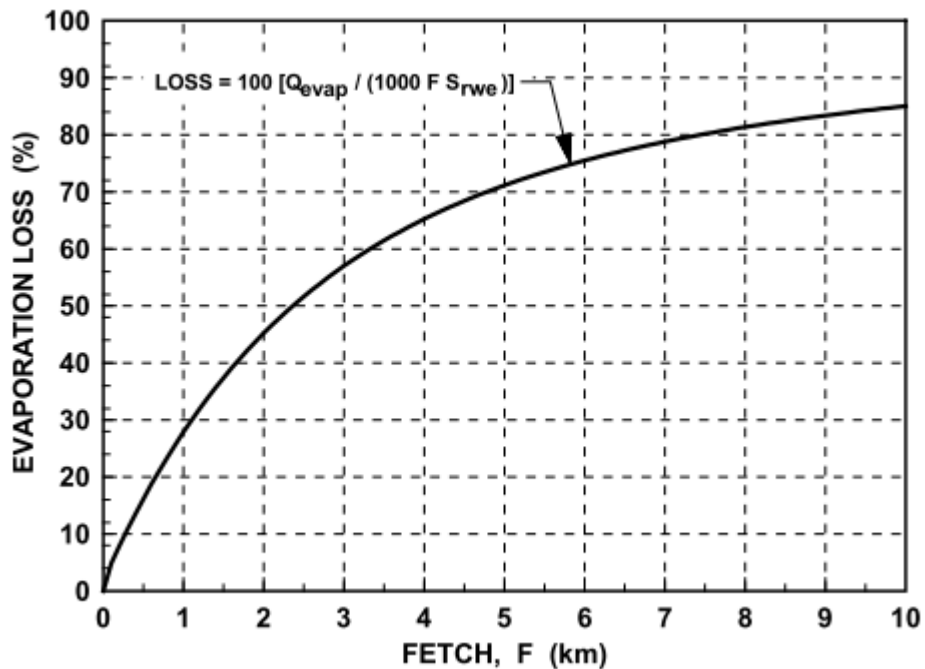


Figure 5 Estimation of loss of snow transport due to evaporation (from Tabler 2003).

2.1.4. Estimation of SRC

Snow relocation coefficient (SRC) represents the ratio of transported snow to available snow in the fetch area. When a fence is located in the fetch area, an acceptable definition for the SRC is provided by the ratio of snow actually deposited at the fence and the amount of snow that would be deposited at the fence if all the snowfall in the fetch area was transported by wind. For a site with constant fetch length, the mass of snow deposit at the fence can be estimated by:

$$Q_{dep} = Q (1 - L_{evap})(1 - 0.14^{F/L}) \quad (7)$$

$$L_{evap} = 1 - (1 - e^{-2F/L})L/2F \quad (8)$$

where L_{evap} is the evaporation loss coefficient, plotted in Figure 5. For a site characterized by different fetch lengths for different wind directions, Haehnel (2019) proposes integrating Equation (7) over different wind directions. Defining a snow transport event as a period of time when snow is actively transported by wind, the amount of snow deposited behind the fence, at the end of the event is given by:

$$Q_{dep} = \Delta t \sum_{i=1}^n Q_i (1 - L_{evap}(\theta_i))(1 - 0.14^{F(\theta_i)/L}) \quad (9)$$

where Δt is the time interval between two consecutive measurements of wind speed, and $L_{evap}(\theta)$ and $F(\theta)$ denote evaporation loss coefficient and fetch length corresponding to different wind directions, respectively. In order to find the snow relocation coefficient, the potential total amount of snow that can be deposited due to wind during the event is calculated as:

$$Q_{spot} = F S_{we}(1 - L_{evap}) \quad (10)$$

where Q_{spot} is the total mass of snow that can be deposited if all of the fallen snow were blown away by the wind, L_{evap} is the evaporation loss coefficient calculated based on predominant wind direction during the event and S_{we} is snowfall water equivalent. If the density of fallen snow is known, snowfall water equivalent is:

$$S_{we} = \frac{snowfall\ depth \times \rho_s}{\rho_w} \quad (11)$$

where ρ_s is the density of fallen snow, $\rho_w = 1000\ kg\ m^{-3}$ is the density of water. However, if the density of fallen snow is not known, S_{we} is approximated assuming the density snow is a tenth of density of water as follows (Tabler 2003):

$$S_{we} = (snowfall\ depth)/10 \quad (12)$$

After calculating the actual amount and the potential amount of snow deposit at the fence, the snow relocation coefficient for the event is represented as follows:

$$\theta = \frac{Q_{dep}}{Q_{spot}} \quad (13)$$

In this study, two different approaches are considered for characterizing SRC of snow transport events: a theoretical approach based on Equations (7) – (13) and an observational approach based on the measurement of the snow deposited behind a snow fence (as subsequently described in section 3).

2.2. Considerations on snow fences

The most often-used drifting-snow prevention measure has been, and continues to be, the deployment of snow fences; they can either be constructed at the site or set in the form of living fences (e.g., shrubs, trees, or local grasses) planted along the road. For constructed snow fences, the typical materials used to build the fence include wood, metal rails, plastic nets, polymer rails

and woven fabric. Fence materials are attached to supporting structures (e.g., posts) made of steel or wood or to truss-type, custom-designed frames set in the ground. Living fences are increasingly used as alternatives to constructed snow fences as they are beneficial not only for protecting the road against snow drifting and accumulation (Nixon et al. 2003), but also for providing important ecological and esthetical benefits.

2.2.1. Structural fences

Snow fences are generally installed perpendicular to the prevailing wind direction and along the roadway. Snow particles are prone to deposit on the snow fence's downwind side, where the wind velocity magnitude is small. The amount of snow that a fence can retain on its downwind side is mainly a function of the fence porosity and the bottom gap's size. Several studies (e.g., Seginer, 1972; Heisler and Dewalle, 1988; Dong et al., 2007 and 2010) have shown that the fence porosity (Figure 7) is the main parameter determining the degree of velocity reduction and turbulence amplification induced in the wake of long fences (i.e., fences whose length is much larger than their height). The turbulent velocity field's characteristics behind the fence control how much snow will deposit and over what distance significant snow deposition will occur (Sañudo-Fontaned et al., 2011).

The bottom gap is the open space between the porous fence's ground and bottom (Figure 6). The role of the bottom gap is to reduce snow accumulation near the fence. The ratio between the height of the bottom gap, G , and the total fence height, H , is a crucial design parameter controlling the total snow trapping capacity of the fence (Tabler, 2003). Constantinescu and Muste (2015) evaluated the role of the fence porosity and gap size for several combinations of these parameters at fences deployed in Iowa.

2.2.2. Living fences

There is a plethora of studies that reports the effectiveness of living snow fences in improving the road safety and reducing snow drifting and blowing (e.g., Tabler, 1993, Nixon, 2003, Blanken, 2009). Distinction must be made between permanent living snow fences (e.g. stands of trees) and temporary or seasonal living snow fences (rows of standing corn left unharvested in the fall). Popular selections for living snow fences are trees and shrubs, wildflowers, and rows of corn. Like the structural fence, the living snow fence causes blowing snow to accumulate in the upwind and down area of the fence. In contrast with structural alternative, the living fence's upwind side captures more blowing snow than a structural fence. Besides the benefit of retaining snow, living snow fences bring eco-friendly outcomes. First, the environmental pollution caused by ongoing traffic and maintenance vehicles on the road can be reduced by the presence of living fences that can store and sequester carbon from atmosphere (Wyatt et al., 2012). Furthermore, they can work as stronghold against soil erosion and provide room for wildlife habitat and micro-organisms (Shaw, 1989).

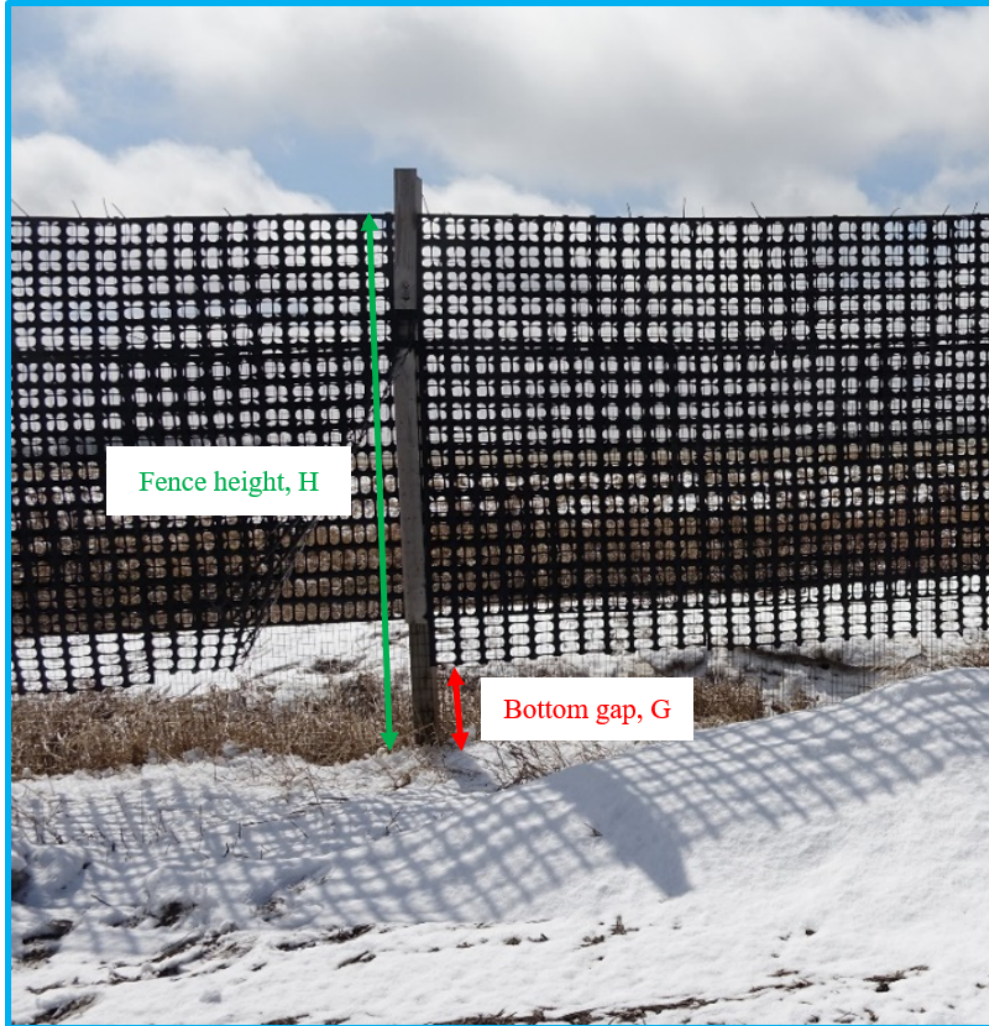


Figure 6. Structural fence located on US-20, Williams, Iowa, U.S.



Figure 7. Overlapping wire and plastic meshes to attain prescribed fence porosity at the US-20 test site (Constantinescu and Muste, 2015).

Tabler (2003) study investigates both permanent and temporary living snow fences. He indicates that the set-back from the road should be at least 35 times the height required for a structural fence at the given location for both sorts of fences. In particular, he notes that standard practice in Minnesota requires a set-back of at least 46 m (150 feet) from the right of way and that a set-back of 30 m (100 feet) proved too close. Other studies suggest smaller set back distances. For example, the Japanese study (HDB, 1996) recommends set-back distance of only 7.5m for forested width of 50 meters. Figure 8 illustrates a typical living snow fence along I-35 investigated in the present study. The fence is set-back at 18 meters (Figure 8) and entails tall brushes 5-m high and 6 meter thick (see Figure 9).

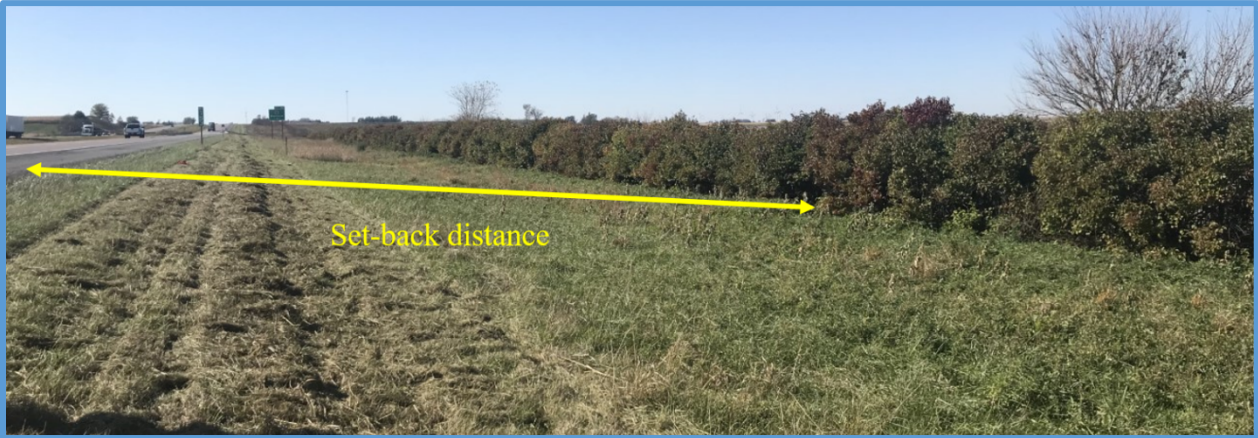


Figure 8. Living fence locates on I-35, Iowa. The set-back from right of way is 18 meters (59 feet).

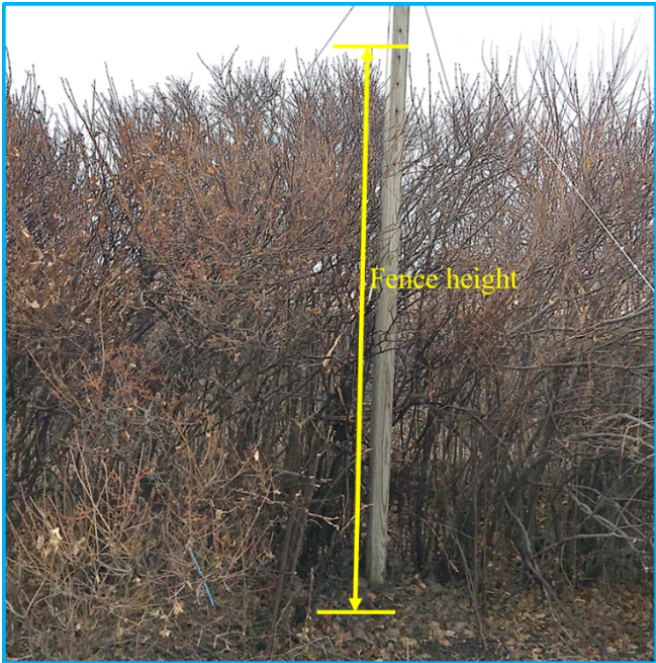


Figure 9. Details on the living fence illustrated in Figure 8.

2.2.3. Design considerations

Irrespective of their type, the design of snow fences is based on a set of local or regional weather conditions estimated over long-term and by taking into consideration the topography of the site. In general, the design of snow fences entails the following steps as outlined by Kaneko et al. (2012):

- 1) Site characterization (i.e., collection of meteorological and snowdrift information on past snowstorms) and selection of a route based on local conditions
- 2) Site survey and analysis (i.e., collection of additional topographic and meteorological information, quantification of the snow drift features at the site)
- 3) Establishment of the orientation, geometry and specifications for the snow fence structural characteristics (i.e., overall geometry, materials and fence porosity)
Evaluation of the snow fence performance (i.e., survey of all aspects of the operational performance from retention efficiency to maintenance costs)

The design of snow fences requires sound engineering judgment regarding two key aspects: a) evaluating the potential for snow blowing and drifting at the site (Step 2 in the design process) and b) providing specifications regarding the snow-fence orientation and construction details commensurate with the estimation obtained through activity a) above (Step 3 in the design process). The layout and dimensions of the fence are determined using formulations related to the annual quantities of drifting snow expected at the site, the roadway alignment, the surrounding terrain features, and the desired efficiency.

3. Experimental approach & implementation details

3.1. Experimental sites

3.1.1. Site selection criteria and experimental design

The ideal experimental sites for this site are locations in open-field areas where snow drifting occur regularly. These sites are typically known to road maintenance personnel in IDOT and engineers in the Iowa's counties due the long-term maintenance issues encountered repeatedly over years. For most of these sites, the road maintenance services are installing mitigation devices such as permanent (structural or vegetation-made curtains) or temporary (structural or standing-crop rows) fences. In selecting the experimental sites for the present studies, we favored sites that had permanent fences in place and, where they were not available, we deployed temporary fences using lightweight plastic snow fences available commercially. This preference is motivated by the fact that fences act as obstacles in the snow drift path where the amounts of snow retained by the fence are easily related to the snow drifted process.

The selection of the sites for this study was made after consulting with engineer representatives and in close collaboration with the project Technical Advisory Committee (TAC). An additional important selection criterion in selecting the sites for the study was that the fence alignment to be perpendicular to the dominant wind direction over most of the winter season. Fulfillment of the last criteria ensure that the snow fence captures the snow drift along the most effective direction of action (i.e., normal to the fence) and also is likely to develop a two-dimensional shape for the snow deposits both upwind and downwind the fence. The last criteria is also narrowing the possibilities for the experiment to be influenced by additional complexities (e.g., secondary

currents in the fence wake, departure of the experimental conditions from the assumptions in the empirical relationships for estimation of SRC).

Following these consultations, the sites selected for investigation during the 2018-19 were: a secondary road in Shueyville (close to US-218, near Cedar Rapids) and a fenced portion of US-20 near Williams (close to the intersection with I-35). Following the analysis of the 2018-19 winter field campaign results, the project team in consultation with TAC have maintained the US-20 site and added a new site on I-35 near Dows to create a pair of sites that captures practically the same meteorological conditions acting on different types of snow fences of similar geometry. Specifically, the US-20 fence is structural, while the I-35 is a mature living snow fence. The practically co-located sites near Williams allow to not only test and compare alternative fence types but also to cross-reference results. Maintenance of the US-20 site for measurements in both project years allow to test the reproducibility of the experiment facility arrangement and ancillary measurement protocols and extending the series of observations over two years for validation purposes. For both investigation years, the sites were observed continuously between mid-November to mid-March. The locations of the two sites along with the seasonal wind roses for each site are illustrated in Figure 10.

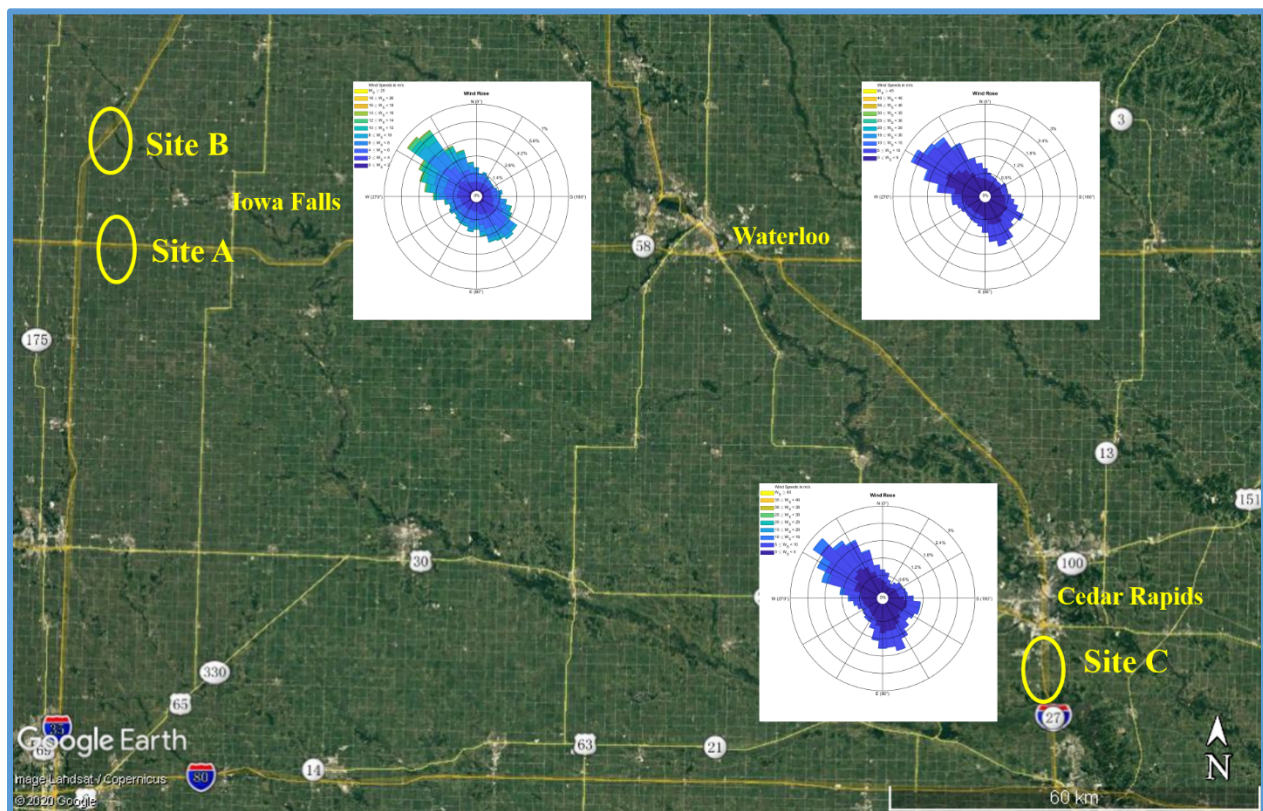


Figure 10. Experimental sites investigated in the study: Site A, structural permanent fence on US-20 near Williams. Site B, living snow fence on I-35 near Dows. Site C, structural temporary fence in Shueyville (image source: Google).

The experimental arrangements at the study sites were based on the familiarity of our team with multiple aspects of snow drifting in Iowa and the progress in investigating it with previous studies

(Constantinescu and Muste, 2015; Tsai et al., 2017). For example, the wind information illustrated in Figure 10 confirm a general trend of the winds over Iowa. i.e., dominant with directions from NW direction with frequent changes of the wind direction from the opposite direction. The data collected during the present two-winter study also concur with the general wind patterns. The fences at the three sites are, non-coincidentally, perpendicular to the dominant wind directions and are known for systematic exposure to snow drifting. Based on this knowledge, the local observations around the fence were concentrated on an area aligned with the NE to SE direction. The experimental facility at the sites were similar and they employed basically the same data acquisition instrumentation and protocols. The components of the experimental facilities include (see also Figures 11, 12 and 13):

- a) **Multiple marker poles** set at short distances apart along a direction perpendicular to the fence (practically along the NW to SE direction). The role of these markers is to capture the development of the upwind and downwind snow deposits created by the fence. The distance of the marker pole transect upwind from the fence was based on observations from prior studies (Constantinescu and Muste, 2015). Downwind from the fence, the marker poles covered the entire width of the right of way (ROW).
- b) **Web-cameras systems** were set at locations with good visibility of the snow fence transect. In the second project year the webcams were backed up with up to three additional cameras. At least one web-camera was equipped with real-time communication capabilities for continuous event monitoring, while all the cameras stored the acquired images.
- c) **Multi-sensor towers** for recording the at-the-site meteorological conditions were deployed at each site.
- d) **Snow-fall measurement installations** were designed for each site to capture locally this important study variable during the first project year. Sheltered areas surrounded by trees and bushes were selected for snowfall measurement deployment at each site. However, these sheltered sites were not sufficient to protect the measurements from the effect of drifting snow. Given the change in criteria of selection of the site in the second project year, a unique central location for the two investigated sites was identified where the sheltering effect was ensured. The second-year installation setup was considerably improved providing high-quality, unbiased and traceable snowfall data. Additional snowfall sensors were installed at the US-20 (in 2018-19) and I-35 sites (in 2019-20).
- e) **Fetch-length tracers** were installed at about 500-yards apart over long distances to substantiate the snow depth within the fetch area and to capture additional information about the dominant wind direction at each site on an event basis. Views of the fetch tracer areas at US-20 and Shueyville sites are shown in Figure 14.



Figure 11. Study area on a secondary road in Shueyville (image source: Google).

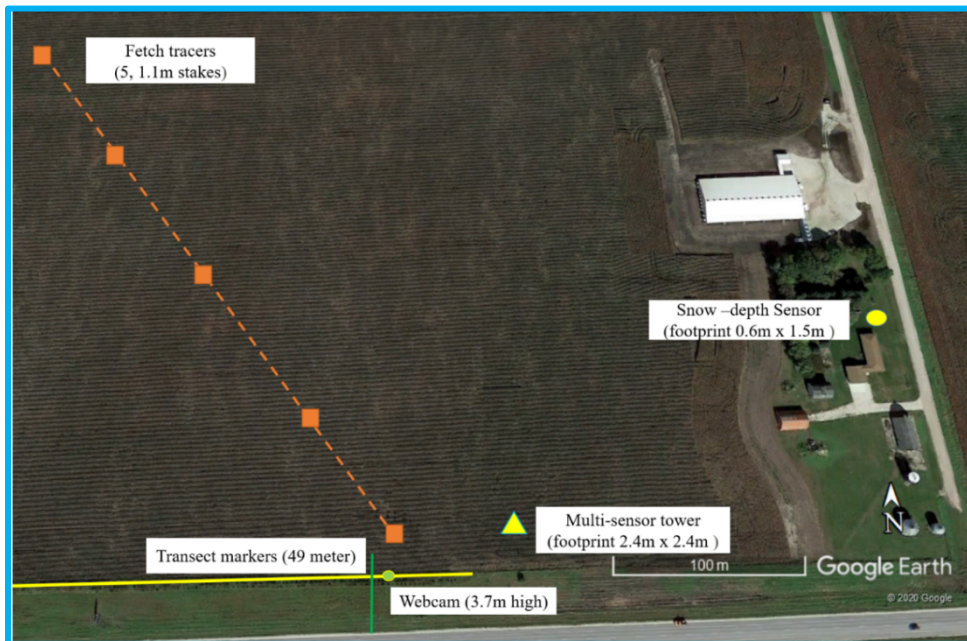


Figure 12. Study area on US-20, near Williams (image source: Google).

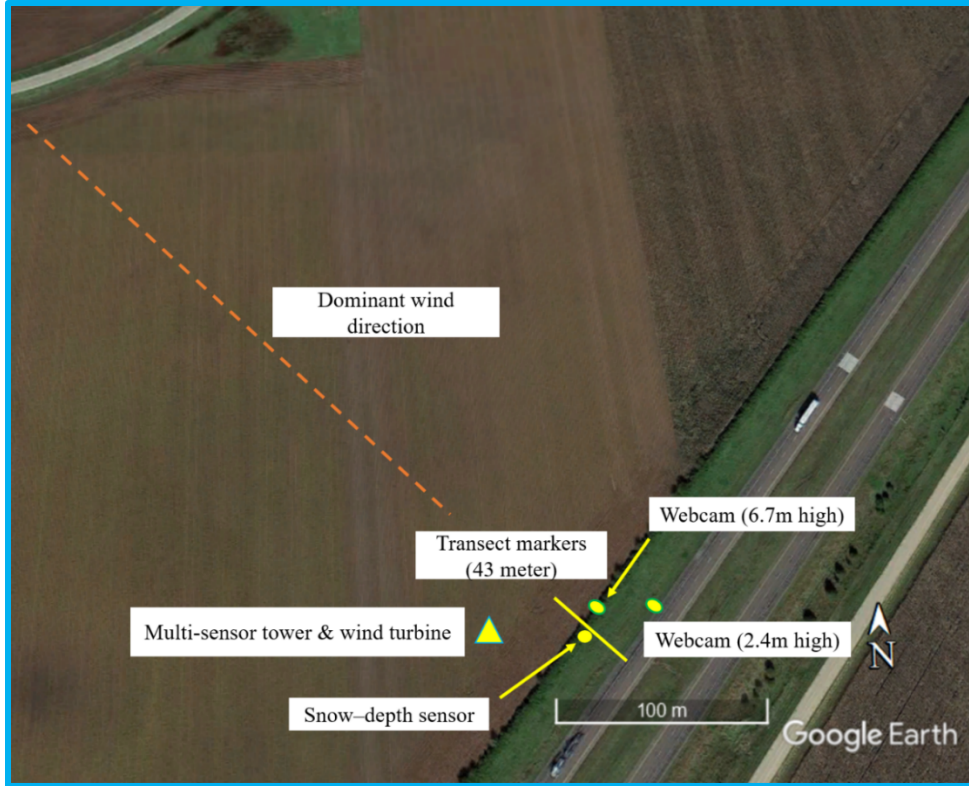


Figure 13. Study area on I-35 near Dows (image source: Google).



(a)



(b)

Figure 14. Fetch tracers installed along the dominant wind direction (i.e., fetch area): a) at US-20 site, b) at Shueyville site.

3.1.2. Description of experimental arrangements

Shueyville site

Shueyville site is located within the city limits at 32 kilometers (20 miles) distance from Iowa City and 16 kilometers (10 miles) south of Cedar Rapids just off I-380. The experimental site is located on a private property (Shueyville United Methodist Church) whose owners agreed to host our experiments. This site was used in the 2018-2019 winter to test all the measurement protocols listed above and, due to its close proximity to the Univ. of Iowa, for testing various proof-of-concept modifications to various components of the observation system. The dominant wind direction during the observation period (from November to March) was steadily from NW with fewer abrupt changes in wind direction than at the other sites. A 24-meter long snow fence made of lightweight plastic material was installed along the SW to NE direction, practically perpendicular to the dominant wind direction (see Figure 15a). Five fetch tracers were installed along the dominant wind direction on the owner property. The web-camera was installed at the SW side of the snow fence, facing NE, as shown in Figure 15a. The site was equipped with a multi-sensor meteorological observation tower and a snow-fall measurement sensor located as shown in Figure 15a.

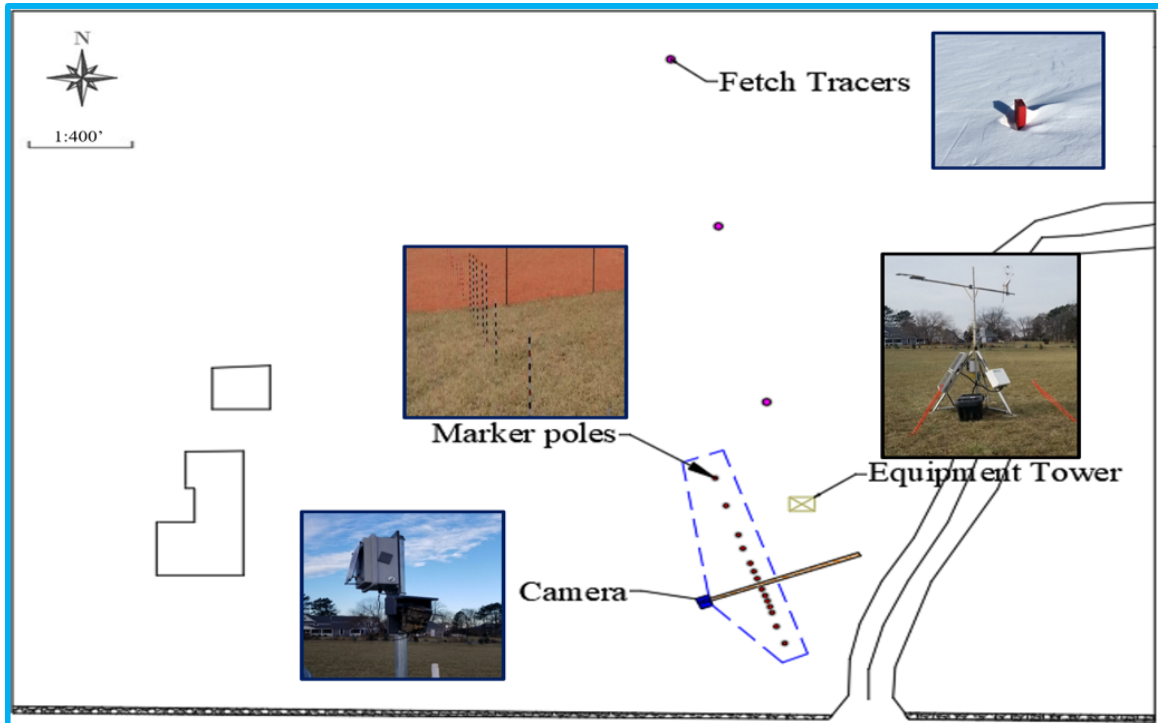
The range of spacing between marker poles was ranging from 0.9 to 6 meters commensurate with the expected shape of the snow deposits from previous observations (Tsai et al, 2017). Since most of the drifting snow was accumulated on the downwind side of the fence, the marker poles were denser in this area compared with the upwind side. Given that the peak of snow deposit was at about 4.5 meters (15 feet) from the fence, the marker poles deployed around this distance were slightly higher. The spacing and distribution of the marker poles along the observational transect are schematically shown in Figure 15b.

US-20 & I-35 Sites

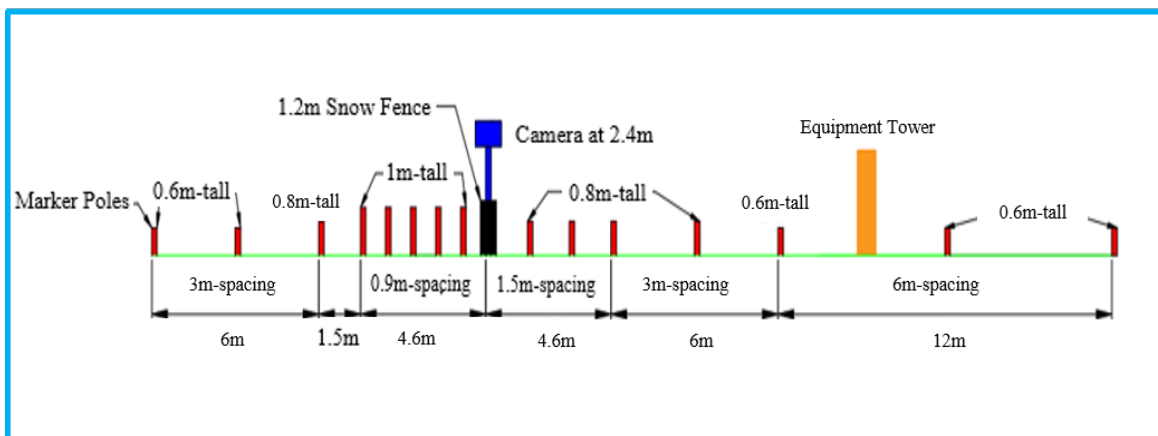
The US-20 and I-35 sites are at located at 241 kilometers (150 miles) and 267 kilometers (166 miles) from Iowa City, respectively. The US-20 site was used for measurement in both project years while the site on I-35 was included in the observation program in 2019-20 winter. The dominant wind direction at both sites over the period of observation (November to March) was from NW. Given the similarity of the geometrical dimensions (with the most important parameter being the fence height) and of the fence porosity for the two alternative types of fences as well as their close proximity, the expectation was for the development of snow deposits of similar shape and magnitude. Consequently, the height of the maker poles at these sites ranged from 0.9 (3 feet) and 6 meters (20 feet). The spacing between the marker poles was gradually changed for the two upwind and downwind sides of the fence to enable capturing of the snow deposit shape with adequate resolution. The markers poles set on the upwind side were generally shorter than on the downwind side due to lesser amount of drifting snow accumulated in this area.

The structural fence of the US-20 is relatively well aligned with in the ES direction. A 49-meters (161 feet) long transect was set perpendicular to the snow fence to establish an observational grid for snow depth measurements of the deposited snow in the fence vicinity. The main production web-camera was installed on one of the poles of the snow fence at a height of 14 meters (45 feet), on the West side of the marker pole line. This position was set to offer a good view of the whole marker pole transect and appropriate image resolution for distinguishing the graduation on all the

marker poles. During the 2019-2020 winter, two more camera unites were installed at the US-20 site for back-up in case of power or camera failures. The cameras' view were oriented toward the marker pole transects. One was located on the East side of the snow fence covering the upwind marker poles. Another web-camera was installed at 2.7 meters (9 feet) on a metallic pole, close to the road for covering the downwind marker poles for the same reasons (see Figure 16a). This camera covered a portion of the road for additional information on the road conditions, especially to observe snow drifting impacts.



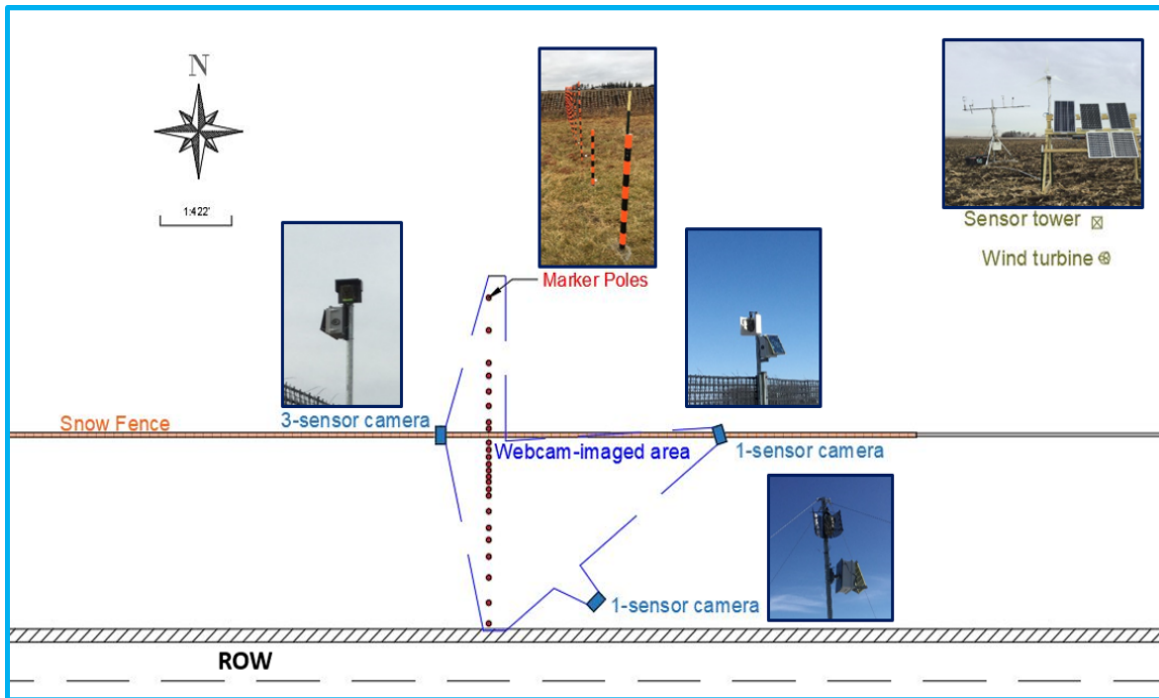
(a)



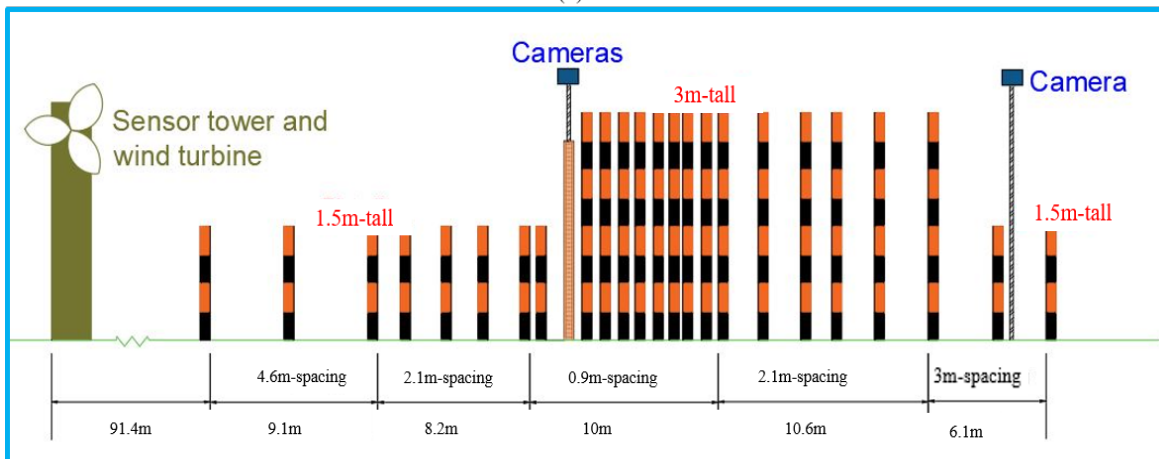
(b)

Figure 15. Site arrangement at the Shueyville site during the 2018-19 field campaign: a) Plan view b) Side view.

The multi-sensor tower and wind turbine was at the 91 meters (300 feet) NE from the marker pole transect in the upwind fence area such that the wake of the wind blowing over the tower platform as a whole did not interfere with the formation of the snow deposits in the test section (see Figure 16a). During the 2018-2019 winter, the range of spacing between marker poles was slightly larger than in the subsequent year, ranging from 2 m (7 feet) to 6 meters (20 feet). Based on that winter observation of the snow deposition patterns, the marker poles spacing within the peak area of the snow deposit was decreased during the 2019-20 field campaign to 0.9 meters (3 feet) as shown in Figure 16b.



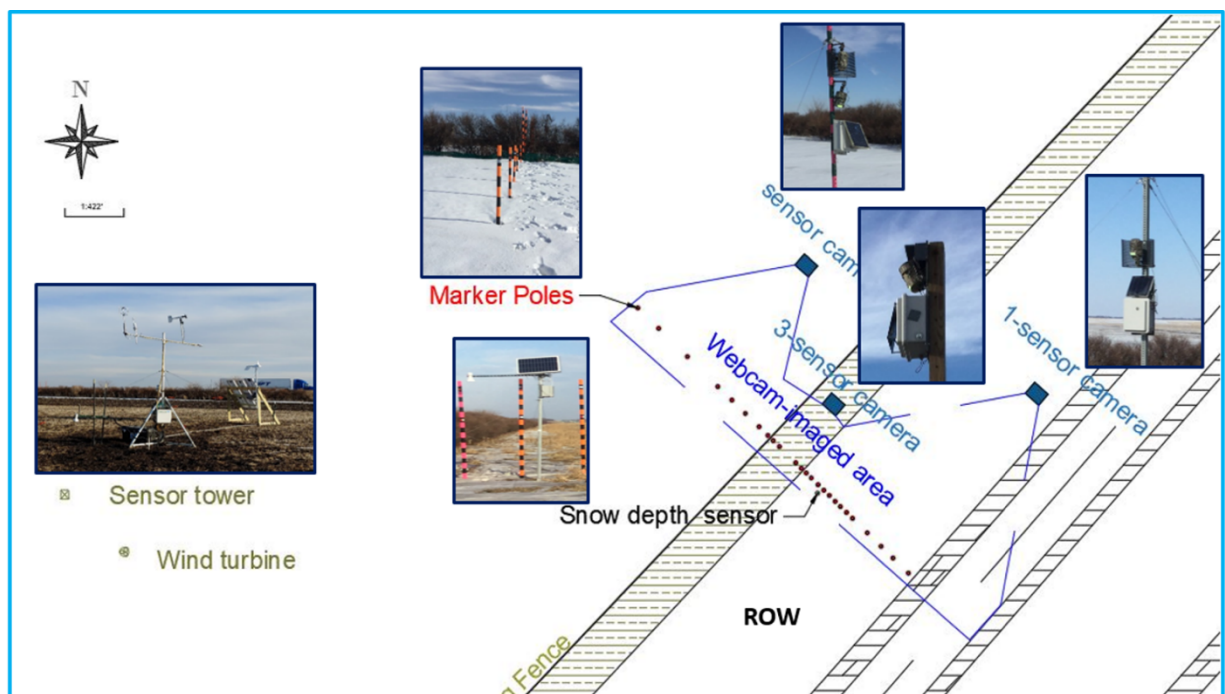
(a)



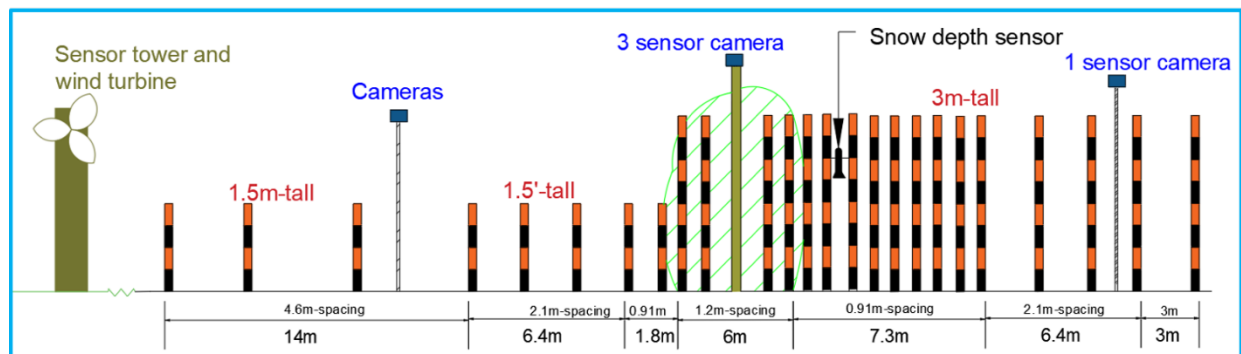
(b)

Figure 16. Site arrangement at the US-20 site deployment during the 2019-20 field campaign: a) Plan view b) Side view.

The overall experimental arrangement for the living fence site on I-35 used in the field campaign of 2019-20 winter is shown in Figure 17. The multi-sensor tower and ancillary turbine were set upwind toward NE at the 91 meters (300 feet) from the marker pole transect (Figure 17a). The site was equipped with one main webcam set atop of the median of the living fence on a 6-meter (20 feet) wood post. Three additional webcams were installed at the site for backup in case of equipment failures and for acquiring redundant image. Two webcams were located downwind next to the road and one in the upwind area all of them facing the marker poles in the respective areas. The 3-meter (10 feet) tall marker poles were densely packed at 0.9 meter (3 feet) to accurately capture the shape of the downwind snow deposit (see Figure 17). The spacing for the remaining poles was set commensurate with the expected shape of the snow deposit as informed by visual information collected during the 2018-19 field campaign. The overall arrangement of the marker poles is provided in Figure 17b.



(a)



(b)

Figure 17. Arrangement at the I-35 site during the 2019-20 field campaign: a) Plan view b) Side view.

3.2. Experimental instrumentation and data acquisition methods

The experimental protocols developed for this study were tailored to address the study objectives listed in Section 1.3. In order to attain the final goal of the study, i.e., estimation of the Snow Relocation Coefficient (SRC), a set of instruments and a suite of customized measurement protocols were set in place to locally estimate:

- snowfall
- volume of snow that is relocated
- the volume of the snow trapped by fence
- how much compaction/melting appears from a day to another and from event to event
- documentation of the at-the site meteorological conditions
- snow density

The above listed estimations have to be made with high spatial and temporal resolution as the storm drifting events unfold. This in turn require to document the snow drifting periods by tracking the development of changes of the snow deposition geometry (extent, shape, orientation) from the initial conditions accounting for the changes in temperature, wind characteristics (magnitude, direction, rates of change) and of the initial deposit conditions with a sampling frequency commensurate with the lifetime of the event. The instruments presented in this section are grouped around the measurement protocols that they pertain to continuous and synoptic monitoring methods.

Selection of the appropriate measurement protocols for quantifying snow drifting events is a challenging task as the observational methods in this area are still under development. Most of the conventional methods (e.g., total station surveys, graduated stakes, and direct snow depth measurements) are outdated and require physical presence in the field during harsh meteorological conditions. During this, as well as through previous studies, we gradually developed our own set of protocols that are currently providing an adequate experimental package to confidently address the estimation aspects listed above. The package includes continuous, unassisted measurements complemented by synoptic measurements acquired through in situ-measurements. The latter type of measurement is needed to verify and improve the continuous method protocols and for verification and validation purposes. The synoptic measurements were typically acquired during or just after the substantial storm events.

3.2.1. Continuous monitoring

3.2.1.1 Web Cameras

The continuous monitoring entailed two sets of observations. The first consisted of a real-time observing system aimed to determine if snow deposition accumulated during storms was significant enough to visit the site and conduct measurements of the snow profiles in situ. For this purpose, Web-camera units were strategically installed at the sites to continue acquire images during the winter field campaigns. Each webcam unit entailed a photo camera with videorecording capabilities, an energy supply component, and a camera protection system. We used two types of web-cameras, i.e., Moultrie P-180i camera (see Figure 18), and Moultrie X-7000i cellular trail

cameras (see Figure 19). The cameras were supplied with power from a battery located inside the housing box that was continuously charged with a solar panel.

The Moultrie P-180i was the optimum choice for the main camera as it assembles internally images from three independent sensors to produce a panoramic image (see Figure 20). This capability plays a critical role in observing the snow accumulation along the whole transect during snowstorms using just one imaging unit. The Moultrie X-7000i cellular trail single-sensor webcams were installed as backup for situations when the main camera was off or encountered recording difficulties due to adverse weather (e.g., blowing snow, extremely low temperatures) or internal failures. Their smaller field of view was focused on the most active areas for snow deposition, both upwind and downwind the fence (see Figure 21). Webcam images were stored on an internal drive and also communicated in real-time via cellular network as thumbnails on a dedicated website (see Figure 20). The availability of the images in real time allows efficient remote monitoring of the experimental site and helpful information for planning of the synoptic measurements field visits. The two-way communication allowed to modify the camera settings (time-lapse, duration of the operation over day, frequency for uploading the images in the camera server) and to observe operational parameters (battery charge level, communication status, temperature and pressure at the location). The cameras were set to record one image per hour for non-event situations and at every 15 minutes during storm event duration. Given that the blowing snow led to camera lens coverage during the high-wind storms, several configurations for protective curtain around the camera sensors were tested during the duration of the study (See Figures 18 and 19).

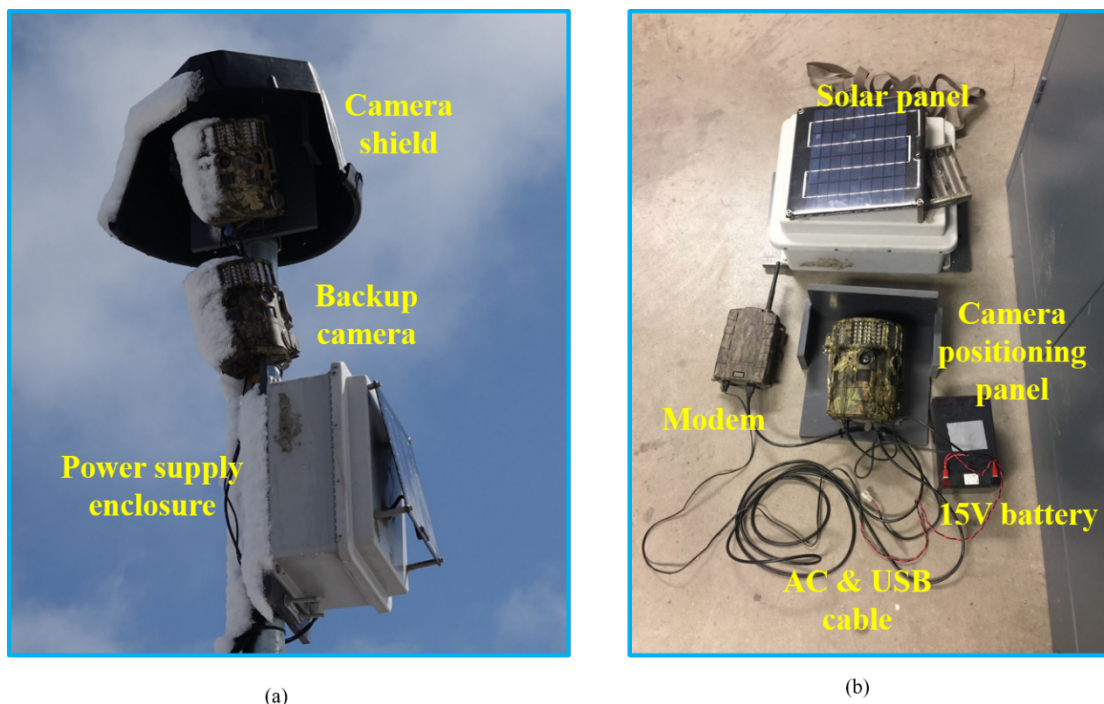


Figure 18. P-180i Web-Camera unit at US-20 site during the Winter 2018-19 deployment: a) overall view including the snow protection shield: b) components of the web-camera unit.

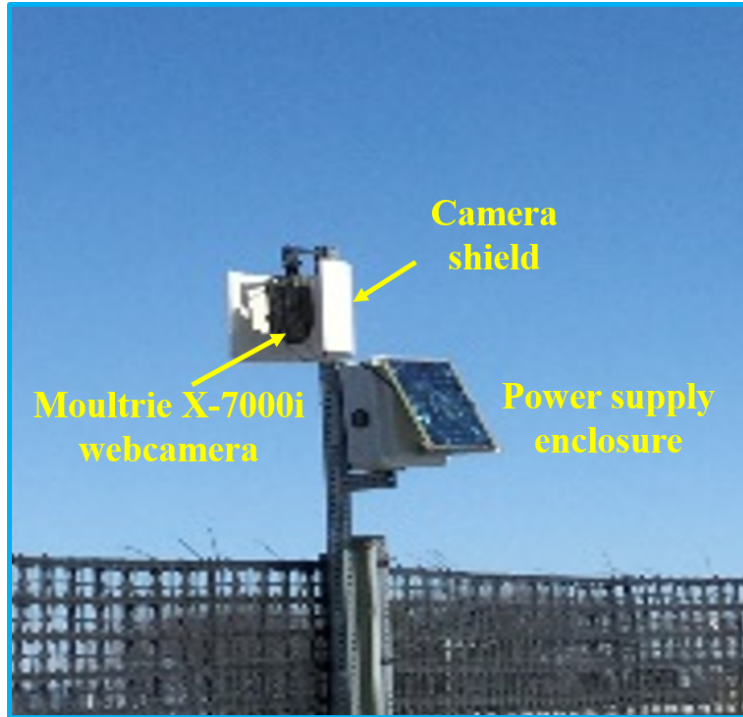


Figure 19. Moultrie X-7000i camera unit deployed at the US-20 site.

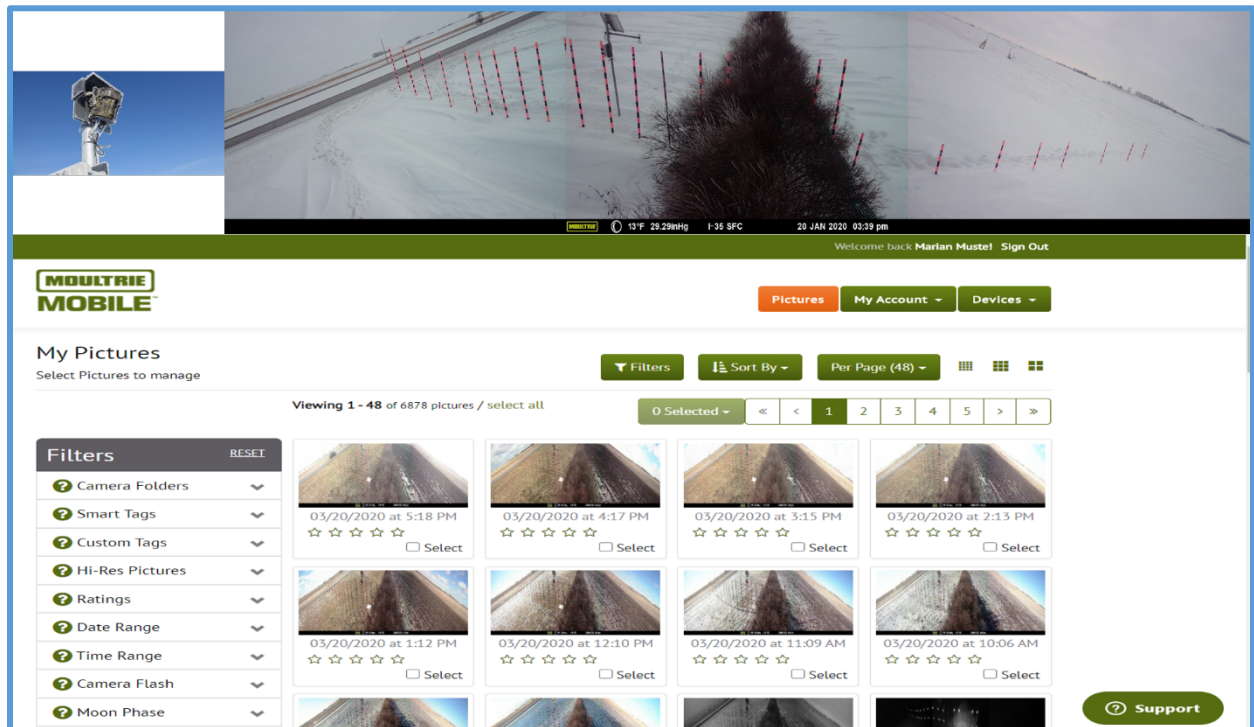


Figure 20. Images recorded by the Moultrie P-180i camera as posted on the real-time Moultrie website: <https://www.moultriemobile.com/images>.



Figure 21 imagines from the two Moultrie X-7000i cellular trail cameras.

3.2.1.2 Multi-sensor meteorological towers (met towers)

For local characterization of the local meteorological conditions, two met towers were deployed to the sites of both fences near Williams. The sensors on the met tower were designed to measure two types of measurements.

- High resolution (10 Hz) measurement of wind speed by a sonic anemometer, and concentration of H₂O/CO₂ by an infrared gas analyzer.
- Low resolution (1 minute) measurement of wind speed, wind direction, temperature, relative humidity, pressure, and radiation by a radiometer.

The towers were powered by solar panels, and a 24 V battery setup. The predominant wind direction at the site is from NW, therefore, the booms of the towers were oriented in this direction, while solar panels were facing south for maximizing sunshine exposure. During the 2018-2019 campaign, the met tower at the US-20 site, was also instrumented by an ultrasonic snow depth sensor (moved to the I-35 site during the 2019-2020 campaign), but strong winds and snowdrifts made it hard to interpret its data. A schematic of the met tower deployed to the US-20 site during the 2018-2019 campaign is shown in Figure 22. This tower was moved to the I-35 site during the 2019-2020 campaign.

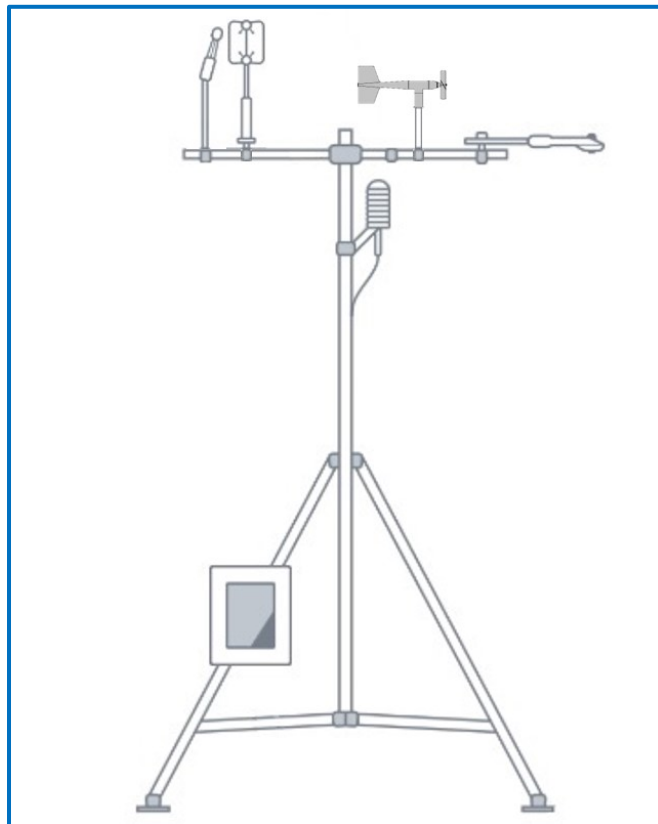


Figure 22. Schematic of the met tower deployed to the study experimental sites (source: <https://www.licor.com>)

A detailed list of the sensors on the tower is provided in Table 1, and Figure 23 shows the tower in the field at US-20 site during the 2018-2019 campaign. This tower was later moved to the I-35 site during the 2019-2020 campaign.

Table 1 List of sensors on the met tower at the US-20 site during the 2018-2019 campaign.

Sensor	Make/Model	Resolution
Sonic Anemometer	Gill - WindMaster Pro	10 Hz
Gas Analyzer	LICOR - LI 7500-RS	10 Hz
T/RH Sensor	Vaisala - HMP 155	1/60 Hz
Pressure Sensor	LICOR	1/60 Hz
Radiometer	Kipp&Zonen - CNR4	1/60 Hz
Wind Speed/Direction	RM Young - Wind Monitor	1/60 Hz
Ultrasonic Snow Depth	Senix - Toughsonic	1/60 Hz

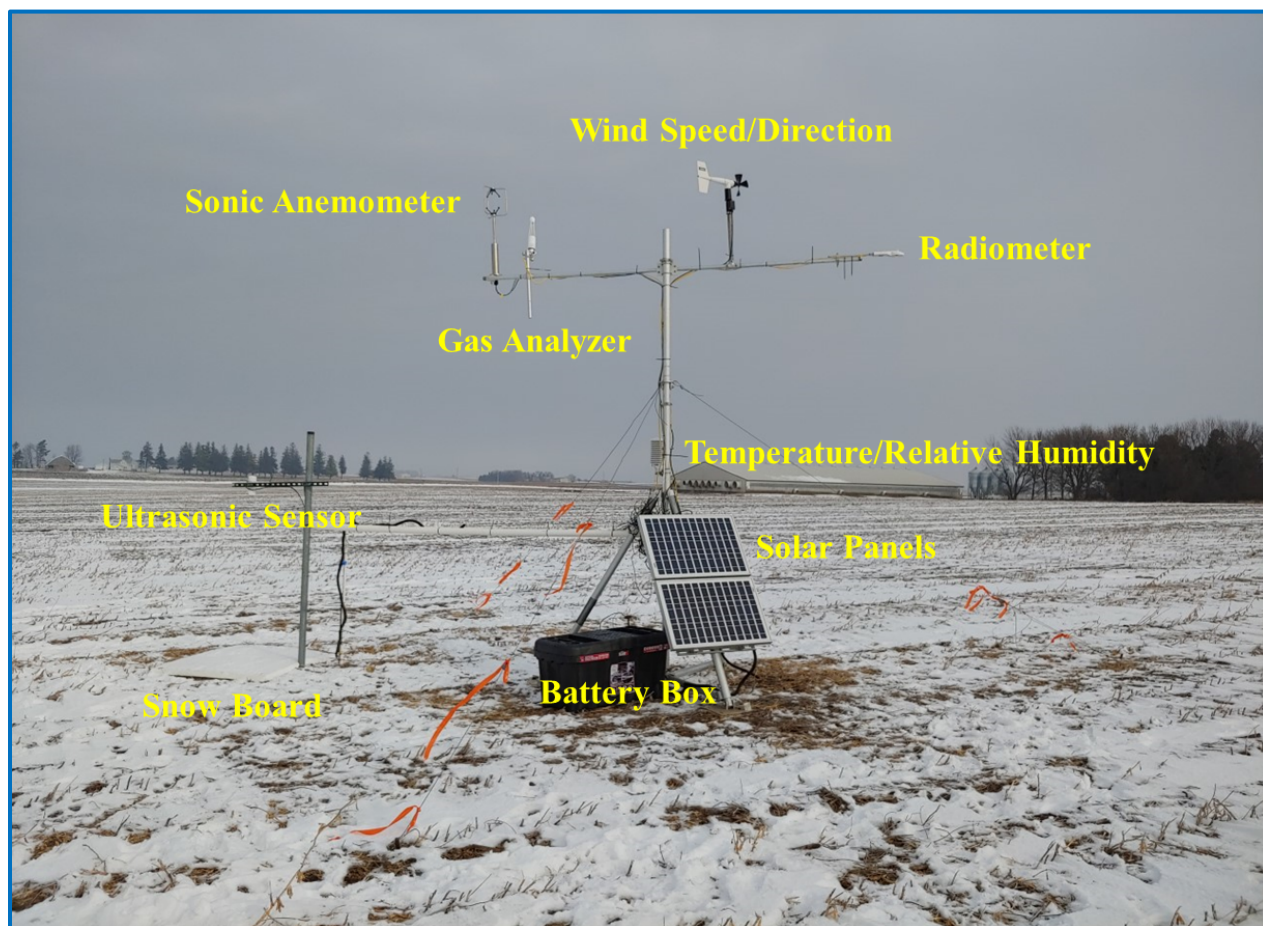


Figure 23. Image of the met tower deployed to US-20 site during the 2018-2019 campaign.

During the 2018-2019 campaign, the met towers experienced several periods of power shortage, due to prolonged cloudy days at the sites. Therefore, during the 2019-2020 campaign, a wind

turbine as well as extra solar panels were added to both towers, in order to minimize periods of power shortage. The wind turbine would provide power during cloudy days when solar panels did not provide any power, and extra solar panels would decrease the time needed for batteries to recharge during sunny days. The wind turbine and the solar panels were mounted on a separate structure as shown in Figure 24.

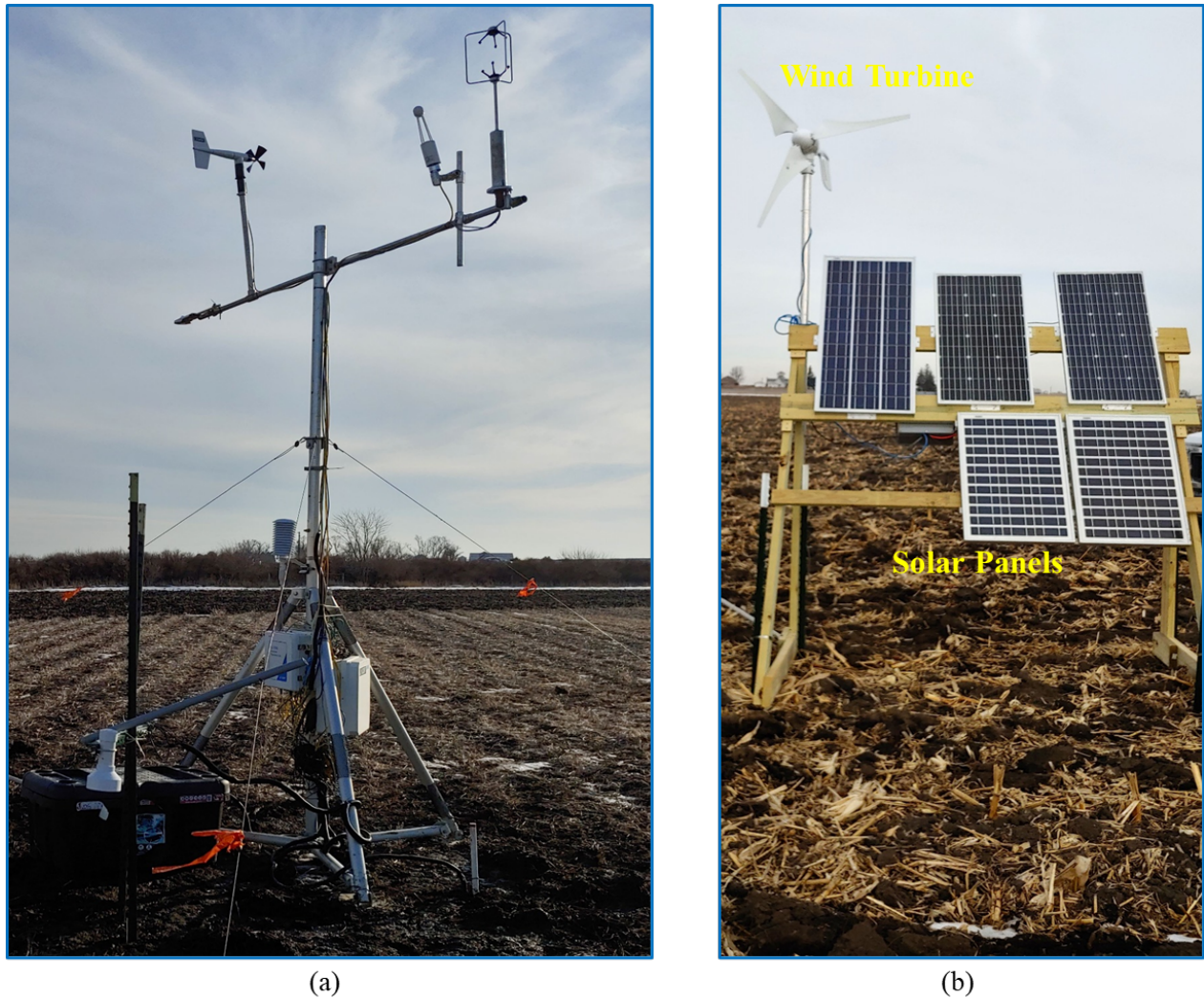


Figure 24. The met tower installation for the I-35 site during the 2019-20 winter campaign: a) overall view; b) wind turbine and multiple solar panels installed on a separate structure in the vicinity of the tower.

The tower deployed to Shueyville site during the 2018-2019 campaign and subsequently moved to the US-20 site during the 2019-2020 campaign has a slightly different set of sensors. A detailed list of the sensors on this tower is provided in Table 2, and Figure 25 shows the tower in the field at the US-20 site during the 2019-2020 campaign. Similar to the I-35 site, a separate structure for wind turbine and solar panels was added to US-20 site during the 2019-2020 campaign.

Table 2 List of sensors on the met tower at the US-20 site during the 2019-2020 campaign.

Sensor	Make/Model	Resolution
Sonic Anemometer	Gill - WindMaster Pro	10 Hz
Gas Analyzer	LICOR - LI 7500-RS	10 Hz
T/RH Sensor	Vaisala - HMP 155	1/60 Hz
Pressure Sensor	LICOR	1/60 Hz
Radiometer	Kipp&Zonen - CNR4	1/60 Hz
Cup Anemometer	A100LK	1/60 Hz
Wind Vane	NRG 200P	1/60 Hz

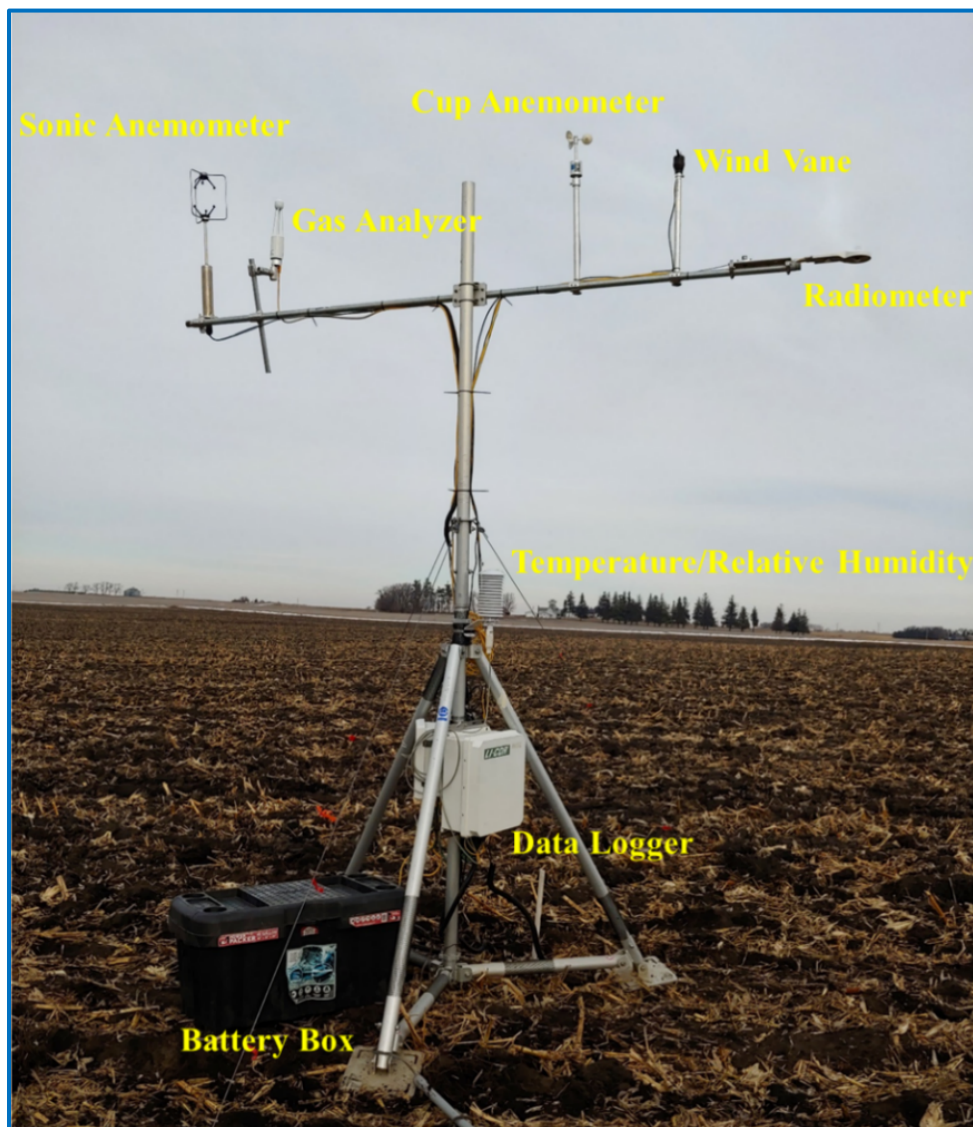


Figure 25. The met tower deployed to the US-20 site during the 2019-2020 campaign.

3.2.1.3 Sensors for local snowfall measurements

Ultrasonic snow depth sensors were deployed to the sites of study, to locally measure snowfall. Comparisons of the local measurements was made with snowfall records from COCORAHS and COOP stations. The TOUGHSONIC ultrasonic sensors (Senix) selected for this study are typically used for detecting objects and measuring distance. The ultrasonic transducer emits an acoustic wave, which is reflected upon hitting a surface or an object such as snow surface, and time it takes for the wave to travel to the surface and travel back to the sensor determines the distance. During the 2018-2019 campaign, the ultrasonic sensor at the Williams site was placed in an area sheltered by trees near the US-20 site, as shown in Figure 26. The presence of evergreen trees on North and West sides of the house suggested that the ultrasonic sensor would be protected from snowdrift. However, results from the 2018-2019 campaign showed significant snowdrift into the effective reading area of the sensor, rendering its data unusable. Therefore, during the 2019-2020 campaign the ultrasonic sensor was moved to a nursery which was enclosed by several rows of tall trees, shown in Figure 26.

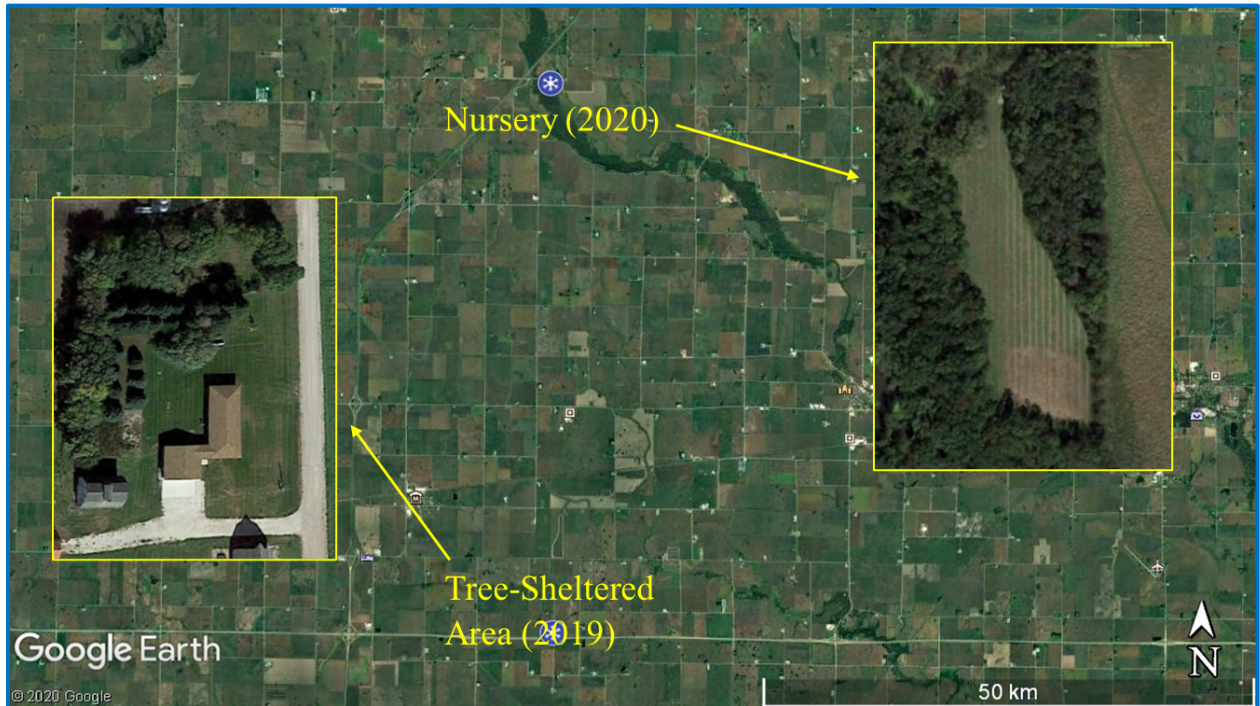
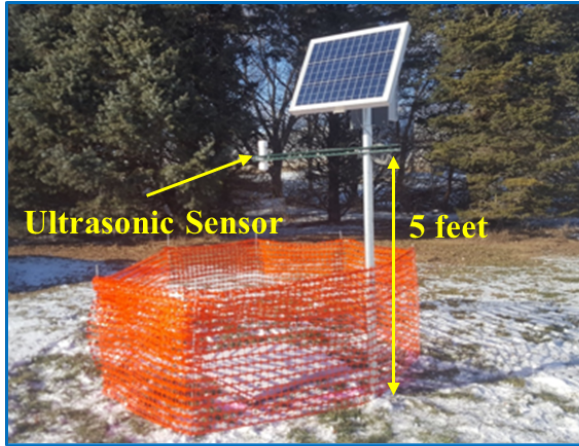
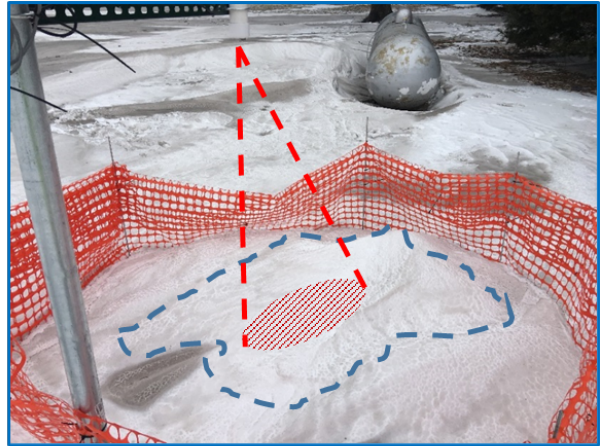


Figure 26. Locations of ultrasonic snow depth sensors during the 2018-2019 and the 2019-2020 campaigns near Williams sites (image source: Google).

Figure 27a shows the ultrasonic sensor at the tree-sheltered area during the 2018-2019 campaign following one of the storm events. It can be seen that the tree curtain did not prevent snowdrift into the sensor measuring area, which resulted in a non-homogeneous snow pile under the sensor footprint, shown in Figure 27b. The non-flat surface of the snow pile does not uniformly reflect the acoustic waves back to the sensor and reading from the sensor were inaccurate during the 2018-2019 campaign.



(a)



(b)

Figure 27. Ultrasonic snow depth sensor located in a tree-sheltered area during the 2018-2019 winter campaign: a) Ultrasonic snow depth sensor assembly; b) visualization of the snowdrift into the measurement area that causes sensor readings to be inaccurate.

Similar deployment considerations were used for setting the ultrasonic sensor for the Shueyville experimental site during the 2018-19 field campaign. This experimental arrangement led to similar problems as for the US-20 site, as illustrated in Figure 28. However, this site was better protected from wind therefore the snow pile under this sensor was more homogeneous than the one at the Williams site. Figure 28b shows that the effect of snowdrift on the snow pile was barely noticeable.



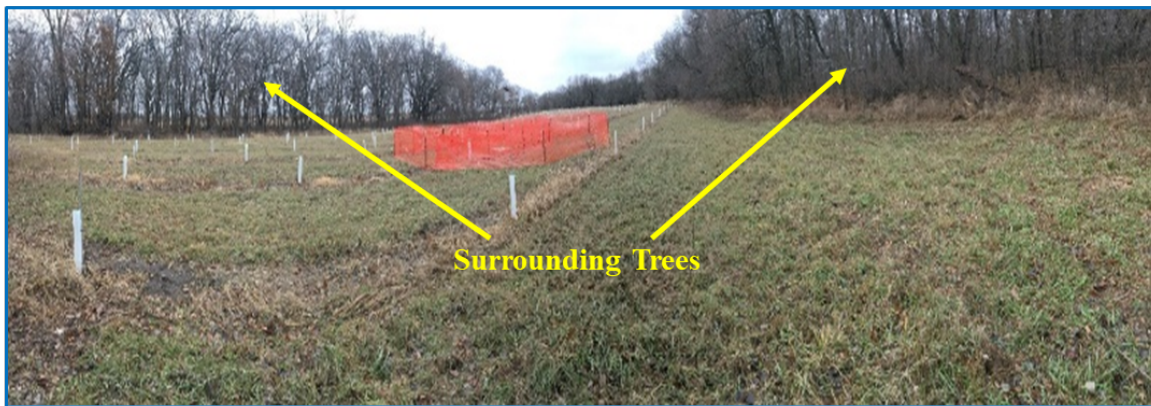
(a)



(b)

Figure 28. Ultrasonic snow depth sensor deployed at the Shueyville site (2018-2019 winter): a) Ultrasonic snow depth sensor powered by a solar panel; b) the snow pile at this location is less developed than the one within the protected area for the sensor deployed at Williams for the same storm event (see Figure 27b).

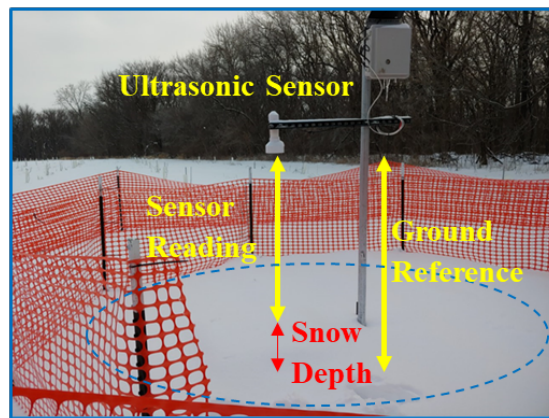
In order to minimize the effect of snowdrifts on snow the depth sensor measurements, a new location was chosen for measurement of snowfall during the 2019-2020 campaign. The new location was a nursery surrounded by a thick curtain of tall trees. Figure 29 shows the overall view and details for the ultrasonic sensor deployment at the nursery. The tall trees surrounding the nursery effectively protected the ultrasonic sensor during snowdrifts. In addition to the protection offered by the curtain trees, two layers of snow fences were placed around the sensor to further prevent snowdrift within the sensor reading area (Figure 29b). The ultrasonic sensor was placed at a height of 1.5 meters (5 feet), hence the reading from the sensor represents the distance between the sensor and snow pile, as illustrated in Figure 29c. Therefore, the difference between the height of the sensor from the bare ground (measured accurately after probe deployment) and the sensor's reading represents the depth of the snow pile. The snowdrift mitigation measures applied for the Williams sites in the winter of 2019-2020 worked well, resulting in practically undisturbed measurement area under the sensor and, implicitly, more accurate readings from this sensor.



(a)



(b)



(c)

Figure 29. Ultrasonic snow depth sensor installed for the 2019-2020 winter field campaign: a) overall view of the nursery where the ultrasonic was deployed, including the tree curtain surrounding the nursery; b) Double-fence arrangement to prevent snowdrift into the effective sensor measurement area; c) Close-up view of the ultrasonic sensor. The dashed blue line shows the snow pile under the sensor which is very homogeneous at this site.

3.2.2. Synoptic monitoring

3.2.2.1 Tape measurement of the snow depth

The simplest and most accurate method for determining the snow depth at an observation point consisted in direct distance measurement at each location. Each point measurement entailed direct reading of the distance between the snow surface and the tip of the marker poles using a tape (see Figure 22). Given that the total length of the marker pole was known from measurements taken at the time of the poles deployment, the snow depth at each marker pole's location was obtained using the on-the-site reading (L_s) and the known pole length (L_m):

$$\text{Snow Depth} = L_m - L_s \quad (14)$$

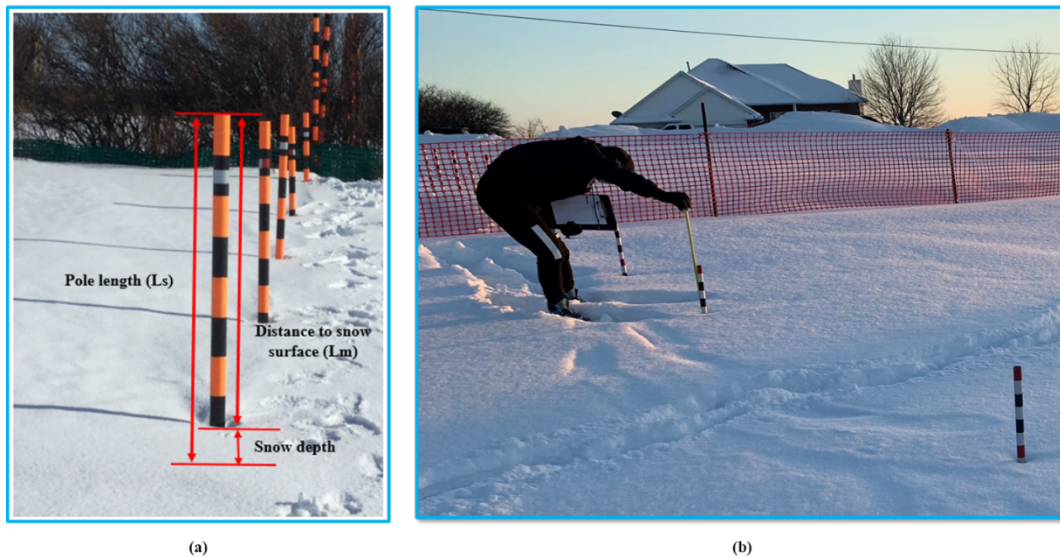


Figure 30. Measurement of the snow depth with tapes: a) marker poles; b) at-the-location measurement.

3.2.2.2 Real-time kinematic survey

Real-time kinematic (RTK) satellite navigation is a surveying technique used for geo-referencing the locations of fixed points on the ground. RTK is a GPS-based positioning system capable of recording the real-time horizontal and vertical elevation of $[x,y,z]$ coordinates. During surveys, RTK is consecutively placed on the top of each reference points to get the final reading. The instrumentation uses the wavelength of the signal to connect to the satellite to obtain accurate coordinates. The RTK accuracy has continued to improve over time such that today the RTK accuracy for locating a survey point is sub-centimeter in the horizontal plane and of the order of few centimeters in the vertical direction.

RTK surveys of various points of interest at the experimental sites were conducted before the first snow event to obtain the bare-ground profile along with marker poles at each of the experimental sites and references for the measurements with the snow depth sensors. During winter season, RTK surveys were conducted after the end of significant snow events to obtain the elevation of the snow cover at the each marker pole's location. In order to reduce the measurement uncertainty, a protective surface (labeled as "snow shoe" in Figure 23) was set lightly on the snow free surface

to disperse the weight to the instrument on the snow surface while the satellite data was received and recorded. Each new RTK survey was referenced with the bare-ground initial surveys of the site to obtain the depth of the snow at each point of interest. Only few RTK measurements were recorded as the instrument does not properly operated in low temperature conditions due to battery failure.



Figure 31. RTK survey conducted at the marker poles located at Shueyville site. The “snow shoe” consists of a $35 \times 20 \times 9.5 \text{ cm}$ ($14 \times 8 \times 4 \text{ in}$) cardboard box.

3.2.2.3 Drone survey

Drone surveys were used extensively by our team in prior studies in order to acquire photogrammetric surveys of the snow deposits developing ad snow drifting sites. The full measurement protocols for photogrammetric surveys using drones is well described by our paper and will be not repeated here (see Tsai et al., 2017 for details). Extensive efforts were made through the previous experiments to determine the best measurement strategy to measure over snow surfaces as they are difficult to be traced by this technique (Basnet et al., 2015).

Using the previous findings as a base, the mapping of the snow deposits in the vicinity of the fences was done by acquiring multiple images from various angles with an unmanned aerial vehicle (UAV) DJI Inspire 1. The camera was attached underneath and was pointing straight down toward the region to be imaged, as illustrated in Figure 24. Given that the drone’s global positioning system does not allow to accurately geotagging the drone position while in flight, a set of ground

reference points were used to complement the photogrammetric processing. For this purpose, twelve ground reference points were temporarily marked with paint on the snow cover in the area of interest and then surveyed by Real Time Kinematic (RTK), as indicated in Figure 24, for post processing. The drone was flew at high altitude first to enclose all the Ground Reference Points in one photo frame. Subsequently, lower altitude flights on smaller spots within the area of interest were repeatedly imaged from various angles. The processing of the acquired images was made with the customized photogrammetric software Agisoft PhototScan.

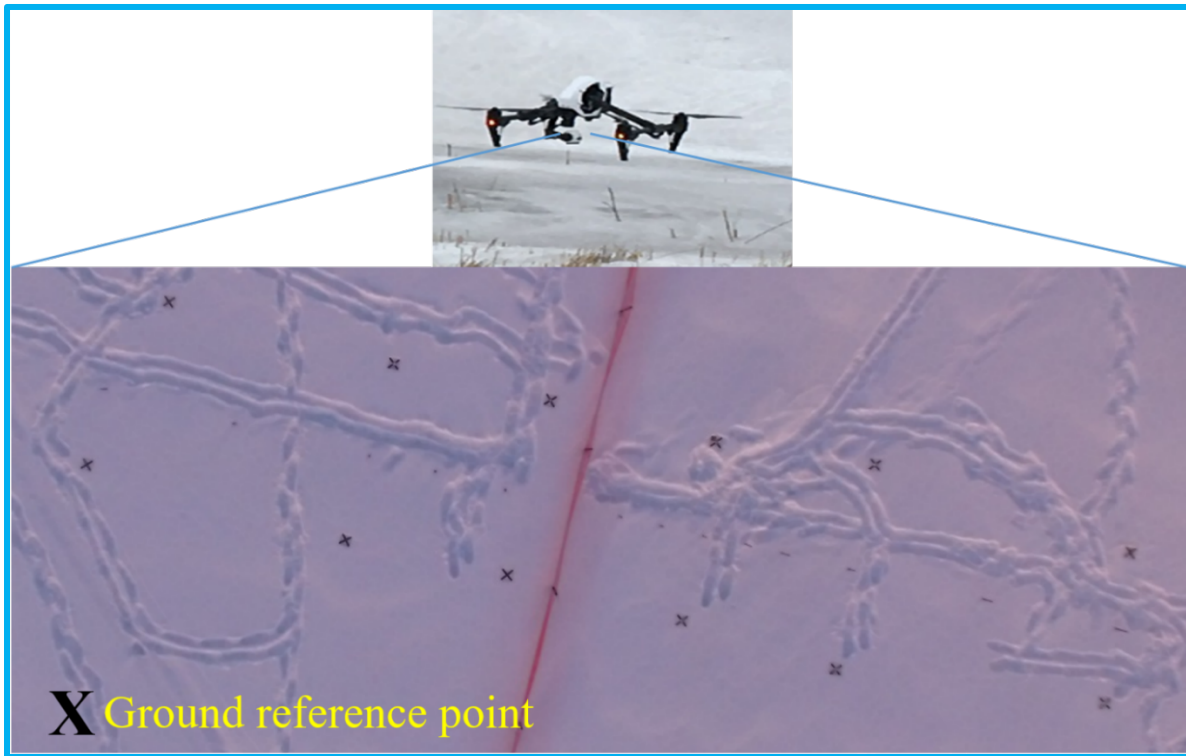


Figure 32 Drone survey executed at the Shueyville site.

3.2.2.4 Mapping/tracing of drifted snow trapped by fences

Measurements of the changes of the snow deposits during and between snowstorms have used various combinations of instruments and methods, commensurate with the time available for acquisition of the measurements at the site. Each storm event was unique in terms of triggering conditions and the amount of time spent for the measurement varied with the event magnitude. Moreover, each site visit involved at times fixings of the installations, therefore the time available for the synoptic measurements vary widely. Repeated measurements of the elevation of the snow surface along the marker pole transects proved that the tape and RTK were the most reliable methods. The agreement between these alternative measurements have been shown in Figure 25 and are reiterated by the plots provided in Figure 33. The actual estimation of the snow profile cross section followed the protocols described in Sections 3.2.2.1 and 3.2.2.2.

The subsequent analysis for estimation of the SRC used as basis the vertical cross section measured as described above. The assumption of this analysis is that the snow deposits are characterized by a strong two-dimensional feature, i.e., there is not variation of the snow deposit shape along its

length. For the structural snow fences, this assumption is well supported both by the multiple site visits after storm events as well as the photogrammetric surveys acquired with the drone during some of these trips. Sample of drone surveys are shown in Figure 34, whereby the two-dimensionality of the deposits in the upwind and downwind areas around the fence is evident.

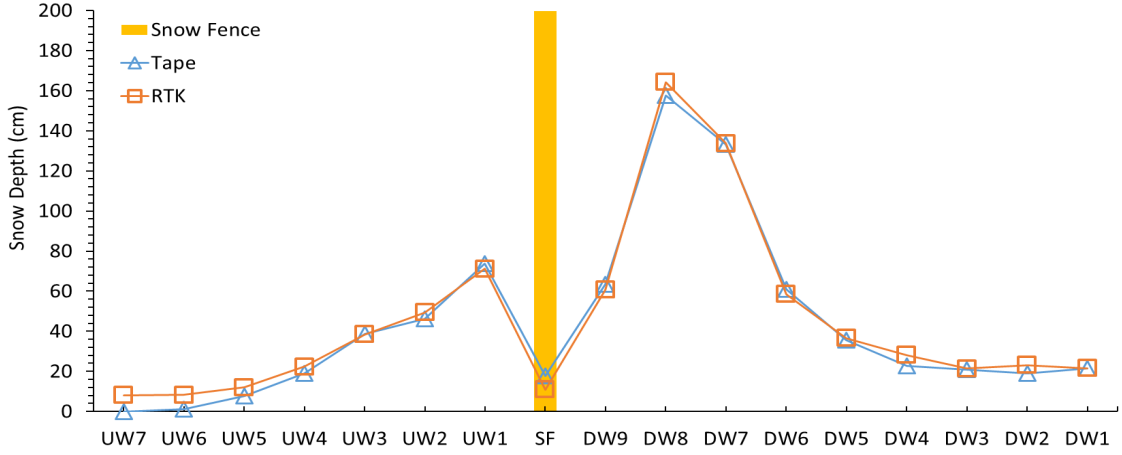
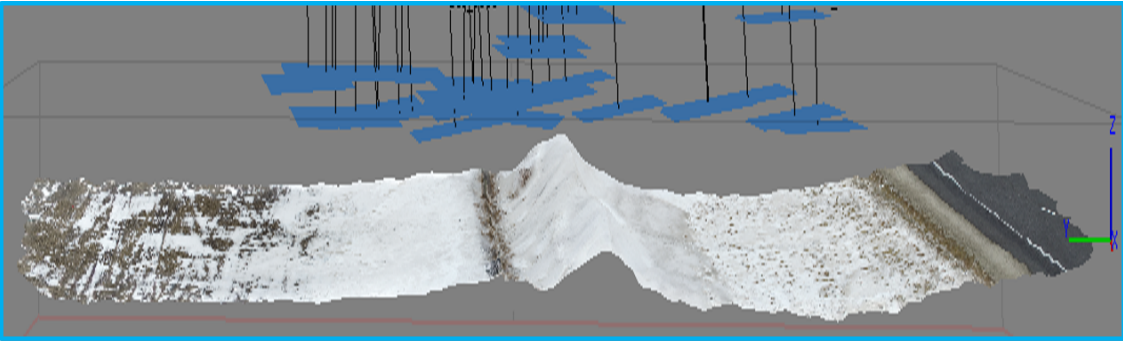
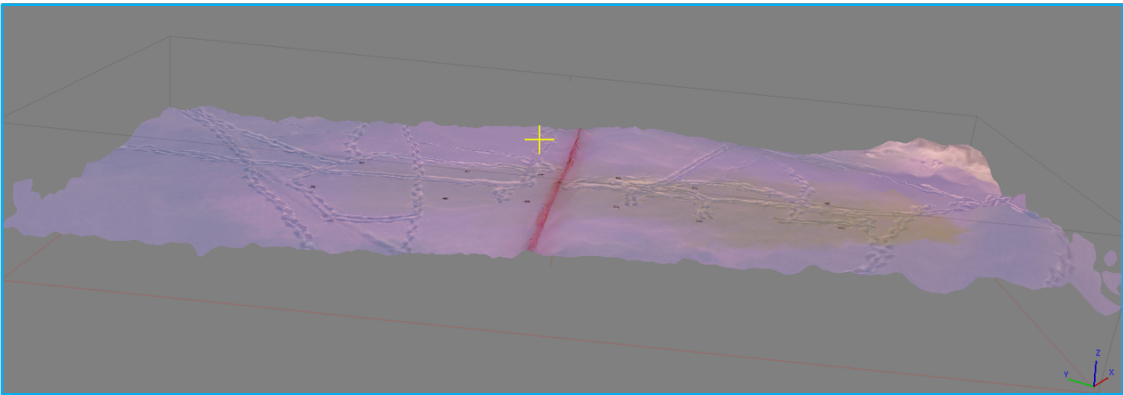


Figure 33. Vertical cross section through the snow deposits along the marker pole lines as documented by tape and RTK measurements.



(a)



(b)

Figure 34. Illustration of the two-dimensionality of the snow deposits accumulated in the fence vicinity with photogrammetric mapping obtained from drone surveys: a) snow cover mapping at US-20 site, winter 2018-19; b) snow cover mapping at Shueyville site, winter 2018-19.

3.2.2.5 Snow density samplers

During the 2019-2020 campaign, core samples of snow were used to determine local snow density. The samples were taken from both snowfall at the nursery site and from the snow deposits behind the fence at US-20 and I-35 sites, near Williams. The core samples from the nursery were used to characterize density of snowfall at Williams, since the nursery is protected from strong winds and snowdrifts. These samples verified the snowfall density records from COOP stations. Moreover, the core samples from snow deposits behind the fences were used to characterize density of transported snow, which has been subject to sublimation and compaction. Figure 35 illustrates the procedures for sampling core samples and determining the snow density with samples from the snow deposits downwind the fence.

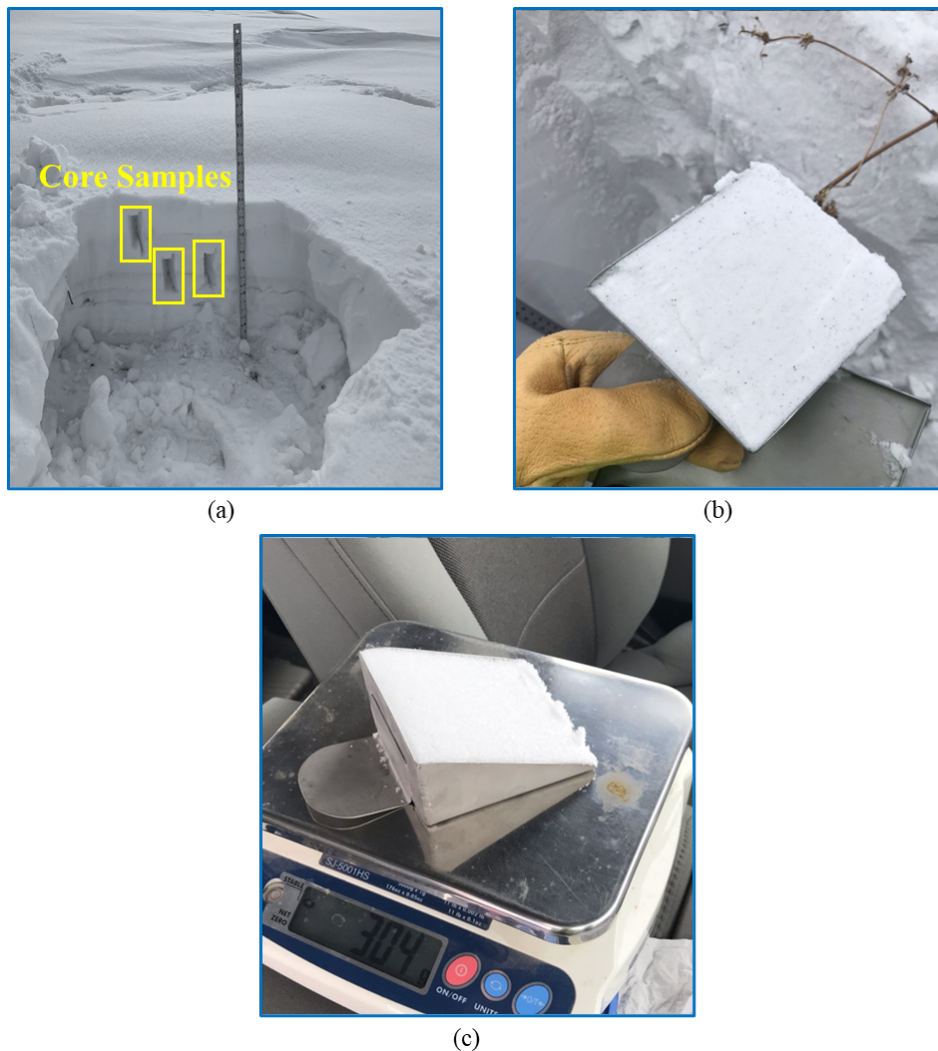


Figure 35. Procedures for sampling cores to determine the snow density: a) a snow trench is dug to ground level from where snow cores are extracted at various locations with a 5 cm × 10 cm × 10 cm snow cutter inserted into the snow pile; b) the extracted samples are shaved to replicate the actual volume of the probe; c) the resulting sample is weighed to measure its mass that is subsequently used to calculate snow density.

3.2.3. Uncertainty considerations

The experimental program undertaken in this study was both extensive and challenging due to the harsh measurement conditions both for equipment and personnel. Given these circumstances, the sources of uncertainty in the study measurements are multiple, with some of them potentially considerable. While it is beyond the resources of the present study to conduct a throughout uncertainty analysis for all the measured variables, it is deemed appropriate to provide several uncertainty considerations and means that we came about to remove or limit their impact of the analysis as a whole.

The most critical measurements for the present study were the images of the changes in the snow deposits continuously monitored with the real-time webcams. These instruments were used both to qualitatively assess the situation at the monitoring sites as well as quantifying the changes in the snow deposition formation due to snow drifting. Despite their critical importance, the webcams were actually the most prone to operational problems among all the deployment instrumentation even if all the imaging unit components and setting on the cameras followed the best practice. For situations where the adverse conditions were absent, the webcams and the associated protocols for quantifying the snow deposit shape at a given time were in quite good agreement, as shown in Figure 36 where webcam, RTK, tape measurements, and cross-section obtained from drone surveys along the marker pole transect are plotted. While accurately capturing the shape of the snow profile, the cross section derived from drone survey is in poor agreement with the other instruments due to the imprecisions in the altitude detection of the flying drones.

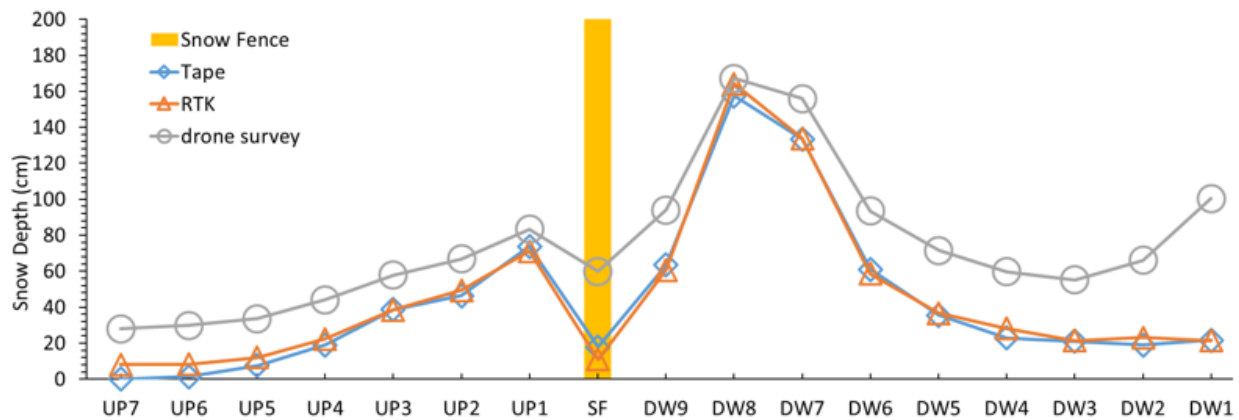


Figure 33. Snow profiles at the US-20 marker pole transect acquired with multiple instruments for the February 2nd, 2020 storm event (left side is located upwind).

One of the most common detrimental situations with the webcams was when the camera lenses were totally or partially covered by snow, ice, or water droplets, as illustrated in Figures 37a and 37.b, respectively. Given the windy conditions at the site, these situations occurred quite frequent and could affect the data acquisition for extended time periods. For avoiding these occurrences we acted along three lines: a) visiting the site in the shortest time possible (note that Williams sites are at about 4 hours driving –at minimum- during snow storms); b) shielding the camera with various snow protection curtains positioned against the dominant wind direction without disturbing the view of the area of interest; c) deploying additional cameras set strategically to not

be fully exposed to the snow drift while covering area of the marker poles located in critical segment of the transect (see Figure 38). The most efficient mitigation measure of this operational problem was the line of action c) that was applied for all the experimental sites.

Another detrimental situation for acquiring data with webcams occurred when reflections of the sun hitting the reflective surface of the snow are sensed by the imaging sensors, as illustrated in Figure 39. This problem was difficult to counteract as the fences at all sites were roughly aligned in the East-West direction, therefore the problem of the sun glare recorded on the sunset was unavoidable for cameras facing toward West. The mitigation of this problem was only possible by adding another redundant webcam sitting on the fence with an Eastern orientation. Additional uncertainties in the quantification of the snow depth at the marker pole locations occurred when the snow deposits built up considerably obscuring the view of the marker poles located downwind or upwind from the snow deposit crest. The positioning of additional webcams from complementary angles was the only good solution for provided the information missing from the main webcam.



(a)



(b)

Figure 34. Image recording obstruction for the P-180i camera located at the US-20 site. a) all lenses covered on January 22th, 2019. b) The lens facing North covered on February 27th, 2019.



Figure 35. Image taken by redundant webcam on January 23th, 2020. Besides providing snow surface elevations while the main webcam is blocked, the strategic positioning of the images acquired with this camera allows to resolve the snow cover elevations for the marker poles located downwind from the snow deposit crest.



Figure 36 Glare produced at sun on the webcam image at US-20 site (January 30th, 2019). The crest of the snow deposit blocks the accurate detection of the marker pole elevations located toward the road (downwind from the fence). The problematic poles are indicated with red circle.

3.3. Complementary public data

3.3.1. Alternative sources for estimation of the local snowfall

A critically important variable in determining snow relocation coefficient, is the amount of snow on the ground which is available to be transported by the wind. For quantifying the available amount of snow, records of precipitation in the form of snow are used. The sources for snowfall data considered in this report include COOP network, COCORAHS network, and local ultrasonic snow depth sensors. The last data for the last listed source is obtained from instruments specifically assembled and deployed by our research team.

3.3.1.1. COOP

The national weather service (NWS) hosts a program called cooperative observer program (COOP) around the country, which includes observation of meteorological conditions reported by volunteers. According to NWS, it is the oldest and largest network of temperature and precipitation records in the nation, with more than 11000 stations across the country. A typical COOP station includes a standard 8-inch rain gage for measuring precipitation, and a snow board for measuring snowfall. Some COOP stations also report snowfall liquid equivalent, which is necessary for determining the density of freshly fallen snow. Figure 40 shows the instruments used in a typical COOP station.

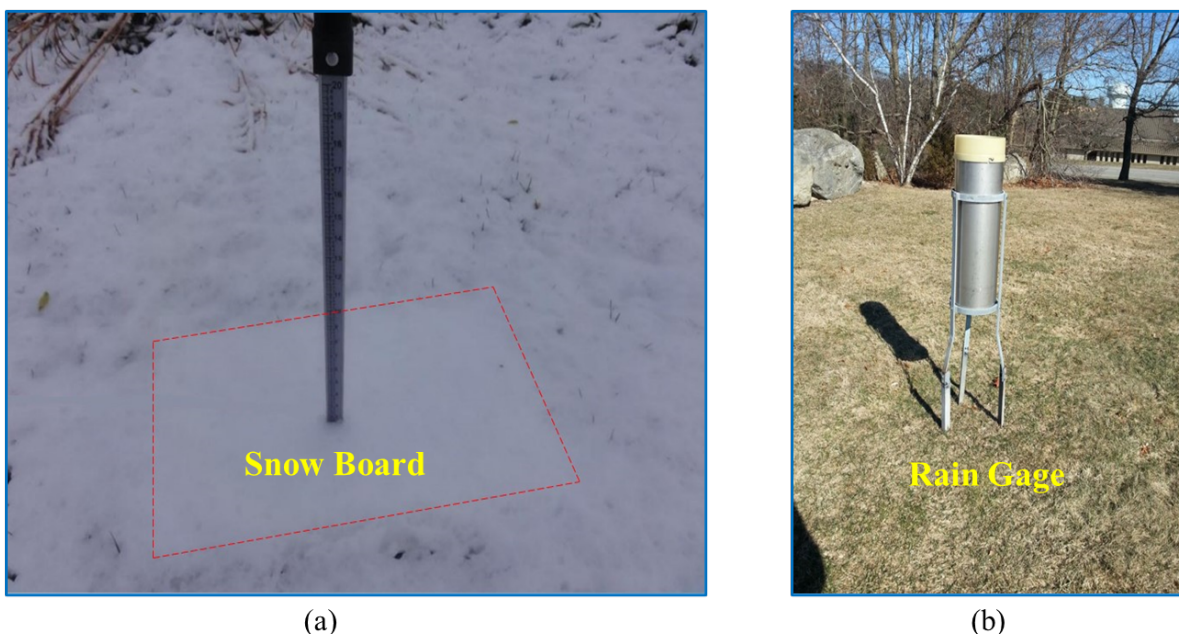


Figure 40. Instruments used at a typical COOP station. a) snow board for measuring snowfall depth. b) standard rain gage for measuring snow density (images: www.weather.gov).

A total of five COOP stations were identified near the two sites near Williams, with the COOP station at Iowa Falls being the closest one, at a distance of 22 km (14 miles) from US-20 site. The locations of the COOP stations used in this study are shown in Figure 41.

3.3.1.2. COCORAHS

Community collaborative rain, hail, and snow (COCORAHS) is another volunteer-based precipitation monitoring network, which is younger than COOP and started in 1998 at Colorado Climate Center at Colorado State University, and currently has more than 12000 stations across the country. A standard COCORAHS station includes a standard four-inch rain gage for measuring precipitation, and an aluminum-foil wrapped Styrofoam hail pad for measuring snowfall. The rain gage at COCORAHS stations can also be used for measuring snowfall liquid equivalent. Figure 42 shows a typical COCORAHS station.

A total of two COCORAHS stations were identified near the two sites of study at Williams, which had continuous report of precipitation history during the period of study. Figure 41 shows the relative locations of the COCORAHS stations.

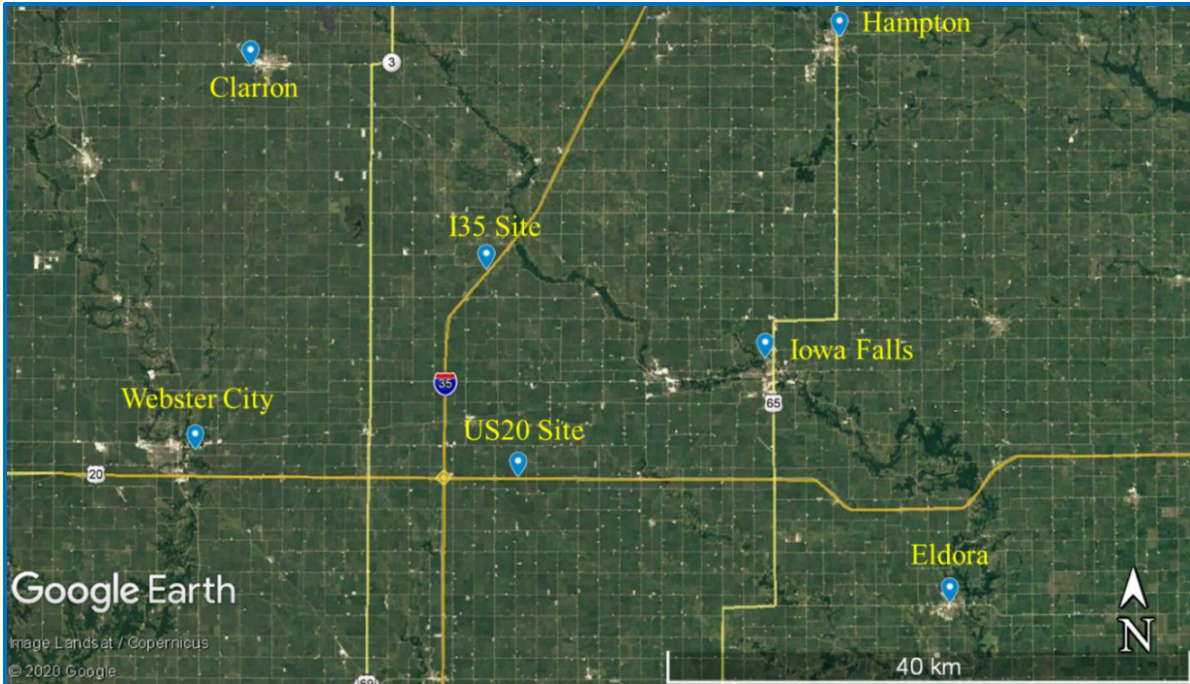


Figure 41. Relative Location of COOP stations near the site of study (image source: Google).

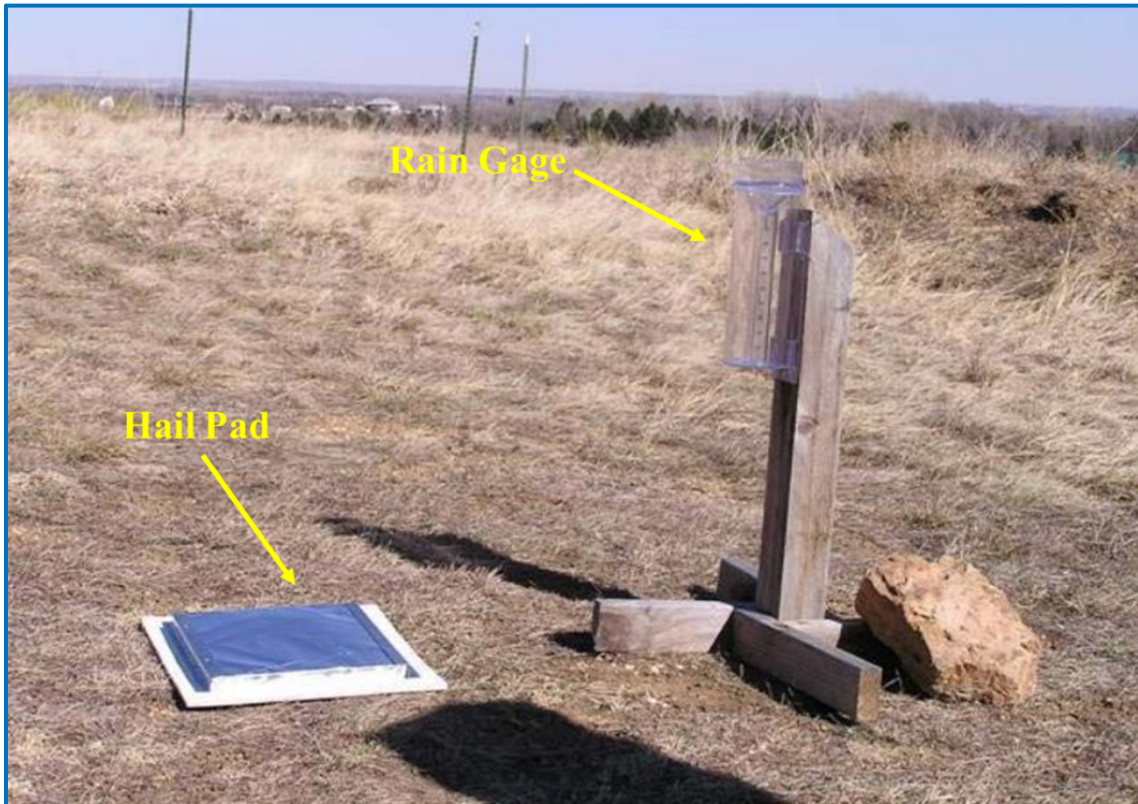


Figure 372. A standard COCORAHS station (image source: www.cocorahs.org).

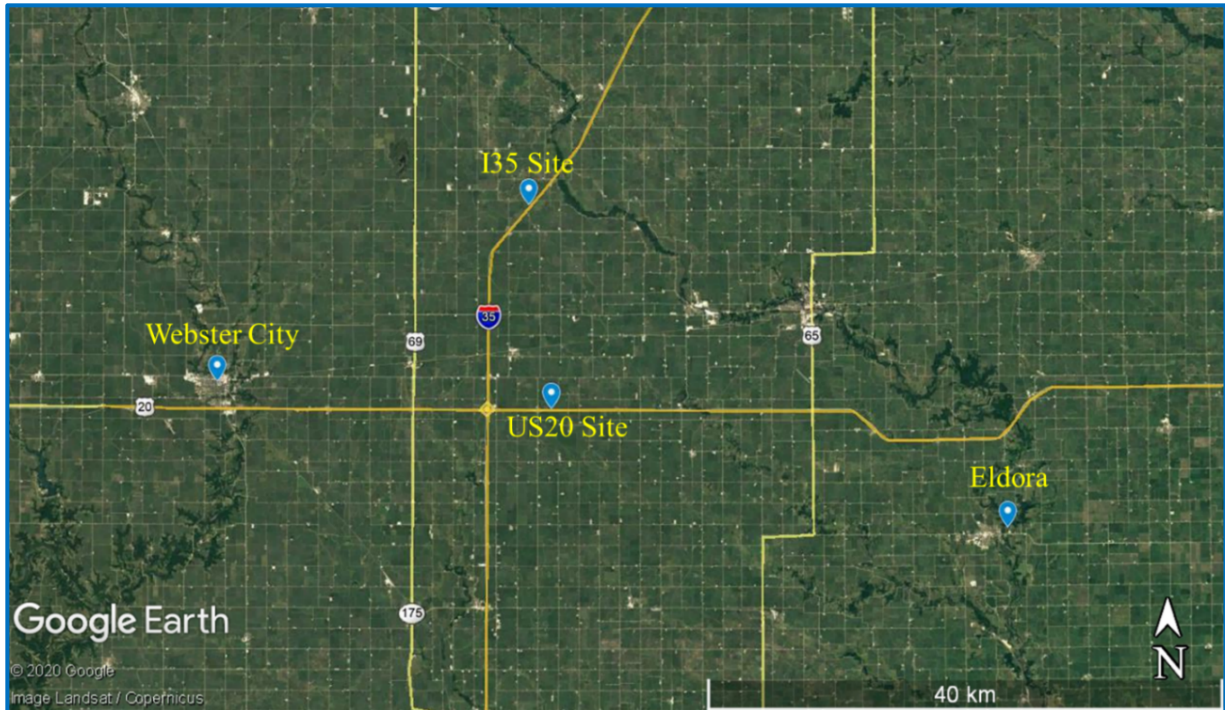


Figure 43. Locations of COCORAHS stations near the Williams experimental sites (image source: Google).

3.3.2 Snow density

Following Equations (10) – (11) in Section 2.1.4, density of snowfall is needed in order to quantify the mass of snow in the fetch area that can potentially be transported to the fence. The calculation of SRC in this report is based on snow density from COOP stations, which have been verified by local measurement of snow core samples.

3.3.2.1. Snow density from COOP

Introduced in section 3.3.1.1, COOP network comprises volunteer-based stations that report precipitation records. The precipitation records from COOP stations include snowfall as well as water equivalent of snowfall. The rain gage provided to COOP stations is used to collect fresh snow, which in turn can be melted to measure the water equivalent of the snowfall. The measured water equivalent can be used to calculate the density of fresh snow. Figure 44 shows the process of measuring snowfall water equivalent at a COOP station.

3.3.3 Wind speed

Ensuing from the descriptions in Sections 2.1.3 and 2.1.4, local wind speed measurements are required for determining the predominant wind direction during snow transport events at the site of study, for quantifying potential snow transport due to blowing wind, and creating wind rose and snow transport rose. Furthermore, temperature measurements are needed to determine freezing and melting periods throughout the observation period. At Williams, Iowa, meteorological conditions were characterized using two on-site meteorological evaluation towers (met towers), a nearby automatic weather observing system (AWOS) tower, and a nearby road weather information system (RWIS) tower. The relative locations of these towers are shown in Figure 45.

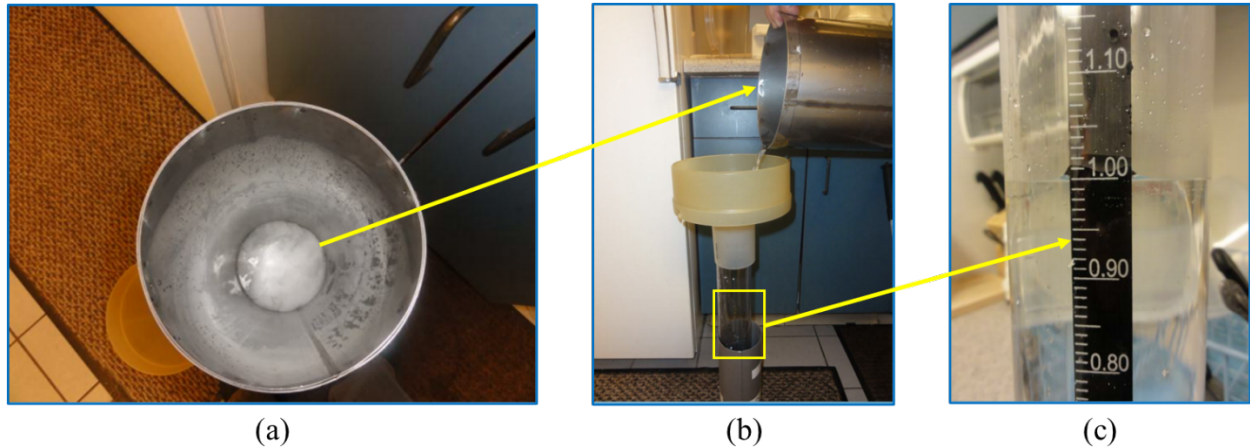


Figure 38. Sample measurement of the snowfall water equivalent: a) the snowfall collected in the rain gage is moved indoors to melt; b) the melted snowfall is poured into a graduated tube; c) the water level in the graduated tube represents the snowfall water equivalent (image source: www.weather.gov).

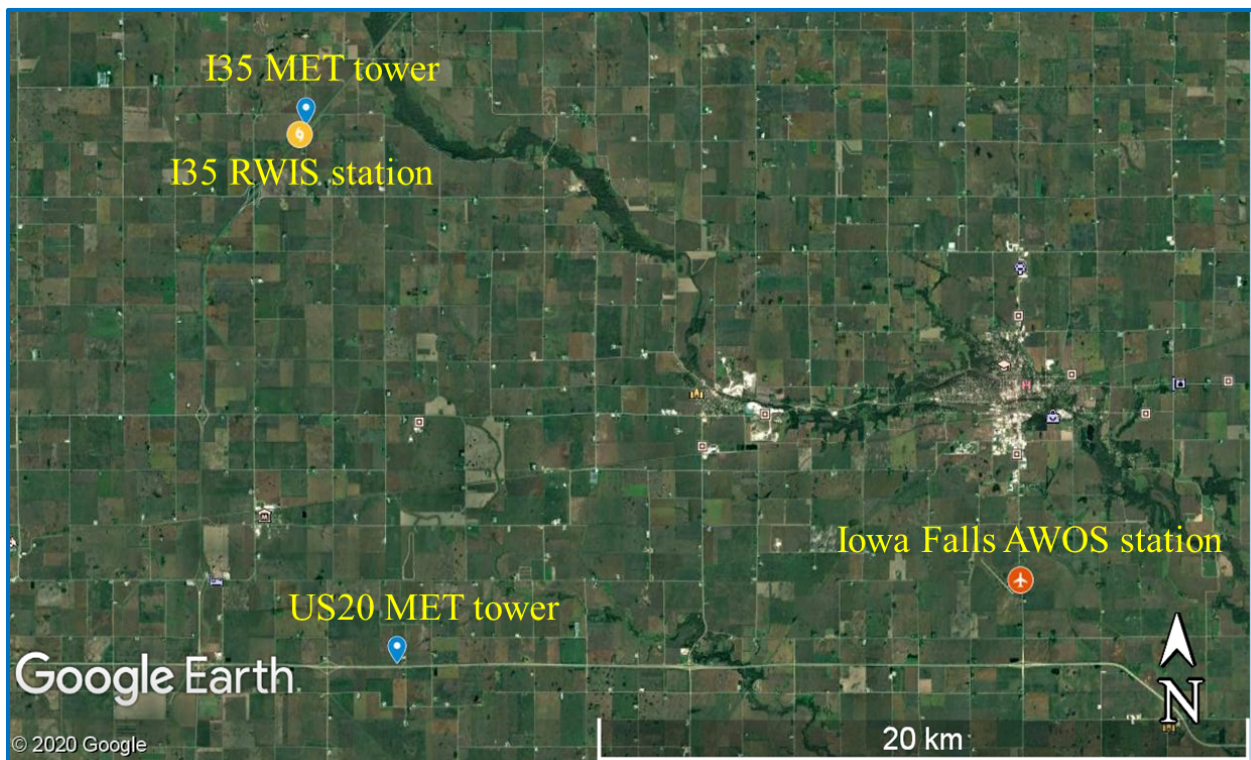


Figure 39. Locations of the two met towers, the RWIS tower at I-35 highway, and the AWOS tower at Iowa Falls airport.

3.3.3.1. AWOS wind speed

Iowa department of transportation maintains a network of 43 AWOS stations which are located at airports around the state of Iowa, with the main goal of providing the aviation community with critical meteorological conditions and real-time weather observations. Typical data from an

AWOS station include wind speed, visibility, current weather, sky conditions, temperature, dew point, and barometric pressure. The closest AWOS station to the sites of study near Williams is located at Iowa Falls Municipal Airport, south of the city of Iowa Falls, at an approximate distance of 19 km (12 miles) from the US-20 experimental site, as shown in Figure 45. A close-up look at this AWOS tower and instruments installed on it, is shown in Figure 46.



Figure 40. AWOS station located at the Iowa Falls Municipal Airport.

3.3.3.2. RWIS wind speed

In order to efficiently maintain roads and improve mobility during cold seasons, it is crucial for road authorities to monitor weather and road surface conditions, which is achieved through RWIS. This system includes a network of environmental sensor stations (ESS) located along highways and roads that are likely to experience hazardous conditions, such as the portion of I-35 highway

chosen for this study. Typical data from ESS includes air temperature, dew point, wind speed and direction, pavement temperature, and subsurface temperature. The closest RWIS station to the site of study is located along highway I-35, very close to the I-35 fence. Figure 47 shows the RWIS tower and its instruments, located on the south-bound side of the highway.



Figure 41. The RWIS station located on I-35 highway.

4. Data analysis

4.1. Snowstorm records

Figures 48 and 49 show snowfall records during winters of 2018-2019 and 2019-2020. The snowfall data from COOP and COCORAHS networks show good agreement for both years. Furthermore, as mentioned earlier, the local ultrasonic data for snowfall were inaccurate during the 2018-2019 campaign. Therefore, only ultrasonic snow depth data for the 2019-2020 winter are shown in Figure 49, which also show good agreement with COOP and COCORAHS networks.

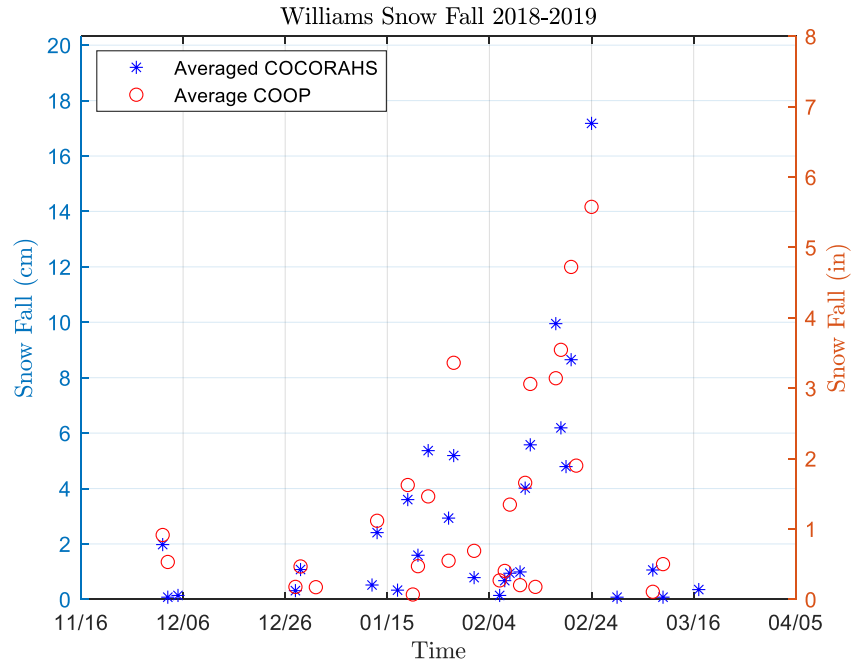


Figure 42. Snowfall records during the 2018-2019 winter season.

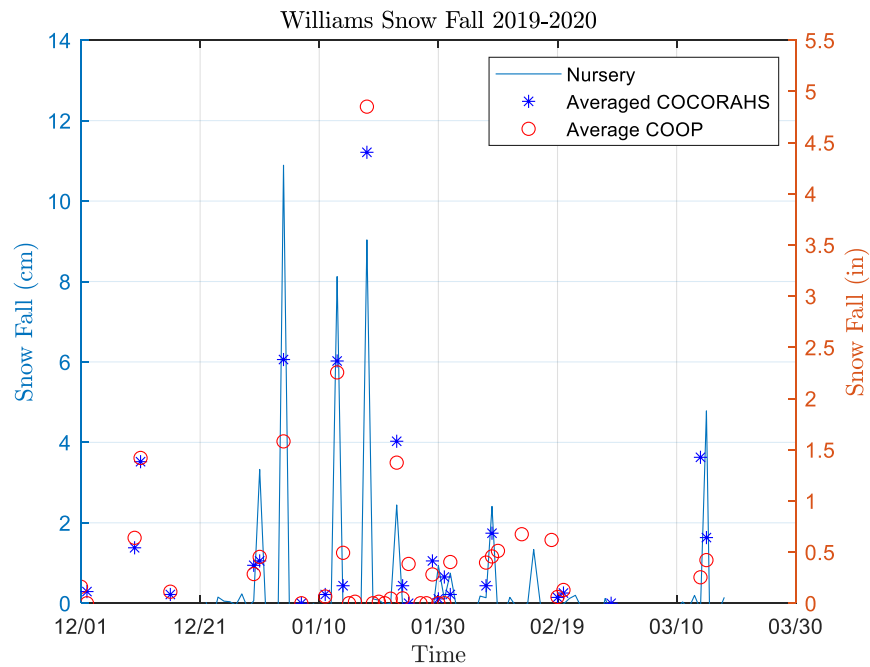


Figure 43. Snowfall records during the 2019-2020 winter season.

Figures 50-53 show temperature and wind speed records for both the winters of the study’s field campaigns. Generally, during the 2018-2019 campaign, we experienced a colder winter season with stronger winds. The 2019-2020 winter season was overall warmer, with fewer snowfall events, and more snow melting events compared with the previous year.

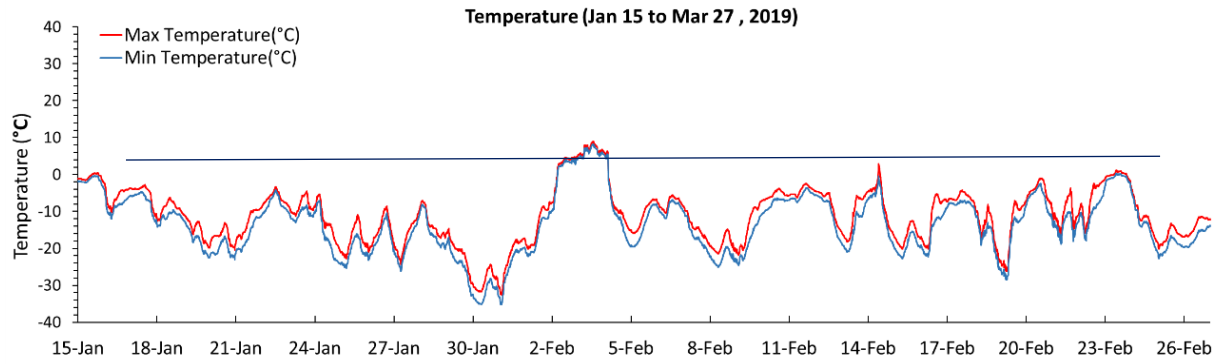


Figure 44. Temperature records during the 2018-2019 winter season.

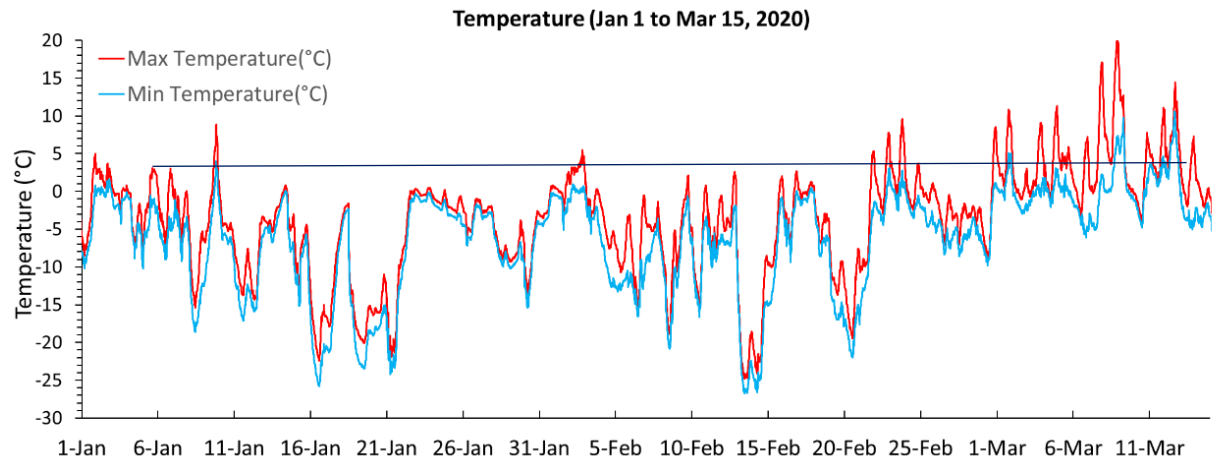


Figure 45. Temperature records during the 2019-2020 winter season.

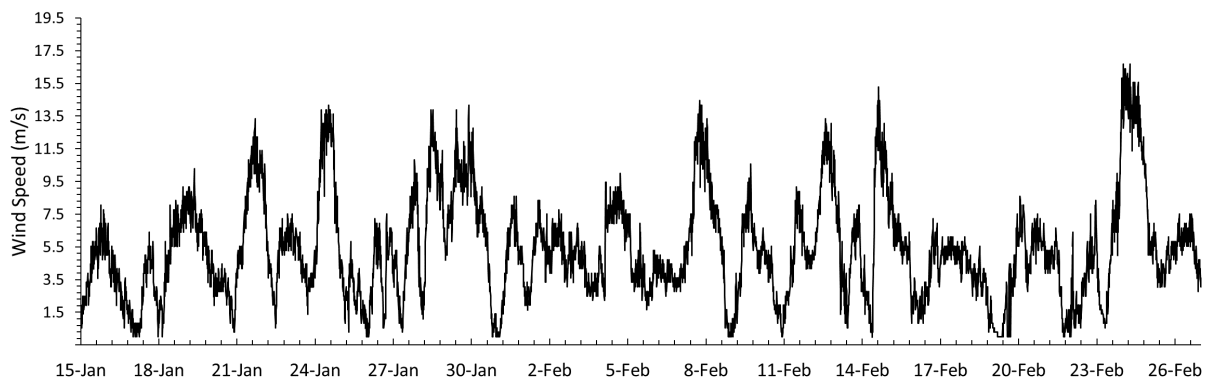


Figure 46. Wind speed records during the 2018-2019 winter season.

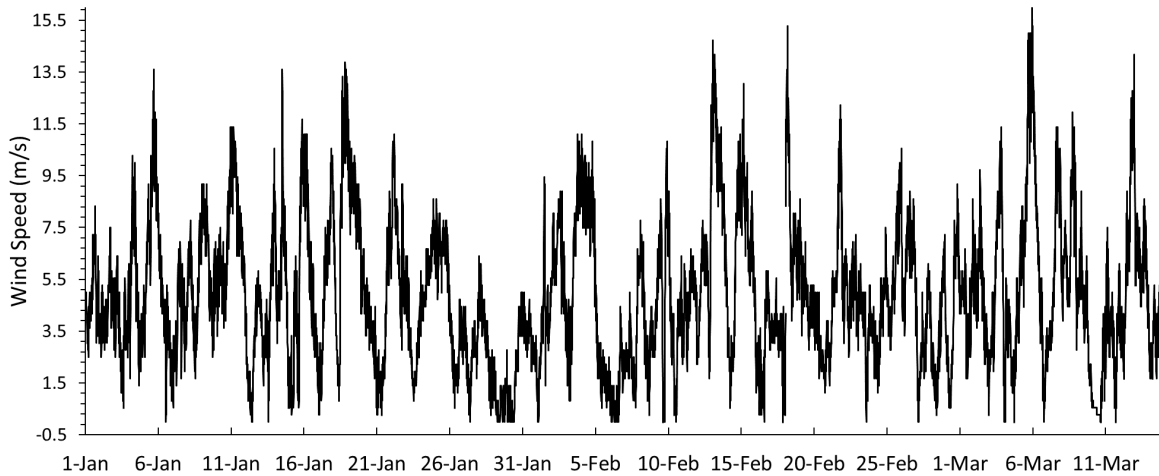


Figure 47. Wind speed records during the 2019-2020 winter season.

Storm event definition

Identification of the storm events is a critical part of the data analysis, as storms are quasi-cyclical physical interactions co-evolving in time. While the cyclical pattern is the dominant aspect of the storms, two events are rarely similar as they are considerably sensitive to the initial conditions of the snow cover on the ground and on the rates of changes, magnitudes, and timing of the changes for the driving variables during the storm event. The event definition adopted for this study is focused on snow drifting, therefore we identify events as those storms that produce “significant” changes of the snow deposits upwind or downwind of the snow fence. Eventually, significant in the present context is related to the capabilities of the continuous monitoring equipment used in the study to detect changes of snow deposits. The key instruments for this detection are the webcams installed on the fence centerline at each experimental site. This is the main reason for which the availability of continuous monitoring (if possible, without interruption during the nighttime) is essential for the quality of the analysis outcomes.

Even adopting this more practical definition it is difficult to find two similar events and to trace the changes in the shape of the snow deposits to the variation of the individual variables. The event identification applied to the two observation winters leads to the conclusion that, for the Iowa conditions, the duration of a storm event is approximately two days. Figures 54 and 55 illustrate the results of this definition implementation for the two winter field campaigns of the study. Due to the limitations of the capabilities of the observational system used in this study, the events provided in these figures do not include sheer snow drifting events whereby the process of snow relocation is not associated with snowfall. Our observational system is most capable to provide reliable data when both snowfall and snow drifting are large. In previous studies, we tested alternative observational approaches to determine snow drift for practically any type of event (i.e., snowfall + drift, drift without snowfall, snowfall without substantial wind) (see Tsai et al., 2017). The alternative observational systems are not however appropriate for the present context where the SRC has to be associated with the season-averaged variables that are required for snow fence design.

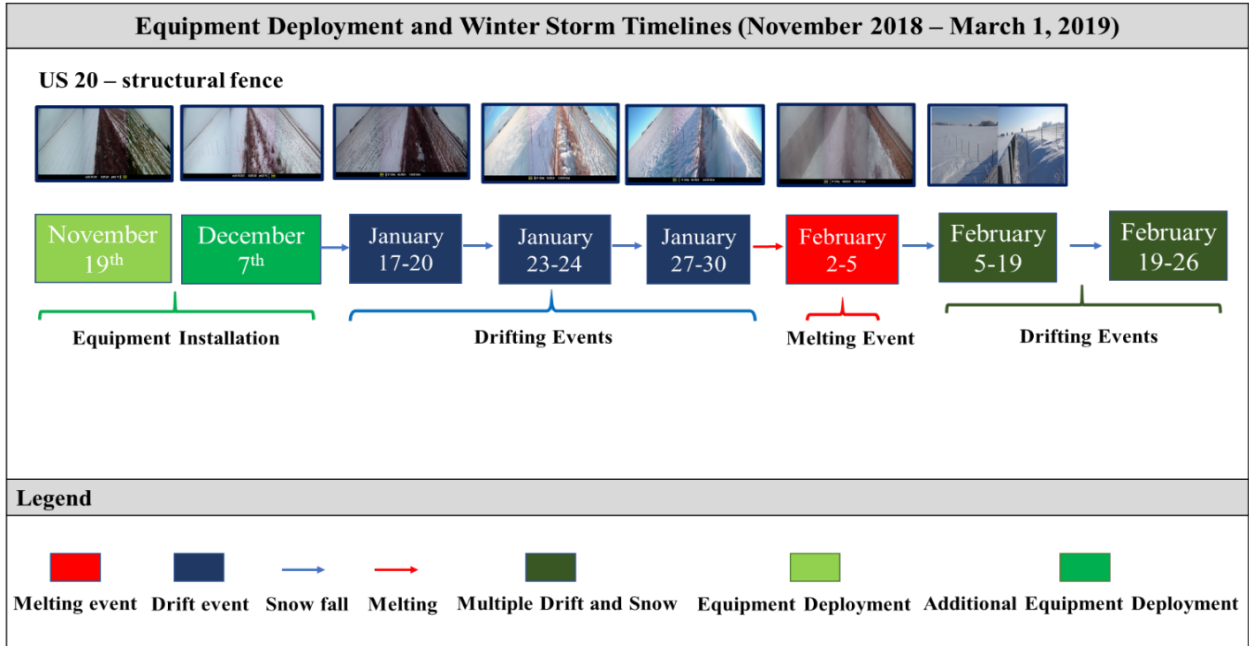


Figure 48. Timeline of the snowstorm events during the 2018-2019 campaign

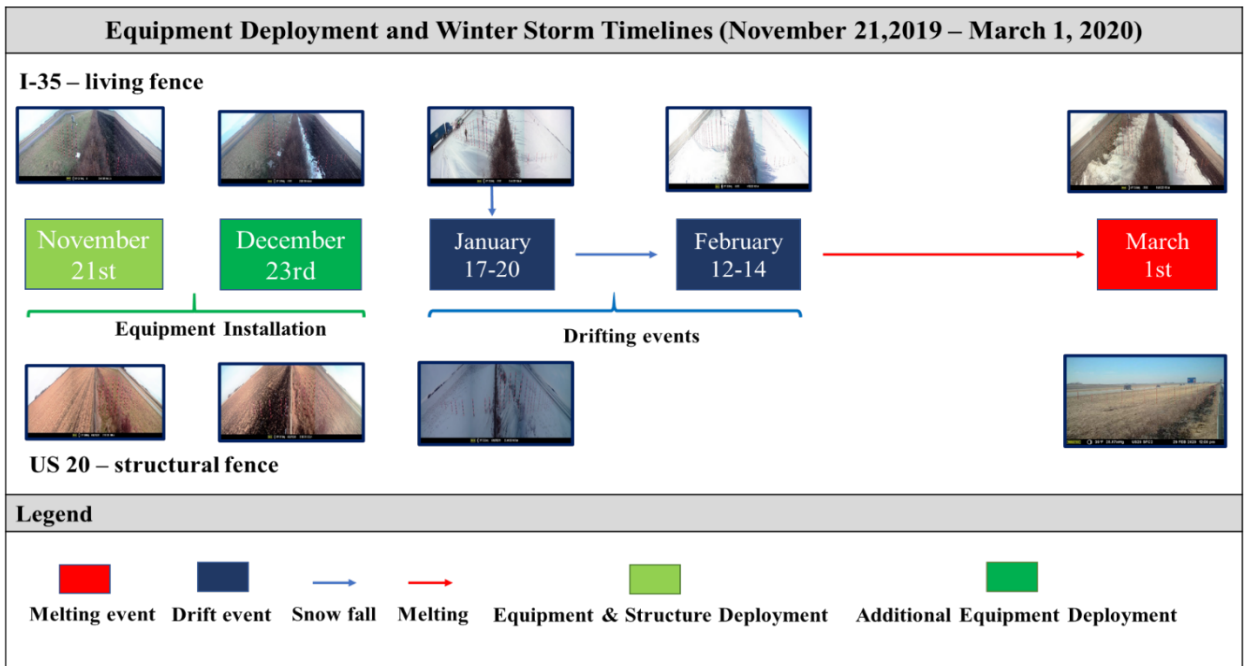


Figure 49. Timeline of the snowstorm events during the 2019-2020 campaign

The Iowa Environmental Mesonet (IEM) provides an alternative definition of the event that is not substantiated with clear-cut definitions. IEM is a multi-set database maintained by the Iowa State University, which gathers data from a number of networks across the state of Iowa and makes them available on their website (<https://mesonet.agron.iastate.edu/>). IEM tracks all major winter storms in the state of Iowa for each year, and chronologically tags each winter storm. Figure 56 shows an example of a winter storm event that occurred during the 2019-2020 as tagged on IEM website.

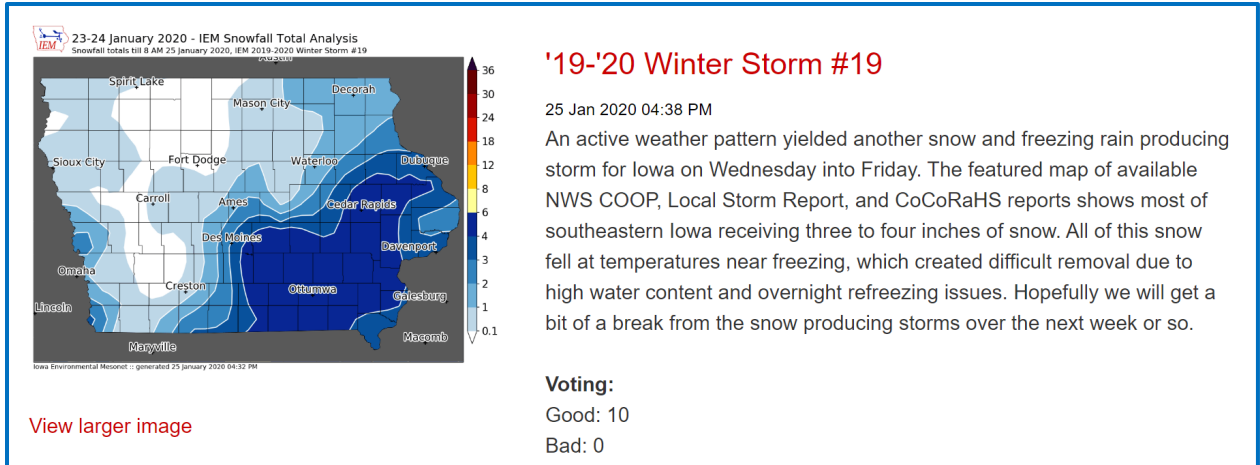


Figure 50. Sample of IEM notification of a winter storm event and its attributes

For a better interpretation of our results, the snow transport events identified in Figures 54 and 55 using our storm event definition, are mapped onto the snowstorms identified on IEM website. Figures 57 and 58 show snowfall records during the identified major events, along with the IEM corresponding tags. The discrepancy between the two alternative definitions is observable in Figure 58, where the IEM tagging includes minor events for the 2019-2020 season during which some snow transport occurred, but the amount of snow transport detected at our sites was not significant enough to be detected on the webcam images deployed at our experimental sites.

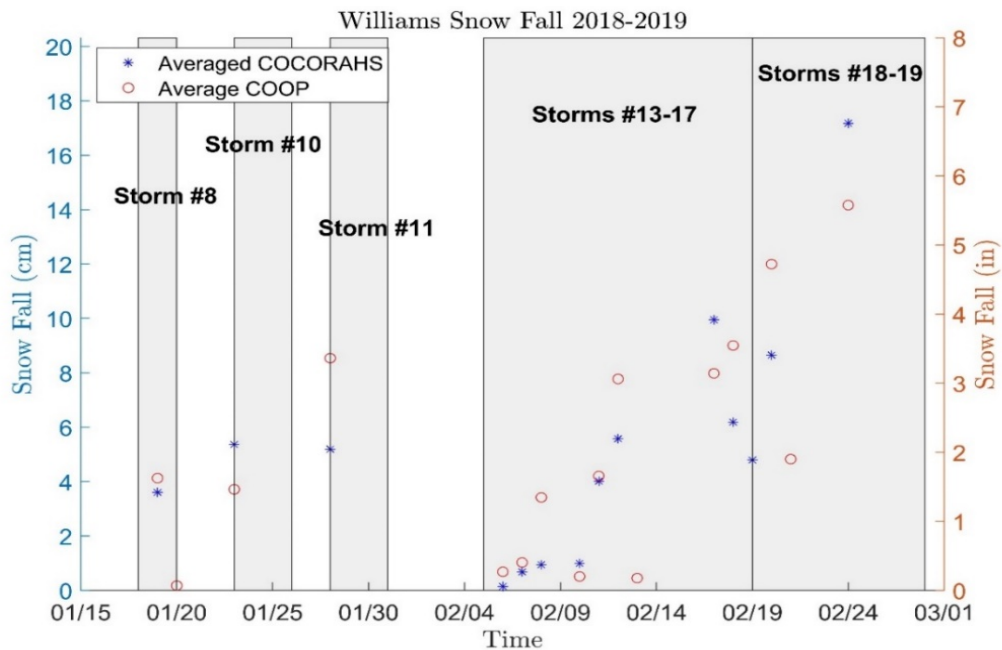


Figure 51. Snowfall records during the 2018-2019 season using this study and IEM event definitions.

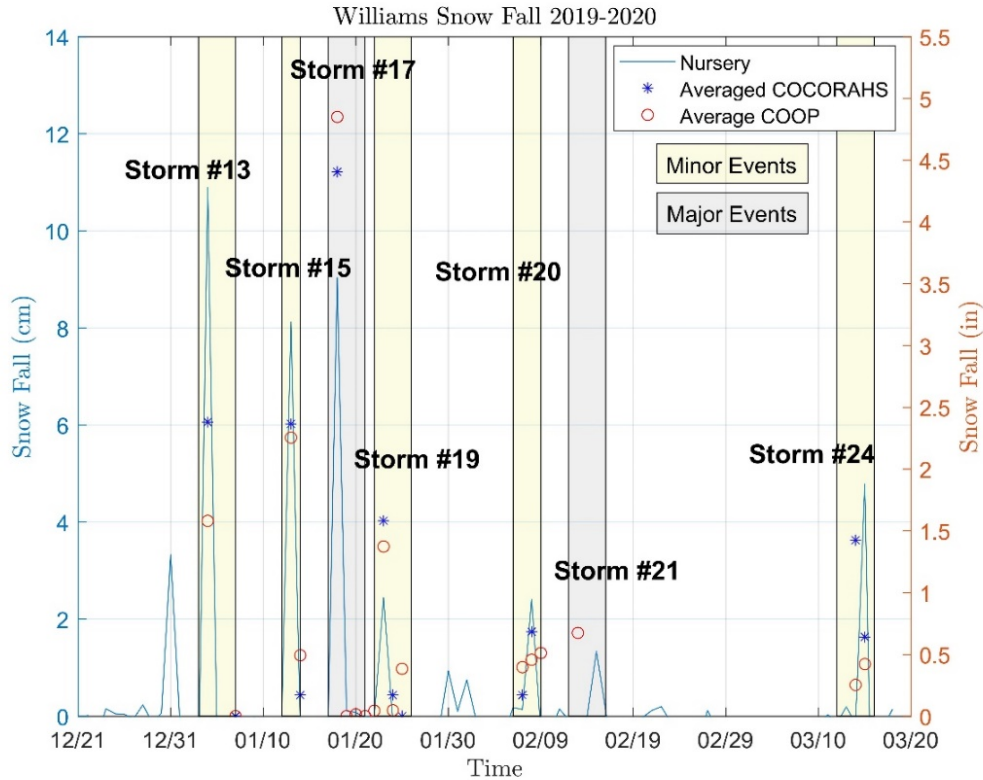


Figure 52. Snowfall records during the 2019-2020 season using this study and IEM event definitions.

4.2. Snow deposit tracking

4.2.1. Snow deposit shape

The overall shape of the snow volume deposits is determined, among other factors, by interaction between the wind characteristics in the undisturbed upwind area, the geometry and texture of the fence, the topography of the ground surface in the fence vicinity and the type of snow transported toward the fence. A common dominant feature of the snow deposits at all the study observations is the prominent two-dimensionality of the snow deposits for each storm event. This feature is expected as the sites were carefully selected to be free of complexities that would affect the use of the available analytical relationships for the result interpretation. In other words, the sites have large fetch areas upwind the fence, the fences are quasi-perpendicular to the dominant fetch direction, and the fences are of regular geometry with uniformly and similarly distributed mesh porosity in verticals and constant patterns along the fence length.

Illustrative examples of the prominent two-dimensionality of the snow fence deposits at the study sites are shown in Figure 59. The illustrations also reveal the impact of the fence characteristics on the snow deposit shape. Notably, the size of the upwind snow deposits is a fraction of those located downwind and that the elevation of the crest on the downwind snow deposit is directly proportional to the fence height. More details about the shape of the snow deposit can be inferred from the numerical simulation results reported in Constantinescu & Muste (2015).



(a)



(b)

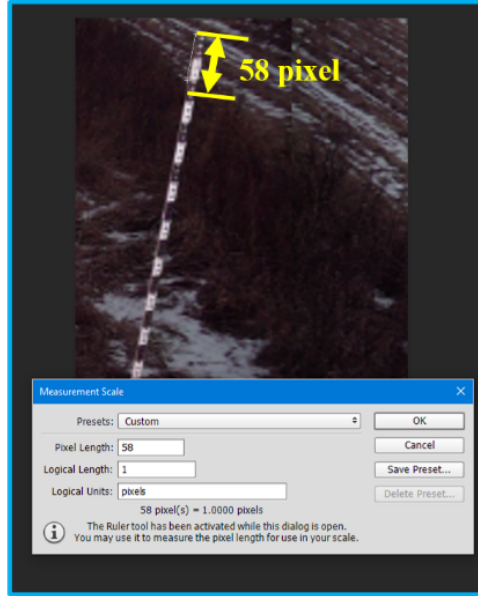
Figure 53. Two-dimensionality of the snow deposits created at fences: a) US-20 site; b) Shueyville site.

4.2.2. Cross-sectional snow deposit profiles using webcam images

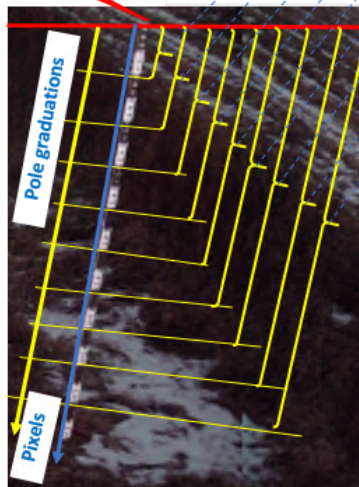
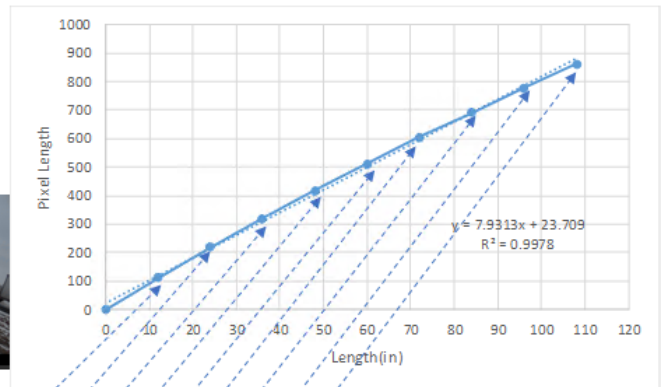
The images recorded with the webcams (see, for example, Figures 20 and 21) entail images of the marker poles and the surrounding areas that are distorted due to the viewing angle and their variable distance from the cameras. While the images give a good qualitative representation of the snow cover along the marker pole transect, these images are critically important to continuously track the snow accumulation in the deposits on a quantitative basis. For this to be possible, a rescaling of images is needed to convert the image coordinates to real-world coordinates. A new customized protocol was developed for conducting this conversion as described below.

The basis of the marker scaling protocol stems in the fact that the individual pole height and size of the colored grading painted on the pole was accurately known from the pole fabrication. Consequently, if the resolution of the image allows good recognition of the pole including the finest graduations over the entire length of the pole a one-to-one relationship can be determined for the distances along the pole and their actual physical dimension. A Photoshop application was developed to automate the scaling process as shown in Figures 60a. Due to the large imaging distance and varying angle of the camera even when imaging individual poles, all graduations on the pole had to be converted one by one to obtain a scaling relationship attached to individual poles, as shown in Figures 60b. The procedure was iteratively applied to individual images of the poles as recorded by each webcam used to track in the real time the snow deposits.

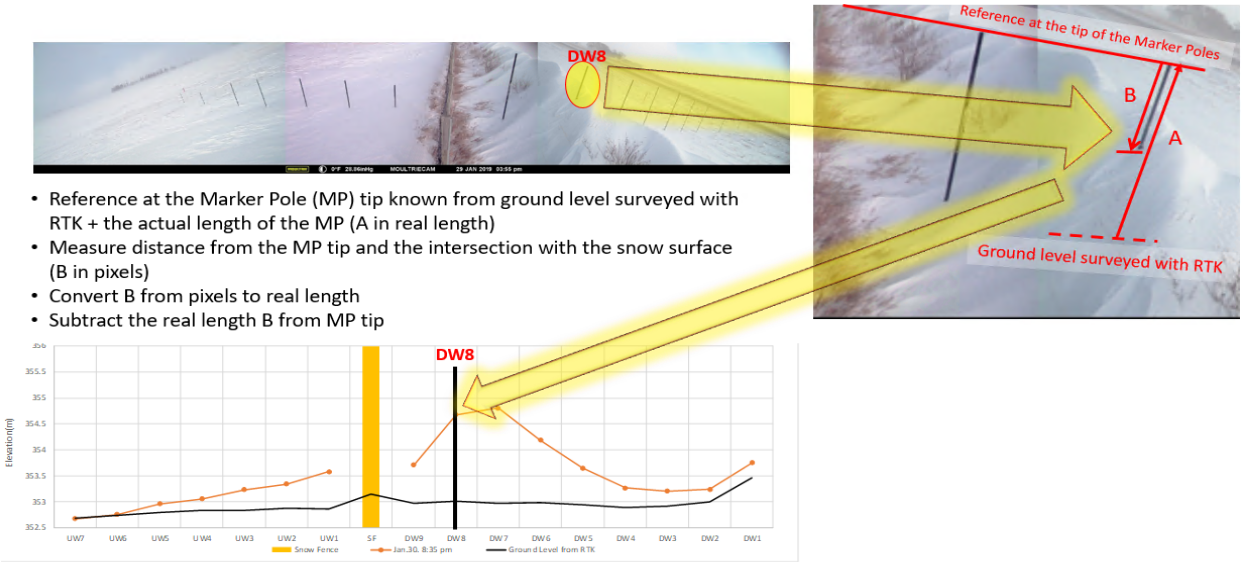
Using the scaling developed for each pole and each camera, the recorded images could be converted in cross-sectional profiles of the snow deposits across the marker pole transect, as illustrated in Figure 60c. The accuracy of the scaling was found adequate for the purpose of the present study as illustrated by the comparison of webcam cross-sectional snow deposit profile with tape measurements acquired directly in the field (see Figure 61a). This information was critically important for tracking the change of the snow deposits during one event and from an event to the other, as illustrated in Figure 61b.



a)

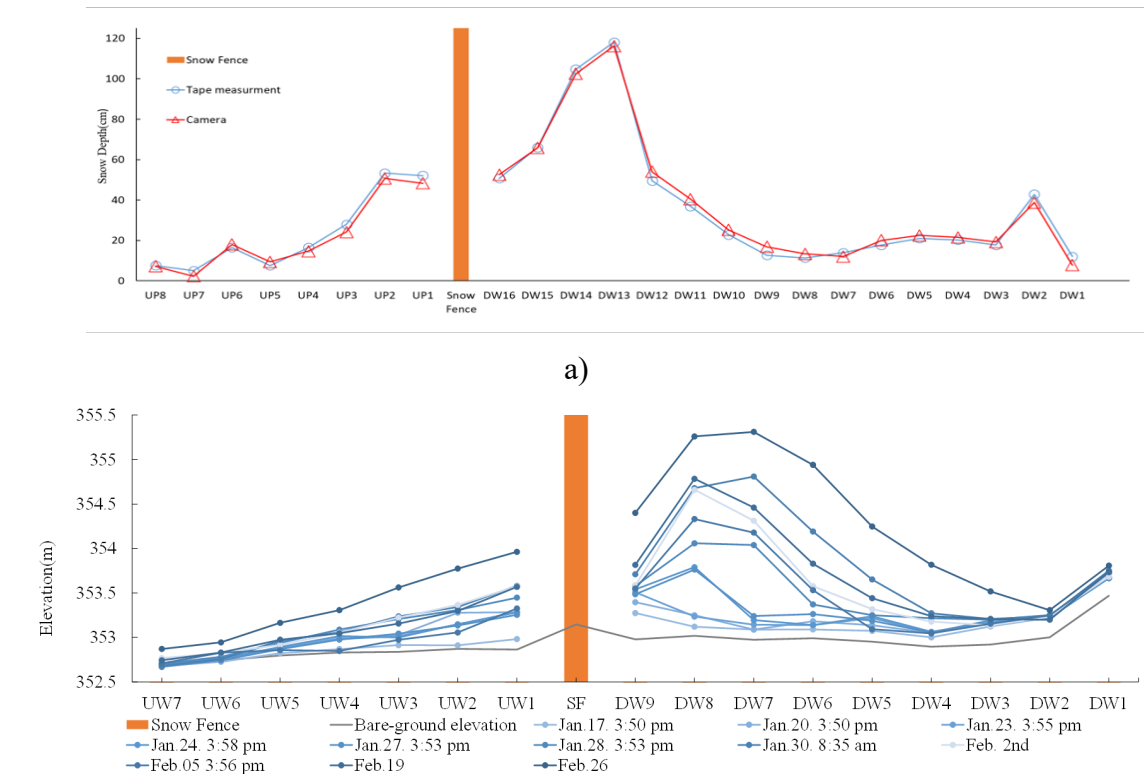


b)



c)

Figure 54. Determination of the snow deposit profiles from the real-time, continuously operated webcams: a) correlation between the actual and image sizes of individual pole graduations; b) development of the scaling relationship for individual poles in the imaged area; c) estimation of the snow depth along the marker pole transect.



b)

Figure 55. Webcam-based snow deposit profiles: a) comparison of the webcam results with tape measurements in the field; b) evolution of the snow deposit cross sectional profile during the 2018-19 field measurement campaign.

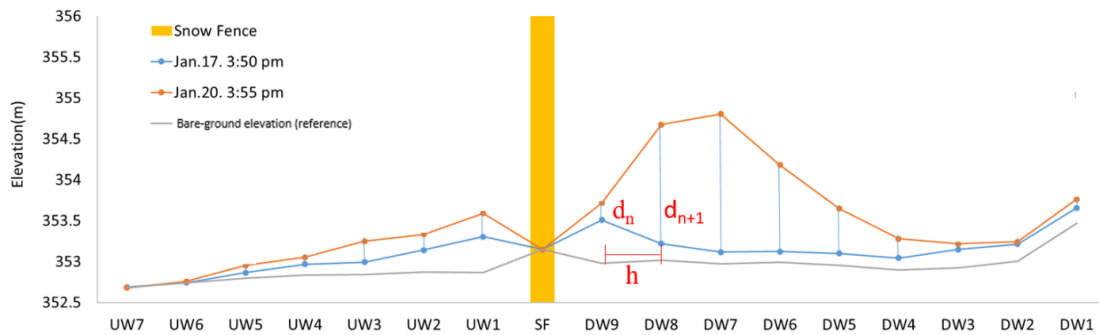
4.2.3. Snow volumes calculation

The calculation of the snow deposits and snow drift volumes are based on the assumption that the geometry of the snow movement in the vicinity of the fence displays a strong two-dimensional nature for all the investigated areas. Consequently, the cross section perpendicular to the fence direction materialized by the marker pole transects at the study sites are representative for all cross sections along the fence. Consequently, the snow deposit volumes per unit width can be obtained by the area under the snow deposit profile at a given time multiplied by the unit width. Irrespective of the method used to determine the cross-sectional profile, the volume calculation retained by the fence per unit width, V_F , is obtained by the summation of the elemental areas between the two successive marker poles along the transect:

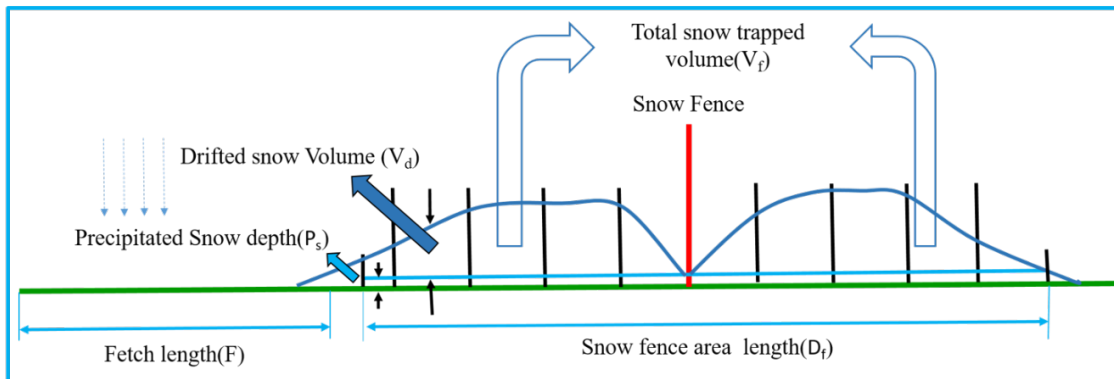
$$V_F = \sum \frac{1}{2} (d_n + d_{n+1}) \times h \quad (15)$$

The notations used in Equation (15) are schematically illustrated in Figure 62a for the estimation of the change in the volumes of the snow deposits trapped by the fence from the beginning to the end of a storm event. Similar assumptions and procedures are used for estimation of the volumes of drifted snow (see Figure 62b). Consequently, the amount of snow drifted downwind from an unobstructed fetch area is calculated by:

$$V_d = V_F - P_s \times D_f \quad (16)$$



(a)



(b)

Figure 56. Snow volume calculations: a) notations for the change in the snow volume trapped by a snow fence; b) notations for the estimation of the amount of drifted snow during an event.

4.3. Data processing for estimation of SRC

Once an event is identified and the data for documenting the event are collected, the SRC can be calculated for each identified event both through the theoretical method described in Section 2.1.4 and the observational method described Section 4.2.2. For illustration purposes, the estimation of the SRC for Storm #11 (January 27th-30th) tracked during the 2018-2019 season is presented in detail below using both methods.

4.3.1. Observational method (M1)

The analytical basis for this method is the Tabler (2003) approach described in Section 2.1.4. The calculations in this section are made in terms of mass of snow deposits, therefore the density of snow is also used in calculations. Our assumption in this calculation is that the density of fresh snow and that in the deposit is the same. The SRC is determined using Equation (13) with the amount of snow deposited behind the fence (Q_{dep}) determined from actual measurements of the snow volumes trapped at the investigated fence and the potential total amount of snow that can be deposited due to wind action during the event (Q_{spot}) determined with Equation (16). The flowchart for estimation of the SRC with this method is provided in Figure 63 with specification of all the experimental procedures and the data sources involved in the estimation process.

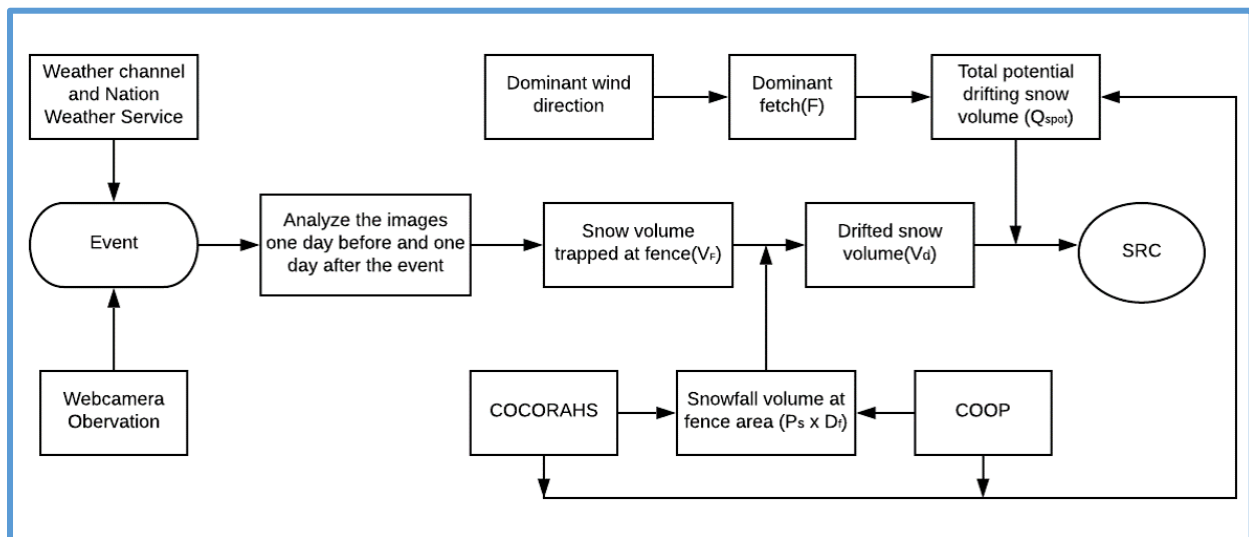


Figure 573. Flowchart of the steps involved and the ancillary data sources involved in the estimation of the SRC using the experimental approach (M1).

The first day of Storm #11 was on January 27th and the end of the storm was on January 30th. The snowfall during this event as reported by the COCORAHS and COOP sources was 5 cm (2 inches) and 8 cm (3 inches), respectively (see Figure 66). Views of the marker pole transects for the two days identifying the start and end of the storm event are provided in Figure 64. Using the images in this figure in conjunction with the procedure for extraction of the snow profiles along the marker pole transect described in Section 4.2.2 lead to the cross sections illustrated in Figure 65. Using Equation (15), the change in the snow volumes from the beginning to the end of the storm event is subsequently estimated. This quantity represents the amount of snow deposited at the fence due to snow drifting. Using Equations (10), (11) and (13) in Section 2.1.4 the SRC can be subsequently obtained using a combination of semi-empirical relationships established by Tabler (2003)

combined with quantitative data collected at our experimental sites. The estimation of the fetch length involved in calculations is described in the next section. The quantification of the experimental data needed for SRC estimation is based on Equations (15) and (16) for estimation of the snow volumes trapped at the fence and the volume of drifted snow, respectively. The summary of the main variables and the estimated SRC for the Storm #11 event are synthesized in Table 3.

Table 3. Data summary for estimation of the SRC for Storm #11, 2018-2019 winter using the observational method (M1)

Snowfall Source	Snow fall(cm)	Snow density(kg/m ³)	Dominant fetch length(m)	Q _{dep} (kg/m)	SRC
COCORAHS	8	90	2600	1869	0.210
COOP	10			1121	0.100



(a)



(b)

Figure 58. Images of marker pole transect at US-20 site on: a) January 27 and 30, 2019.



Figure 59. Snow profile along the marker pole transect in January 27th and January 30th.

4.3.2. Theoretical method (M2)

Following Equations (4) – (13) presented in Section 2.1, a theoretical value for the amount of snow deposit at the fence, and consequently a theoretical value for SRC can be obtained for each event, based on wind speed and snowfall data without the need of any local snow deposit measurements.

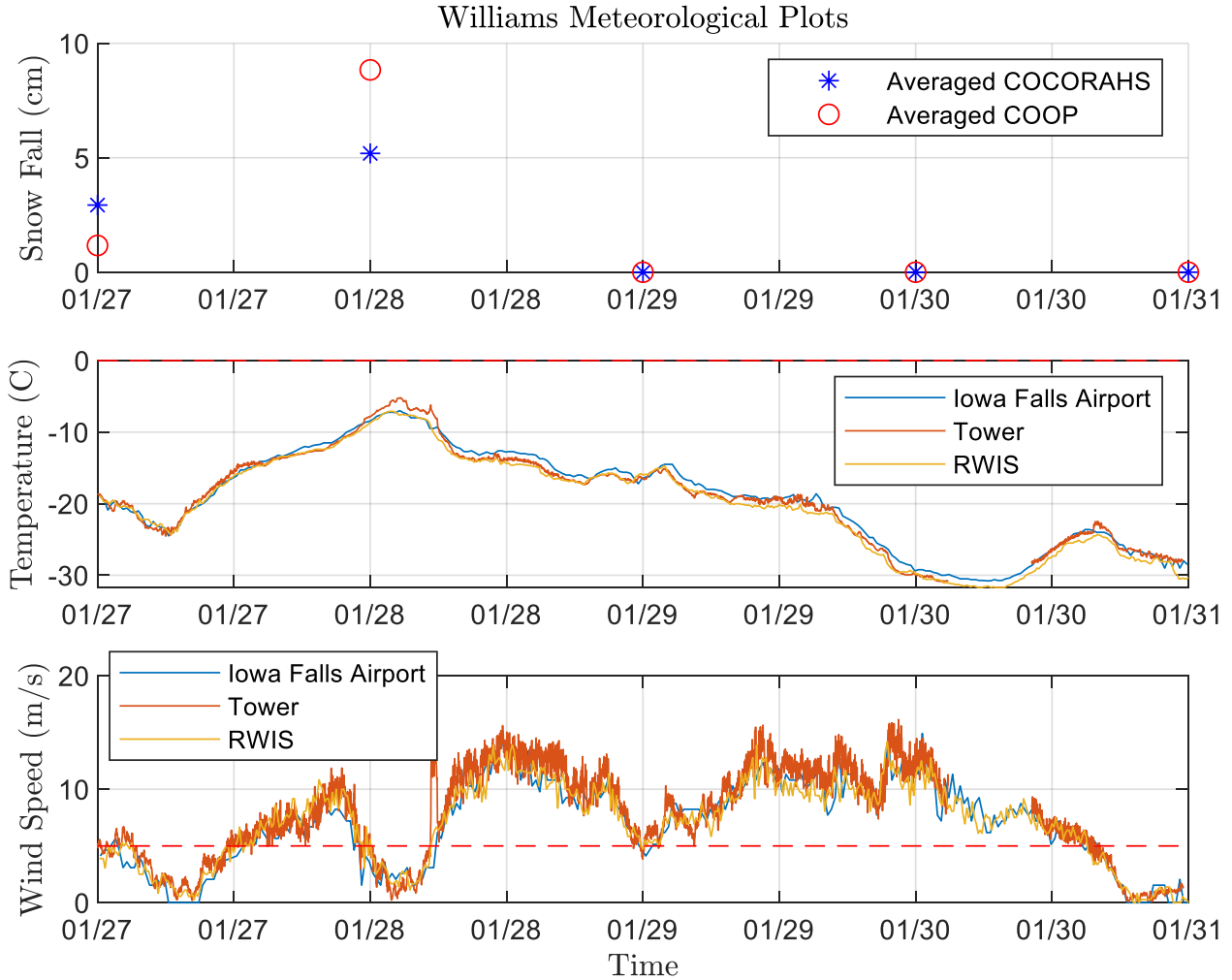


Figure 60. Meteorological conditions during Storm #11, 2018-2019 winter.

Figure 66 shows the meteorological conditions during this event. Total snowfall during the event was 8-10 cm (3-4 in), temperature was below 0 °C (32 °F) throughout the event, suggesting there was no melting and wind speed during this event reached as high as 14 $m s^{-1}$ (31 mph).

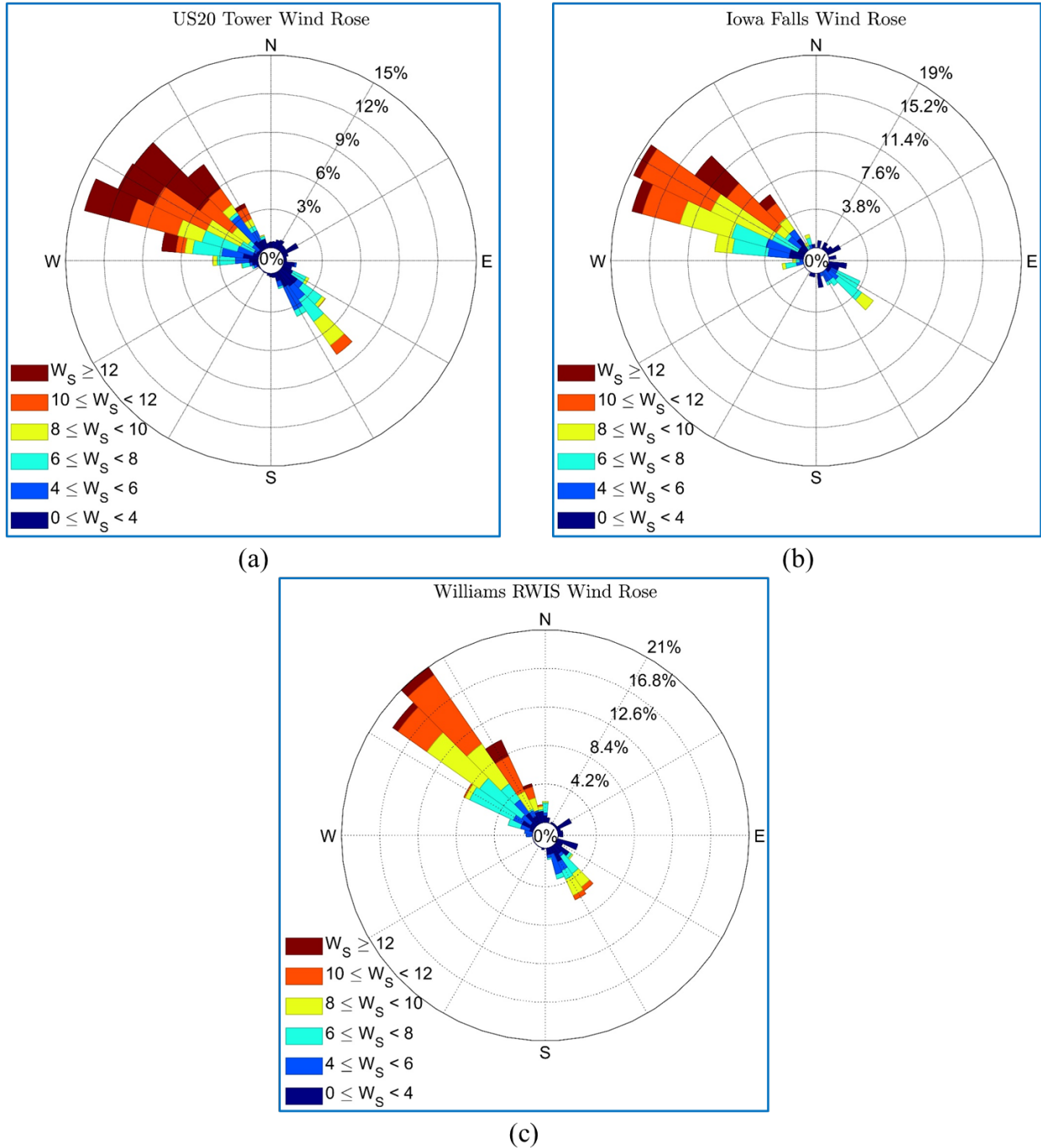


Figure 61. Wind rose during Storm #11, 2018-2019 using a) local tower anemometer, b) Iowa Falls AWOS tower and c) RWIS tower.

Three different sources of wind speed are used for calculation of SRC include local met tower, AWOS tower at Iowa Falls municipal airport, and RWIS tower at I-35. Wind speed records from these three sources are slightly different during the event as shown in Figure 66, while wind roses shown in Figure 67 show wind directions from RWIS tower are slightly in disagreement with the other two sources. Furthermore, the timescale at which wind speed is recorded differs among these

sources. RWIS stores wind speed records at ten-minute intervals, AWOS records are every twenty minutes, and the tower wind speed records are stored every minute. For calculating SRC, all wind speed records are synchronized and are averaged at hourly intervals.

Once wind records are processed, Equation (9) is used to calculate theoretical mass of snow deposit at the fence. Besides wind speed, the theoretical value of snow deposit depends on fetch length as well, and the fetch length at both US-20 and I-35 sites differ with wind direction. Figure 68 shows the possible fetch lengths occurring at this site commensurate with the dominant wind directions during specific events.

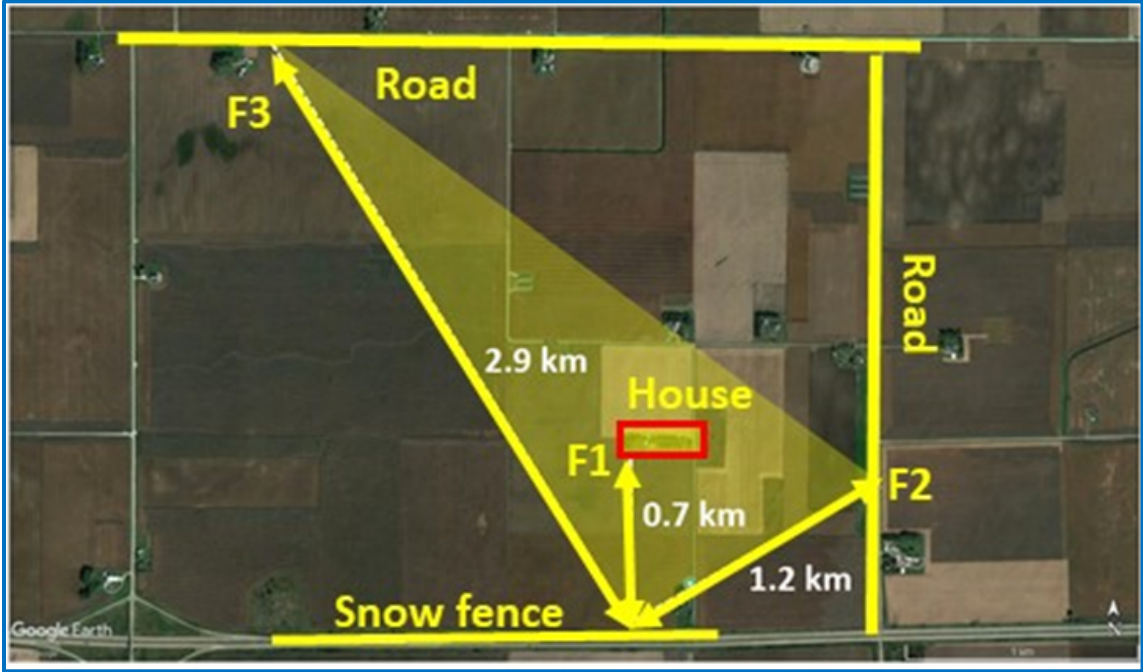


Figure 62. Illustration of the possible fetch lengths corresponding to dominant wind directions occurring during storm events at the US-20 site.

Since wind direction affects fetch length, Haehnel (2019) proposes to divide wind data into 20 directional bins, each bin corresponding to a 18° sector of fetch area, and calculate snow deposit for each bin, using Equation (9). Integrating snow deposit over all wind directions would result in total snow deposit at the fence. Furthermore, normalizing snow deposit from each directional bin by total snow deposit, shows the ratio of contribution of that directional bin to total snow deposit, which can be used to create a transport rose. Transport roses are used to determine the predominant direction of snow transport. Figure 70 shows transport roses for this event, generated by wind data from three different sources. The blue lines show contribution of each directional bin to the total snow transport at the fence. The dashed red line represents the direction of predominant snow transport, which is determined through vector summation of hourly snow transports. All three transport roses suggest that the predominant snow transport direction for this event is from NW, which coincides with predominant wind direction during the event at this site.

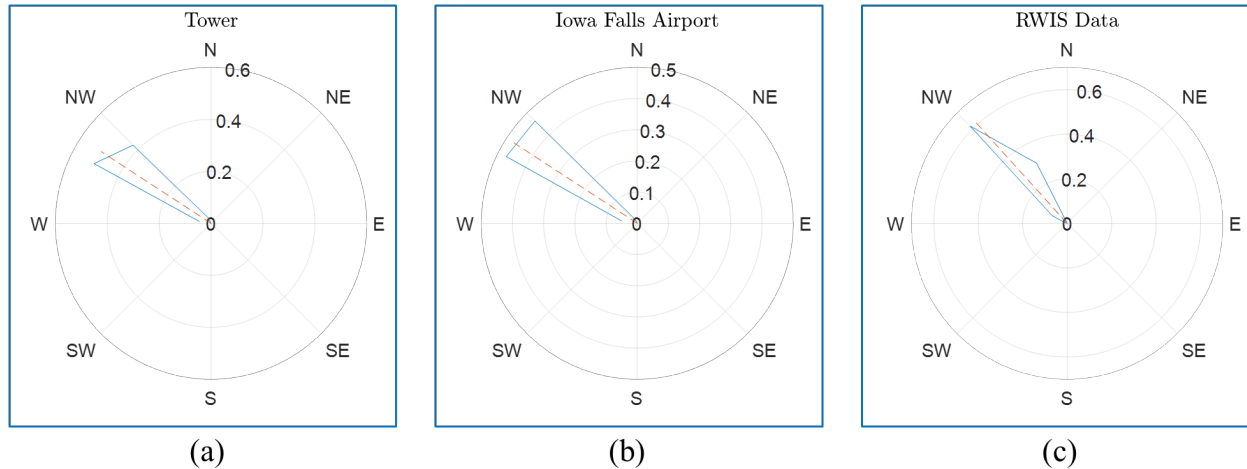


Figure 63. Snow transport rose during Storm #11, 2018-2019 winter using: a) tower anemometer, b) Iowa Falls AWOS tower and c) RWIS tower. The dashed red lines show the direction of total transport resulting from vector summation of all hourly transports.

The snow deposit (Q_{dep}) calculated through Equation (9) and plotted in Figure 69, represents the theoretical amount of snow transport to the fence area. However, the value of SRC also depends on Q_{spot} which represents the amount of snow deposit at the fence, if all of the available snow in the fetch area were to be transported behind the fence by wind. Q_{spot} depends on both the amount of snowfall and the value of snow density during any specific event. Once Q_{spot} is calculated, Equation (13) is used to calculate the value of SRC for the event. Using a combination of COOP and COCORAHS as sources of snow fall, and the met tower, Iowa Falls AWOS tower, and RWIS tower at I-35 results in different values for SRC. The range of SRC values calculated for Storm #11, 2018-2019 is presented in Table 4. Two different sources for snowfall and three different sources for wind speed, result in six different values for SRC. The highest calculated value for SRC is highlighted in yellow and the lowest calculated value is highlighted in blue. A flowchart of steps needed to calculate SRC for a transport event is shown in Figure 70.

Table 4 Snow deposit and SRC results for Storm #11, 2018-2019 using the theoretical and different sources for wind speed and snowfall

Snowfall Source	Snowfall (cm)	Dominant Fetch Length (m)	Snow Density (kg/m ³)	Wind Speed Source	Average Wind Speed (m/s)	Q_{dep} (kg/m)	SRC
COCORAHS	8	2600	90	MET Tower	7.69	2712	0.3
				Iowa Falls	7.02	2163	0.24
				RWIS	7.03	1844	0.21
COOP	10			MET Tower	7.69	2712	0.24
				Iowa Falls	7.02	2163	0.19
				RWIS	7.03	1844	0.17

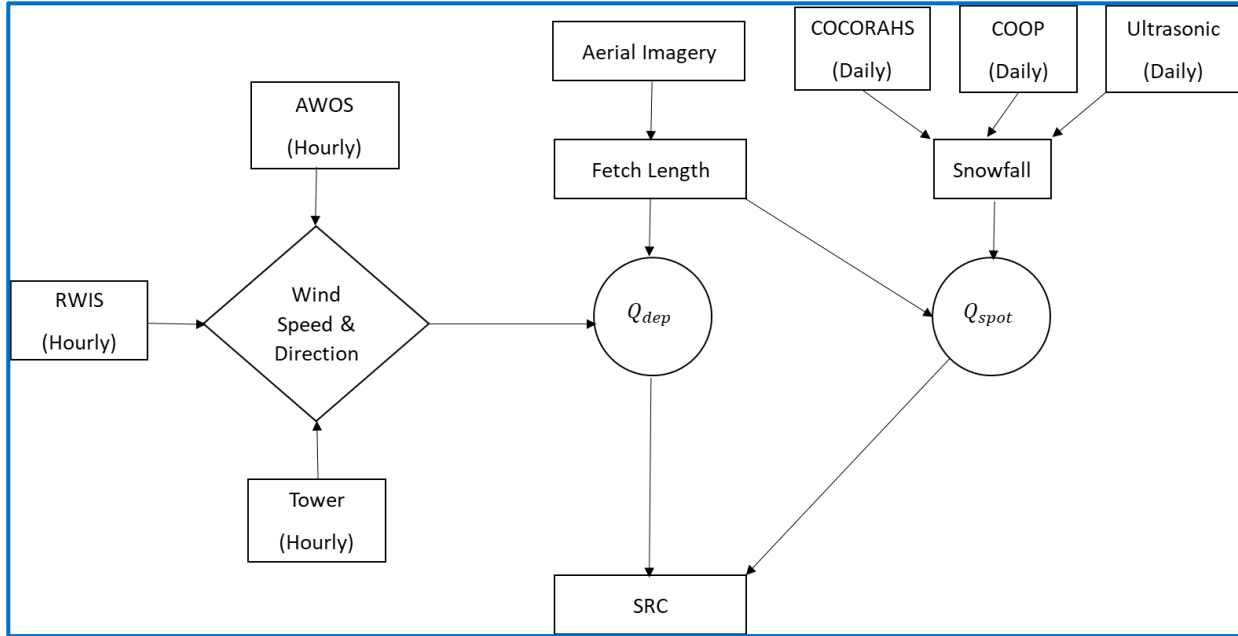


Figure 64. Flowchart of steps needed for calculation of SRC and the data sources needed for the theoretical approach (M2).

4.3.2. Uncertainty considerations for SRC calculation

Details of calculating SRC for a snow transport event are explained in Section 4.3.1. for both observational and theoretical approaches. Both approaches entail measurement of a number of different variables including volume of snow deposit at the fence, snowfall, snowfall density, density of snow deposit at the fence, wind speed and direction, and fetch length. The uncertainties associated with measurement of these variables, contribute to uncertainties in calculation of SRC. The volume of snow deposit at the fence is mainly measured through the continuous monitoring method described in Section 3.2.1, using cameras at the sites. Moreover, the snow deposit profile and volume are validated by synoptic monitoring methods including tape measurement, RTK and drone surveys to reduce uncertainty. For snowfall, data from several COOP and COCORAHS stations described in Section 3.3.1., are averaged to reduce uncertainty associated with snowfall measurements.

Similarly, records from several COOP stations are considered for density of fresh snow and the average value of these records are used to reduce uncertainty. Also, during a field visit on January 20th, 2020, the core sampling method described in section 3.2.2.5. was carried out which resulted in similar values of snow density as COOP records. The snow density for deposit behind the fence was measured at several different sections of the snow pile behind the fence during the visit on January 20th, 2020 resulting in a range of measured densities from 300 kg m^{-3} to 500 kg m^{-3} , which is in good agreement with the results reported in Paterson (1994). All the observed values for Q_{dep} and SRC in the following section are based on this range of densities for snow deposit at the fence. Furthermore, the three sources for wind speed including RWIS tower, AWOS tower and

local met towers result in a range of values for Q_{dep} in the theoretical approach, which in turn results in a range of possible values for theoretical SRC.

Moreover, in this study it is assumed that only fresh snow in the fetch area is available for transport during each event and old snow remaining from previous events cannot be transported by wind. Therefore, only fresh snowfall is considered in the calculation of Q_{spot} . Furthermore, the contribution of snowfall to snow deposit at the fence is assumed to be negligible. In other words, it is assumed that all the snow deposit at the fence is due to transport from the fetch area and not fresh snow. These assumptions contribute to the uncertainty in calculation of SRC as well.

5. Summary of results

5.1. SRC Estimates

This study includes two experimental campaigns during the 2018-2019, and 2019-2020 winter seasons with the broader goal of characterizing SRC in the state of Iowa. During each winter season, the instruments were deployed to the sites of study, described in Section 3, to measure meteorological conditions and snow deposit behind snow fences. The procedure described in Section 4.1 was applied to observations from both winter seasons to identify major snow transport events during each season. Five major transport events were identified for the 2018-2019 winter season, while the 2019-2020 season records showed two major events and five minor events. Once the events for the two campaigns were identified, the value of SRC for each event was calculated through both a theoretical approach and an observational approach, which have been laid out in Section 4.3.2.

The calculated values for SRC during major transport events are presented in Table 5 and 6. Table 6 also includes minor events during the 2019-2020 season, highlighted in yellow. However, Storm #15 and Storm #24 are not included in this table. During Storm #15, wind direction was from SE which is the roadside of the snow fences. Therefore, this event is omitted from Table 6. Furthermore, during Storm #24 temperature at the sites were above 0°C, resulting in melting of fallen snow. Hence, this minor event is also omitted from Table 6. The theoretical and observed values of Q_{dep} and SRC are generally smaller for minor events, compared to major events, as shown in Table 6.

Table 5. Results of SRC for US-20 site during the 2018-2019 winter field campaign. M1 refers to the observational approach described in Section 4.3.2.1 and M2 refers to the theoretical approach described in Section 4.3.2.2.

Event	Snowfall (cm)	Snow Density (kg/m ³)	Dominant Fetch Length (m)	Q_{dep} (kg/m) Theoretical (M2)	Q_{dep} (kg/m) Observed (M1)	SRC Theoretical (M2)	SRC Observed (M1)
January 17-20 Storm #8	4	100	700	243 - 477	433 - 722	0.11 - 0.13	0.19 - 0.32
January 23-25 Storm #10	5	100	2900	1298 - 2013	141 - 235	0.2 - 0.32	0.02 - 0.04
January 27-31 Storm #11	8 - 10	90	2600	1844 - 2712	1121 - 1869	0.17 - 0.3	0.1 - 0.21
February 5-19 Storm #13-17	40 - 42	90	2600	3119 - 6318	629 - 1048	0.07 - 0.14	0.01 - 0.03
February 19 -26 Storm #18-19	26 - 31	120	2300	1060 - 4225	1504 - 2506	0.03 - 0.11	0.03 - 0.07

Table 6. Results of SRC for US-20 and I-35 sites during the 2019-2020 winter field campaign. The events highlighted in yellow are minor events.

Event	Site	Snowfall (cm)	Snow Density (kg/m ³)	Dominant Fetch Length (m)	Q_{dep} (kg/m) Theoretical (M2)	Q_{dep} (kg/m) Observed (M1)	SRC Theoretical (M2)	SRC Observed (M1)
January 4 Storm #13	US20	4 - 10	125	2900	98	435 - 725	0.01 - 0.02	0.03 - 0.11
	I35			800	94	360 - 600	0.01 - 0.03	0.05 - 0.19
January 17 Storm #17	US20	9 - 13	100	2300	1361	600 - 1000	0.09 - 0.13	0.04 - 0.1
	I35			1500	1359	774 - 1290	0.11 - 0.16	0.06 - 0.15
January 24 Storm #19	US20	4 - 5	113	2600	279	156 - 260	0.04 - 0.05	0.03 - 0.05
	I35			1500	266	150 - 250	0.05 - 0.06	0.03 - 0.06
February 7 Storm #20	US20	2 - 4	100	2600	4	150 - 250	0	0.03 - 0.1
	I35			800	4	156 - 260	0	0.08 - 0.21
February 12 Storm #21	US20	2 - 3	66	3000	988 - 1580	426 - 710	0.4 - 0.9	0.17 - 0.42
	I35			1500	998 - 1208	408 - 680	0.56 - 1	0.22 - 0.55

5.2. Snow deposit volume change between events

A factor that has generally been unaccounted for in the design of snow fences is the additional storage created at the fence (particularly between the fence and the road) due to melting and snowpack consolidation between snowstorms. The approach undertaken in this study, whereby the estimation of the SRC was made on an event-by-event basis, provided an opportunity to track changes in the snow deposits due to additional snow drift, and shrinking of the deposit following storm events. As shown below, the combined effect of these factors can result in a gained in storage capacity at the fence. Therefore, traditional designs may be unnecessarily conservative.

Figures 71 and 72 illustrates the changes in the snow deposits trapped between the snow fence and the road during the season (for the US-20 and I-35 sites during the 2018-19 and 2019-20 winter field campaigns). For the experimental sites investigated in this study, all the snow deposition

areas were confined within the road right of way. In order to limit the uncertainties in the snow volume estimation, the volumes corresponding to the start and end of each storm were estimated using the quantification of the snow deposit profiles procedure described in Section 4.2.2 applied to three consecutive webcam images. As expected, the capacity at the snow fence is increased due to the shrinking of the snowpack over time. While this conclusion cannot be readily generalized for this sites or other regions of the state because of the short time of the study carried over only two winters. However, the results illustrate the capabilities of the developed methodology to document this consideration that is not included in current methods of snow fence design.

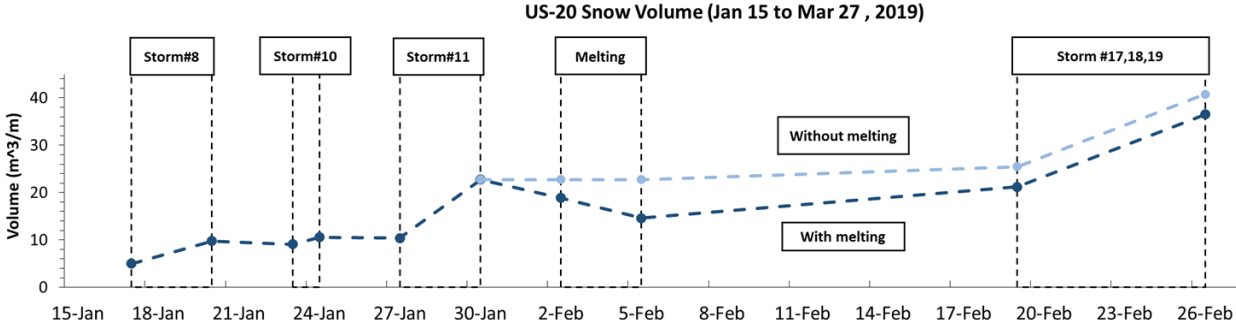


Figure 65. Changes in the snow volumes accumulated at the snow fence between storm events at US-20 site, winter 2018-19.

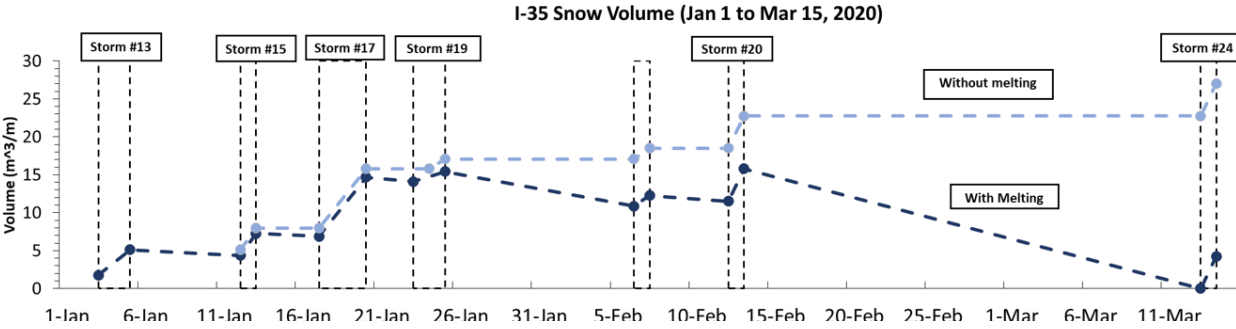
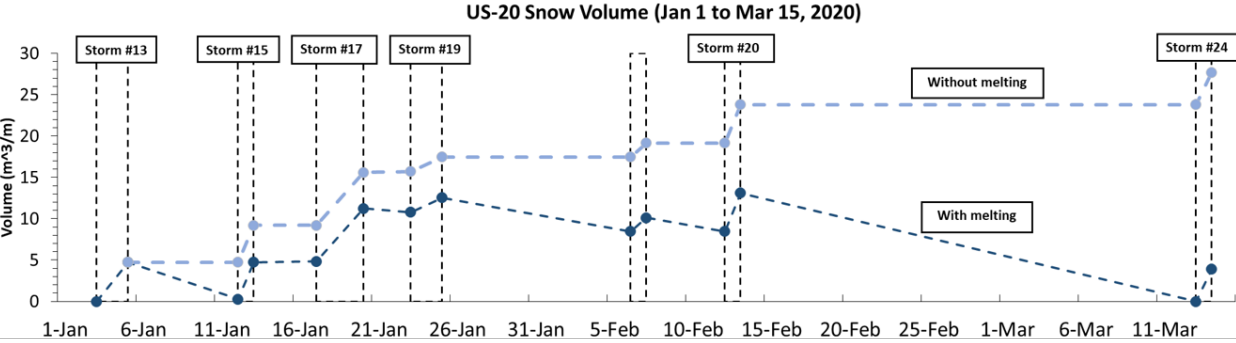


Figure 66. Changes in the snow volumes accumulated at the snow fence between storm events at the US-20 and I-35 sites, winter 2019-20.

Theoretically estimated SRC does not always match the value derived from observed quantities, but they are generally of similar magnitude.

6. Conclusion and future work

The present research study addresses two critical aspects of snow fence design: estimation of snow relocation coefficient and of the seasonal storage capacity of the snow fences to retain the drifted snow. It does so by developing customized, verifiable, and repeatable monitoring methods that are capable to continuously monitor the snowfall and snow drift fluxes by mapping of the snow volumes accumulated at the snow fences. The developed methods are non-intrusive and acquire the data automatically with high spatial and temporal resolution without the need for operator presence in the field. This is in contrast with conventional measurement methods in this area, whereby deployment of instrumentation and personal at the site for extensive periods of time in a harsh winter environment is required.

The most important outcome of this project is directly measured quantitative values for Snow Relocation Coefficient determined based on an event-based approach where the drifting process accounts for the local topography, climate, and weather conditions typical for Iowa. For the first time, specific values and protocols for SRC estimation for Iowa-specific conditions using global measurements, based on tracking snow accumulation at snow fences. The range of values observed for Iowa SRC estimates is considerably smaller for individual events. SRC was found to vary from one event to another depending on wind direction, snow type, air and ground temperature, and accumulation of snow in the fetch area at the beginning of the event. Theoretically estimated SRC does not always match the value derived from observations, but they are generally of similar magnitude indicating a level of robustness between the measurement and theoretical methods in spite of uncertainty in both methods. The seasonal average SRC was found to vary between 0.2 and 0.3 for the two winter seasons observed. This value is significantly less than the default SRC of 0.5 currently used by Iowa DOT Design office.

The study also shows that fences provide additional storage capacity for the accumulation of drifted snow, an important factor that is currently overlooked in the design of the snow fences. The observations revealed additional storage ranges from 10% to 90 % for the two sites investigated during the winter of 2019-20. This aspect of the fence design needs further investigation as this aspect has been barely demonstrated because of the absence of snowdrift conditions at the monitored sites over the observation time.

Additional products of the present research include:

- a) methods and protocols for local measurement of snowfall and snowdrift fluxes,
- b) methods for mapping snow accumulated at snow fences.

The above listed methods can be used as a solid basis for a thorough step-by-step estimation of the Snow Relocation Coefficient and characterization of the Iowa-specific snow transport and accumulations at snow fences during and between storms irrespective of the geographic location. The developed methodologies can be bundled in standardized methodologies for SRC estimation through a systematically laid out program. Repetition at the above monitoring programs at several

sites is suggested to capture the spatio-temporal variability of the snow transport processes in other Iowa regions confronting snow drifting issues.

The observed SRC and snow fence capacity need to be put into context. They depend on specific locations within the state, details of the local landscape and highway right of way geometry, and winter climatology. The observations presented in this report represent two years, which is challenging to contextualize in terms of the average snow drift year or average capacity usage for snow fences. Meteorological data recorded for 20 or 30 years could be used with the theoretical approach (M2) to determine how the two years of this study compare with the average and extreme years. The approach could then be extended to evaluate an acceptable risk for design based on associated return periods for snowstorms (including snowfall and wind velocities). This would be similar to a flood frequency analysis for hydraulic design of culverts or bridges. For example, a 10- or 25-year SRC and fence capacity could be defined and used in design rather than the average year (2-year return period). Just as design criteria for roadway overtopping due to flooding is defined based on traffic statistics and using sound hydrologic engineering, a similar criterion could be defined for blowing and drifting snow over roadways.

7. References

- Basnet, K., Muste, M., Constantinescu, G, Ho, H.C. and Xu, H. (2015). Close-range Photogrammetry for Dynamically Tracking Drifted Snow Deposition, *Cold Regions Science and Technology Journal*, doi: 10.1016/j.coldregions.2015.08.013.
- Blanken, P. D. (2009). "Designing a living snow fence for snow drift control". *Arctic, antarctic, and alpine research*, 41(4), 418-425.
- Constantinescu, G. and Muste, M. (2015). Optimization of Snow Drifting Mitigation and Control Methods for Iowa Conditions, *Report for the Iowa Department of Transportation*, The University of Iowa, Iowa City, IA.
- Dong, Z., Luo, W., Qian, G., and Wang, H. (2007). "A wind tunnel simulation of the mean velocity fields behind upright porous fences." *Agricultural and Forest Meteorology*, 146, 82-93.
- Dong, Z., Luo, W., Qian, G., Lu, P., and Wang, H. (2010). "A wind tunnel simulation of the turbulence fields behind upright porous wind fences." *Journal of Arid Environments*, 74, 193-207.
- Giudice AL, Nuca R, Preziosi L, Coste N (2019) Wind-blown particulate transport: A review of computational fluid dynamics models.
- Haehnel, R. B. (2019). "Blowing Snow Transport Analysis for Estimating Drift Orientation and Severity." *Journal of Cold Regions Engineering*, 33(2), 05019002.
- Heisler, G. M. and Dewalle, D. R. (1988). "Effects of windbreak structure on wind flow." *Agriculture, Ecosystems and Environment*, 22/23, 41-69.
- HDB (1996). Snowbreak Forest Book, Highway Snowstorm Countermeasures Manual (Hokkaido Development Bureau Book, translated by FHWA in 1996.
- Iowa Environmental Mesonet (IEM): <https://mesonet.agron.iastate.edu/>
- Kaneko, M., Watanabe, T., Matsuzawa, M. and Ito, Y. (2012). Revision of Highway Snowstorm Countermeasure Manual: Focus on Snowbreak Woods (WM-STW12-131), *International Conference on Winter Maintenance and Surface Transportation Weather*, Coralville, Iowa.
- Martinelli, M. Jr., R. A. Schmidt, and R. D. Tabler. 1982. Technology transfer in snow control engineering. *Journal of Technology Transfer* 6(2): 27-37.
- Mellor, M. 1965. *Blowing snow*. CRREL monograph, Part III, Section A3c, and U.S. Army Corps of Engineers, Cold Regions Research and Engineering Laboratory, Hanover, NH.
- Moultrie Mobile camera: <https://moultriemobile.com/>
- Nixon, W. A. (2003). Living snow fences. Iowa Highway Research Board Project TR 460. IIHR Technical Rep, 460.
- Pomeroy, J.W. 1988. *Wind transport of snow*. Ph.D. dissertation, University of Saskatchewan, Saskatoon, Canada.
- Pomeroy, J.W. 1989. A process-based model of snow drifting. *Annals of Glaciology*, vol. 13. pp. 237-240.
- Ohara, N. 2014. A practical formulation of snow surface diffusion by wind for watershed-scale applications, *Water Resources Research*, 50, doi: 10.1002/2013WR014744, pp. 5074-5089
- Paterson, W. S. B. (1994). *Physics of glaciers*. Butterworth-Heinemann.
- Sañudo-Fontaned, L.A., Castro-Fresno, D., del Coz-Díaz, J.J., and Rodriguez-Hernandez, J. (2011). "Classification and comparison of snow fences for the protection of transport infrastructures." *Journal of Cold Regions Engineering*, 25, 162-181.

- Seginer, I. (1972). "Windbreak drag calculated from the horizontal velocity field." *Boundary-Layer Meteorology*, 3, 87-97.
- Shaw, D. L. (1989). *Living snow fences: Protection that just keeps growing*. Colorado Interagency Living Snow Fence Program, Colorado State University, Fort Collins.
- Tabler, R. D. 1980a. Geometry and density of drifts formed by snow fences. *Journal of Glaciology* 26(94): 405-419.
- Tabler, R. D. 1980b. Self-similarity of wind profiles in blowing snow allows outdoor modeling. *Journal of Glaciology* 26(94): 421-434.
- Tabler, R. D. and R. L. Jairell. 1980. Studying snowdrifting problems with small-scale models outdoors. In: *Western Snow Conference (Laramie, Wyo.; April 15-17, 1980) Proceedings* 48: 1-13.
- Tabler, R. D. 1993. Trapping efficiency of snow fences and implications for system design. *Transportation Research Record No. 1387, Snow Removal and Ice Control Technology (Papers presented at a Symposium Sept. 14-18, 1992, Minneapolis, MN)*. Transportation Research Board, National Research Council, National Academy Press, Washington, DC, pp. 108-114.
- Tabler, R. D. 1994. *Design guidelines for the control of blowing and drifting snow*. Strategic Highway Research Program, Report SHRP-H-381.
- Tabler, R.D. (2003). "Controlling drifting and blowing snow with snow fences and road design." *Final Report, NCHRP Project 20-7 (147)*, Transportation Research Board of the National Academies, Washington, D.C.
- Tabler, R.D. (2006) "Algorithms for generating snow fence profiles" Tabler & Associates, Niwot CO.
- Tsai, H.W., Muste, M., Constantinescu, G. and Rehmann, C. (2017). Improving Traffic Safety through Better Snow Fences: Image-based Methods to Measure trapped Snow Volume and the Snow Relocation Coefficient, Report for Midwest Transportation Center, Ames, IA.
- Wyatt, G., Zamora, D., Smith, D., Schroeder, S., Paudel, D., Knight, J., Gullickson, D. &. (2012). Economic and environmental costs and benefits of living snow fences: safety, mobility, and transportation authority benefits, farmer costs, and 435 carbon impacts. Final Report, MN/RC 2012-03, MN Department of Transportation.